Summer 2022

Tire-wear-particle leachate toxicity to Americamysis bahia: analysis of sublethal and molecular effects

Karrin Leazer
Western Washington University, knleazer@gmail.com

Tire-wear-particle leachate toxicity to *Americamysis bahia*: analysis of sublethal and molecular effects

By

Karrin Leazer

Accepted in Partial Completion
of the Requirements for the Degree
Master of Science

ADVISORY COMMITTEE

Dr. Ruth Sofield, Chair

Dr. Markus Hecker

Dr. Rebecca Bunn

Dr. Robin Kodner

GRADUATE SCHOOL

David L. Patrick, Dean

Master's Thesis

In presenting this thesis in partial fulfillment of the requirements for a master's degree at Western Washington University, I grant to Western Washington University the non-exclusive royalty-free right to archive, reproduce, distribute, and display the thesis in any and all forms, including electronic format, via any digital library mechanisms maintained by WWU.

I represent and warrant this is my original work, and does not infringe or violate any rights of others. I warrant that I have obtained written permissions from the owner of any third party copyrighted material included in these files.

I acknowledge that I retain ownership rights to the copyright of this work, including but not limited to the right to use all or part of this work in future works, such as articles or books.

Library users are granted permission for individual, research and non-commercial reproduction of this work for educational purposes only. Any further digital posting of this document requires specific permission from the author.

Any copying or publication of this thesis for commercial purposes, or for financial gain, is not allowed without my written permission.

Karrin Leazer

08/15/2022

Tire-wear-particle leachate toxicity to *Americamysis bahia*: analysis of sublethal and molecular effects

A Thesis
Presented to
The Faculty of
Western Washington University

In Partial Fulfillment
Of the Requirements for the Degree
Master of Science

by
Karrin Leazer
August 2022

Abstract

Tire-wear particles (TWPs) are considered among the largest contributors of microplastics to the environment. They are subject to break-down due to environmental weathering, which allows for potentially toxic chemicals to be released from and sorbed onto the particles. In this study, leachate generated from "weathered" and "un-weathered" TWPs were used for sublethal toxicity tests with *Americamysis bahia*. Organisms were exposed for 2, 4, and 6 days and the effects endpoints included changes in respiration rate and molecular responses (i.e., changes in the abundance of transcripts after 4 days of exposure). A threshold for stimulated respiration rate was detected for weathered leachate on day 2 only between 0.133 and 0.67 g/L TWP leachate. For the un-weathered leachate, the threshold was on days 4 and 6 and was between 0.54 and 1.08 g/L TWP leachate. There were dysregulated contig sequences, in all tested concentrations for weathered (0.67, 1.34, and 2.68 g/L) and un-weathered (0.27, 0.54, and 1.08 g/L) TWP leachates; the contigs had sequences orthologous to specific gene descriptions in arthropods and were considered significantly dysregulated at an FDR ≤ 0.05 and $|\log2FC| \geq 1$. There were 80 dysregulated contigs across all tested weathered leachate concentrations and 139 dysregulated contigs across all tested un-weathered concentrations. Upregulated contigs at 2.68 g/L for weathered and 1.08 g/L for un-weathered leachates showed enrichment compared to the *de novo* reference transcriptome; this coincided with a significant respiration stimulation observed at 1.08 g/L in the un-weathered leachate. There were five enriched pathways in the weathered group and 10 enriched pathways in the un-weathered group; serine hydrolase, serine-type peptidase, and peptidase activity were enriched in both groups. Many contig sequences mapped to gene descriptions that regulated physical body structure, inflammatory response, and mediated protein-protein interactions, signifying that TWP leachate exposure disrupts many internal molecular processes in *A. bahia*.

Acknowledgements

I would like to thank my graduate adviser, Dr. Ruth Sofield, and thesis committee, Dr. Markus Hecker, Dr. Rebecca Bunn, and Dr. Robin Kodner, for their insight and help with project planning, setup, and interpretation. I would like to gratefully acknowledge Scott Wilkinson and Rose Kawczynski for their logistical support, Scott in the laboratory and Rose with international travel. I offer thanks to the many undergraduate students that assisted with sublethal respiration tests, specifically: Sierra Alden, Brook Ashcraft, Rachel Henden, April Reed, Angela Reisman, Avni Sharma, Saeda Suhm, and Jacob Warren (Western Washington University). I would like to acknowledge Stefanie Birzer and Anna Schmid from PreSens Precision Sensing for helping with technical support surrounding their products. I offer special thanks to Shakya Kurukulasuriya (University of Saskatchewan) for completing the RNA extraction for my samples. I would like to acknowledge the support of the Freiburg Galaxy Team: Beatriz Serrano-Solan and Björn Grüning, Bioinformatics, University of Freiburg (Germany) funded by the Collaborative Research Centre 992 Medical Epigenetics (DFG grant SFB 992/1 2012) and the German Federal Ministry of Education and Research BMBF grant 031 A538A de.NBI-RBC. I would like to thank Dr. Andy James from University of Washington Tacoma's Center for Urban Waters as well as Matt Roberts and Robert Rauschendorfer from Western Washington University for conducting the lab work and data cleaning for leachate chemistry analysis. I would like to specially thank Dr. Alper James Alcaraz (University of Saskatchewan) for his essential project support, encouragement, assistance, expertise, and his work with assembly and annotation of the *de novo* reference transcriptome. Finally, I would like to thank Western Washington University's Research and Sponsored Programs and Huxley College of the Environment, as well as Sigma Xi Grants in Aid of Research for providing the funding needed for this project.

Table of Contents

List of Appendices:

List of Tables:

List of Figures:

1.0 – Introduction

1.1 – Tire particles as microplastics and tire particle composition

Small particles of plastic pollution, including microplastics ranging from >100 nm to < 5 mm in diameter and nanoplastics <100 nm in diameter (Nguyen et al. 2019), are becoming more prevalent in the marine environment due to the continued production, degradation, and chemical persistence of plastics (Galgani et al. 2015, Gunaalan et al. 2020). Although it is difficult to quantify the amount of plastic input into the oceans, it is estimated that nearly 8 million tons of plastic per year are discharged to the ocean from both land and sea-based sources (Gallo et al. 2018). According to the United Nations Environment Programme (2018), of these 8 million tons of plastic discharged to the environment during various stages of its production or degradation, 36% (or approximately 3 million tons) are at the micro scale. Of these 3 million tons of microplastics, approximately 47% are from tire particles that come from the abrasion of tires, making tire particles the largest single contributor of microplastic inputs to the environment. Although not originally considered a microplastic due to their elastomeric properties, tire particles are more recently referred to as microplastics in the scientific literature (e.g., Kole et al. 2017, Wagner et al. 2018, Hartmann et al. 2019, Hüffer et al. 2019, Halle et al. 2020) and will be considered as such in the current study.

Tire particles are thermoset polymers, which are polymers that are irreversibly hardened by curing, or cross-linking (Halle et al. 2020). Tire particles are further classified as elastomers, which are defined by ISO (2012) as macromolecules with the ability to rapidly return to their initial dimension after deformation. They are divided into natural elastomers, commonly known as latex rubber, and synthetic elastomers, both of which are present in tires (Halle et al. 2020). Typical types of synthetic rubber include styrene butadiene rubber (SBR), polybutadiene rubber

(PBR), butyl rubber (IIR), and synthetic polyisoprene (IR) (Lin and Teng 2002, Hüffer et al. 2019). Tires are produced using different formulations and ratios of natural and synthetic elastomers to change the properties of wear, grip, and rolling resistance (Halle et al. 2020). They are also composed of a mixture of fillers and additive chemicals that contribute to the tire's performance, functionality, and durability (Hirata et al. 2014). The weight composition of a generic tire includes 21% synthetic rubber, 29% natural rubber, 26% reinforcing fillers, 6% additive chemicals, 3% organic fiber cord, 10% steel cord, and 5% bead wire (Hirata et al. 2014).

Tire particles contain a variety of additive chemicals depending on the brand and type of tire, and some of those additive chemicals differ from those associated with traditional microplastics (Halle et al. 2020). These tire-associated additives can include several kinds of carbon black and other fillers such as silica and calcium carbonate, extender oils and softeners (that can include polycyclic aromatic hydrocarbons, or PAHs), pigments, vulcanization chemicals such as sulphur and zinc oxide, curing agents, stearic acid, plasticizers that adjust the processability and hardness of the compounds, protective agents such as 6-PPD, and several different antioxidants, biocides, and oxonates which include compounds like aniline, benzothiazole, and methylbenzothiazole (Lin and Teng 2002, Kreider et al. 2010, Hirata et al. 2014, Hüffer et al. 2019, Wagner et al. 2018, Halle et al. 2020).

1.2 – Sources of tire particles and input to the environment

Tire-wear particles (TWPs) are defined as secondary microplastics produced by the abrasion of tires in contact with road surfaces (Kole et al. 2017, Wagner et al. 2018). TWPs are different from "crumb rubber granulate" (CRG), also called "crumb tire rubber" (CTR) by some studies, which are particles purposely ground from end-of-life tires and re-purposed for use as filler in artificial turf fields, playgrounds, safety surfaces, and walkways as a method of recycling

used tires (Capolupo et al. 2020, Halsband et al. 2020). There are different names in the literature for tire particles depending on their source and depending on whether road dust or road-related chemicals are associated with them (Halle et al. 2020). In my study, "TWPs" refers to tire-wear particles that were produced via abrasion of tires.

There is increased recognition of TWPs as a large source of microplastics to the environment (Kole et al. 2017, Wagner et al. 2018). Tire consumption has exponentially increased over time; according to a 2022 report by Global Industry Analytics, Inc., as of 2021, the US market was 544.3 billion units and currently accounts for a 27% share in the global market (GIA, Inc. 2022). In a study by Kole et al. (2017), the authors obtained an approximate global estimate of the amount of TWPs emitted into the environment per capita; this estimate predates the percentage estimate of total TWP inputs to the environment given by the United Nations Environment Programme (2018) but is the newest estimate of per capita TWP emissions. Kole et al. (2017) looked at either national tire-wear particle emissions estimates (when available) or data on the mileage and number of vehicles driven for thirteen countries (The Netherlands, Norway, Sweden, Denmark, Germany, United Kingdom, Italy, Japan, China, India, Australia, United States, and Brazil) and found that the average per capita TWP emission rate ranges between 0.23-4.7 kg/year, with a global per capita estimate of 0.81 kg/year (Kole et al. 2017). In general, more TWPs are generated in urban areas than in rural areas due to the larger number of tires on the road (Verschoor et al. 2016, Kole et al. 2017). Sommer et al. (2018) further suggests that the usual focus on traffic density as the only way of characterizing the TWP emission conditions at any given roadside is not sufficient, and they state that considering traffic mode and speed is also important. A study conducted by the Dutch government reported the contributions of total TWP emissions to different environmental compartments. They determined

that TWPs on road surfaces represent the largest percentage of all TWPs across environmental compartments: 3% enter surface waters directly, 8% enter water via sewage, 5% becomes airborne, 36% is deposited in the soil, 43% remains on road surfaces as residue, and the rest of the TWPs are retained in sludge (Verschoor et al. 2016).

The size of TWPs generated is dependent on factors such as the type of pavement, temperature, speed of travel, as well as the age and composition of the tire (Kole et al. 2017). There can be considerable variation in the size of TWPs, with different studies reporting different size ranges depending on the method of TWP collection or generation; the generally reported range of TWP sizes is between 10 nm to several 100 μm (Verschoor et al. 2016, Kole et al. 2017). The fate and transport of TWPs in the environment are largely dependent on their size, with smaller particles usually emitted into the air and subsequently dispersed, and larger particles deposited on road surfaces close to their source of generation and transported by rainwater runoff into surface waters, soils, and sewers (Kole et al. 2017). Atmospheric transport and runoff during rain events are considered the two most important modes of TWP transport in the environment (Wik and Dave 2009, Kole et al. 2017), although 90-99% of generated TWPs are non-airborne and remain on the roadside, subject to transport by runoff into freshwater and marine waterbodies (Wagner et al. 2018).

1.3 – Environmental weathering of TWPs

Once TWPs and other microplastics enter the environment, they are subject to further break-down due to a variety of degradation processes. These processes can include hydrolysis, UV photodegradation, mechanical abrasion, and biodegradation. As degradation and break-down continue, new surface area on the particles is exposed, allowing for chemicals both to be released

from the particles into the environment, and to be sorbed from the environment onto the particles (Alimi et al. 2018).

1.3.1 – Leaching additive chemicals into the environment

TWPs can leach many additive chemicals that are associated with them, some of which can be toxic, into the environment (Sadiq et al. 1989, Ozaki et al. 2004, Bocca et al. 2009, Degaffe and Turner 2011, Rhodes et al. 2012, Wachendorf et al. 2017, Halsband et al. 2020). Sadiq et al. (1989) compared concentrations of metals in tire particles to concentrations of the metals in roadway soil samples normalized to background un-contaminated soil and found that Zn, Ba, Pb, and Ni were higher in roadway soils, indicating that both tires and traffic volume contribute to environmental metal contamination. In another study, researchers found that tire particles contained a high ratio of Zn and Cd compared to background roadway dust and were cited as sources of Zn and Cd into the environment (Ozaki et al. 2004).

Halsband et al. (2020) investigated the metal and organic chemical content of both un-weathered, or "pristine" (collected directly from a commercial supplier) and naturally weathered (collected from outdoor sports fields in Norway) crumb rubber particles from end-of-life tires and the corresponding seawater leachates. Through various mass spectrometry methodologies, the authors found similar organic chemical profiles for both un-weathered and weathered crumb rubber leachates, which included a range of polycyclic aromatic hydrocarbons (PAHs) and phenolic compounds like bisphenols, benzothiazole, N-1, and 3-dimethylbutyl-*N*'-phenyl-*p*-phenylenediamine (Halsband et al. 2020). The authors also found Zn (in g/kg quantities) and Fe, Mn, Cu, Co, Cr, Pb, and Ni (in mg/kg quantities). They discovered that the most abundant organic chemical and metal compounds in the crumb rubber leachates were benzothiazole and Zn, respectively (Halsband et al. 2020). The authors also reported that metals are released from

the tire particles over a longer time period than are the organic chemicals, with the metals continuing to leach into solution over the course of the authors' 30-day leaching period, while the organic chemical concentrations stabilized in the leachate solution within only a few days.

In a study based out of Western Washington University, a variety of leachates created from "weathered" and "un-weathered" TWPs across 6 different years (2013-2018) were analyzed for metal content (Roberts 2021). It was found that, for all 6 years, out of 6 analytes (i.e. Al, Co, Cu, Mn, Ni, and Zn), Zn was present at the highest concentrations in the leachate, from 1-3 orders of magnitude greater than the other metals. In addition, Zn content in the "un-weathered" leachates was consistently higher than in "weathered" leachates for 5 out of the 6 years, with one exception in 2014.

An earlier study examining the chemical constituents of TWP leachate agree with Halsband et al.'s (2020) conclusion that Zn is a major component of the leachate (Bocca et al. 2009). Bocca et al. (2009) investigated the content of 25 metals leached from synthetic turf, or crumbled granulates from recycled tires, collected from 32 different playgrounds in Italy. The authors compared the amount of each element leached under acidic conditions (pH = 5) with the amount leached in deionized water and found that Zn was the component with the highest concentration in leachate in each type of leaching condition (Bocca et al. 2009). However, when the authors normalized the mass (in mg) of each leached metal found in the acidic solution to the mass (in kg) of metal in the original rubber particles, they found that Zn only leached 1%, whereas Mg, Mn, and Sr leached 10% of the concentration that was found in the rubber particles themselves, indicating that more Zn was available for release beyond the 24 hour leaching period (Bocca et al. 2009).

Many environmental factors can impact the amount of chemical that can leach from tire particles, including tire particle size, the amount of light present during leaching, the amount of time spent leaching, the salinity of the water, and the pH of the water. Two studies looked at the environmental influences affecting the amount of Zn leached into various solutions. In general, the amount of Zn leached into solution was higher when the tire particle size was smaller, in the presence of light, longer leaching periods, lower salinities, and lower pHs (Degaffe and Turner 2011, Rhodes et al. 2012). Wachtendorf et al. (2017) conducted a series of artificial weathering experiments on synthetic sports mats/surfaces which contain a mixture of TWPs and binding polymers, synthetic turf mats, and ground TWPs that had been coated with a green colored polyurethane protective coating as well as those that had been left un-coated. The authors used a variety of weathering methods, including ozone exposure, UV exposure, humidity, sub-zero temperatures, and simulated rainwater and paired these weathering methods with leaching. The authors initially found a general decline in Zn, PAHs, electrical conductivity, and total organic carbon (TOC) in the leachate, indicating depletion of additives and fillers accessible from the TWP surface. After an initial decrease in concentrations, the authors observed an increase of chemicals in the leachate again, which they suggested was caused by further degradation of the polymeric matrix and the opening of new cracks and pores in the material, allowing the release of additional fillers, additives, and products from the polymer matrix degradation that were not able to be released before (Wachtendorf et al. 2017). They also found that the green polyurethane protective coating on some of the TWPs resulted in a decrease in the TWP-associated chemicals that leached into solution as compared to the un-coated TWPs, indicating the utility of protective coatings. In another study, natural weathering of tire particles was investigated; the authors found that the out-gassing of ten volatile chemicals, including benzothiazole, other PAHs, and

antioxidants, was reduced in tire particles collected from two-year-old turf fields when compared with tire particles collected from newly manufactured turf fields (Li et al. 2010). These various studies collectively show that environmental weathering of tire particles can alter the chemical composition of the particles themselves as well as the leachate created from them, and that the amount of chemicals released from tire particles is dependent on a variety of environmental conditions and interactions.

1.3.2 – Sorption of chemicals from the environment

In addition to leaching additive chemicals into the environment, TWPs can also act as a substrate on which a variety of toxic chemicals from the environment, such as metals and organic contaminants, can sorb (Alamo-Nole et al. 2010, Kreider et al. 2010, Sommer et al. 2018, Halle et al. 2020, Hüffer et al. 2020). TWPs have an affinity for both metals and organic contaminants due to their physical properties, including the interaction of metals with specific filler chemicals and the interaction of organic chemicals with the large number of amorphous regions on the particles, and so can be expected to have an elevated chemical load relative to other types of particles (Halle et al. 2020).

In 1974, Netzer and Wilkinson investigated the potential for TWPs to remove metals from wastewater. They discovered that up to 99% metal removal was achieved for Cu, Hg, Ag, Pb, Al, Cr, Fe, Ni, Zn, Cd, Co, and Mn at varying pH levels, indicating that TWPs are effective at adsorbing metals. The authors suggested that carbon black was the primary constituent of the tire particle that binds to metals, drawing from earlier work (Netzer and Norman 1973), while the removal of metals by reaction with other parts of the tire such as with sulphur, synthetic rubber, or other types of fillers was a secondary mechanism (Netzer and Wilkinson 1974). TWPs can also remove mercury (II) from aqueous solutions (Knocke and Hemphill 1981, Gunasekara et al.

2000) via adsorption onto carbon black molecules (Knocke and Hemphill 1981), further supporting Netzer and Norman (1973). Rowley et al. (1984) further investigated the mechanisms of metal adsorption to tire rubber particles from aqueous solutions containing a variety of different metals and discovered an ion exchange mechanism that displaces Zn (II), present in the tire as a vulcanization chemical aid, and replaces it with cadmium or mercury from the solution. In short, these various studies indicate that TWPs are effective at adsorbing metals from the environment primarily through interaction with carbon black, but also through interactions with other constituents of the tire.

In addition to their ability to adsorb metals, TWPs have a particular affinity for organic contaminants (Halle et al. 2020). According to Fried's (2003) book on Polymer Science and Technology, the ratio of crystalline to amorphous regions in various types of polymers could influence the sorption of organic contaminants, as those are more likely to interact with amorphous regions of the polymer. Because all polymers are made up of both crystalline and amorphous regions, the affinity of organic contaminants for the particle will depend on the number of amorphous regions it contains (Hüffer et al. 2019, Halle et al. 2020). Elastomers like TWPs tend to have more amorphous regions relative to crystalline regions, which increases their affinity for binding organic contaminants (Halle et al. 2020). Some organic chemicals that have been found to bind to TWPs are toluene and xylene (Alamo-Nole et al. 2010), naphthalene (Gunasekara et al. 2000), n-hexane, cyclohexane, benzene, chlorobenzene, di-n-propylether, and 2,6-dimethyl-2-heptanol (Hüffer et al. 2020). It has been suggested that organic chemicals bind to tires primarily by being absorbed into the polymer matrix of the tire and by being adsorbed onto the carbon black filler through hydrophobic interactions (Alamo-Nole et al. 2010, Hüffer et al. 2020).

TWPs can accumulate some of these chemicals from physical interactions with road surfaces, allowing road dust, automobile fluids, the erosion of brake pads, and the weathering of pavement to contribute to the chemical load that the tire particles may accumulate in the environment (Kreider et al. 2010, Sommer et al. 2018, Wagner et al. 2018, Halle et al. 2020). The sorption of environmental chemicals onto TWPs can impact their physical capacity for further sorption as well as their potential toxicity (Day et al. 1993, Kreider et al. 2010, Wagner et al. 2018, Hüffer et al. 2019, Halle et al. 2020, Hüffer et al. 2020).

1.4 – Aquatic toxicity of TWPs

The toxicity of TWPs to organisms is difficult to determine due to a variety of factors. These factors include varying routes of exposure (e.g. whether the toxicity comes from ingestion of the particles themselves or from exposure to the chemicals associated with those particles), the amount of additives and environmental contaminants that are potentially present on the particles, the migration tendencies of the various chemicals, and whether the chemicals associated with TWPs are bioavailable and under what conditions (Wik and Dave 2009, Hansen et al. 2013, Auta et al. 2017, Halle et al. 2020).

1.4.1 – Particles compared to leachate

Recent research on both freshwater and marine organisms has focused on differentiating between the toxicological effects of the tire particles themselves as compared to TWP leachates (Khan et al. 2019, Cunningham et al. 2022, Siddiqui et al. 2022). Khan et al. (2019) exposed *Hyallela azteca* to both tire particles and TWP leachates and measured the effects on mortality, reproductive output, and growth. The authors found that the acute toxicity of the tire particles was distinct compared to that of the leachate, with the toxicity profile of the particles suggesting a different mechanism than that of the leachate (Khan et al. 2019). Similarly, Cunningham et al.

(2022) discovered that tire particles showed unique particle-specific toxicological effects in *Daphnia magna* and *Danio rerio* (zebrafish), although the leachate component was still the larger contributor to the observed toxicity. In another study, two marine indicator species, *Americamysis bahia* (mysid) and *Menidia beryllina* (inland silverside) were exposed to nano- and micro-sized tire particles as well as TWP leachates, and their behavioral responses and growth were measured (Siddiqui et al. 2022). The authors found that *A. bahia* exposed to tire particles exhibited significant decreases in growth as well as some alterations in behavior, whereas *A. bahia* exposed to TWP leachate did not experience any significant decrease in growth but did show some significant behavioral alterations (Siddiqui et al. 2022).

These studies show that toxicity due to TWPs can either be derived from exposure to the particles themselves (e.g. via ingestion), or exposure to the chemicals that leach from the tire particles. The goal of my study was to focus on TWP leachate-induced toxicity for two different environmental weathering treatment groups in order to build on previous knowledge of the toxicity of TWP leachate exposure to *A. bahia* (Roberts 2021).

1.4.2 – TWP leachate toxicity – case studies

Many studies have examined toxicity resulting from exposure to TWP leachates; these studies have investigated a variety of different species and endpoints, tested both freshwater and saltwater organisms and measured both sublethal and apical effects. A study was conducted by Wik and Dave (2006) on the sublethal effects to *Daphnia magna* neonates after exposure to TWP leachate derived from particles originating from 25 different used tires. The authors artificially created the TWPs, then leached the particles at 44°C for 72 hours, and subsequently used the leachate in 48-hour acute toxicity tests where the percent immobilization of *D. magna* was measured as an endpoint. They found that the EC50 values, or the concentrations at which

D. magna experienced 50% immobilization, ranged from 0.5 g/L to over 10 g/L depending on which specific tire the particles originated from.

In a recent study by Cunningham et al. (2022), *D. magna* and *D. rerio* were exposed to concentrations of TWP leachate ranging from 10% to 100% and sublethal and apical effects were measured for *D. rerio* and *D. magna* respectively. TWP leachate was generated by cutting a new, undriven standard passenger car tire into 2-4 mm pieces with a stainless-steel blade, milling the pieces and then suspending 3.25 g of the milled particles in 300 mL of liquid, and then filtering the tire particles through a 20 µm, 1 µm, and 0.02 µm filter to remove micro- and nano-sized particles. The remaining leachate stock was set at 100% and was subsequently diluted. For *D. rerio* sublethal toxicity tests, the authors found that the EC50 for overall toxicity (with percent normal zebrafish embryos as the endpoint) at 120 hours post-fertilization was at a TWP leachate concentration of 88.65% of the stock. Zebrafish exposed to TWP leachate at concentrations above 80% developed unique abnormalities including malformed jaws, snouts, eyes, as well as yolk sac edemas. For *D. magna* acute toxicity tests, with mortality as the endpoint, the authors calculated a 48-hr LC50 value of 20.50% TWP leachate concentration.

In another study, both *A. bahia* and *M. beryllina* were exposed to TWP leachate at different salinities (i.e. 15, 20, 25 PSU) and sublethal responses (i.e. changes in growth and behavior) were measured (Siddiqui et al. 2022). The authors found that TWP leachate had no significant effect on either organism's growth, but they did find that it had a significant effect on several behavioral endpoints. Both *A. bahia* and *M. beryllina* exposed to TWP leachate experienced significant differences in six of the seven measured behavior variables (i.e. freezing, movement, in zone duration, frequency, meander, and turn angle) compared to control animals (Siddiqui et al. 2022).

The adverse effects of a variety of microplastic leachates, including leachate derived from "crumb tire rubber", on three aquatic organisms: the freshwater microalgae *Raphidocelis subcapitata*, the marine microalgae *Skeletonema costatum*, and the Mediterranean mussel *Mytilus galloprovincialis* were studied by Capolupo et al. (2020). The authors found that crumb tire rubber leachates were the most toxic of all the tested leachates for every measured endpoint and to all organisms. Crumb tire rubber leachates inhibited algal growth, with a 72-hr EC50 of 0.5% of the total leachate concentration for the freshwater algae and a 72-hr EC50 of 19% for the marine algae. The leachate also affected the mussels; notably, the lysosomal membrane stability, percent egg fertilization (EC50 36.38%), percent larval motility (48-hr EC50 18.75%), percent larval survival (144-hr EC50 59.38%), and embryonic development (48-hr EC50 2.22%).

In another study, leachate was created from "crumb rubber granulate" and two species of marine copepods, a smaller lipid-poor *Acartia longiremis* and a larger lipid-rich *Calanus* sp., were exposed over the course of 14 and 17 days, with mortality as the endpoint (Halsband et al. 2020). The authors created crumb rubber granulate leachate from both "pristine" and "weathered" particles. The leachates were subsequently diluted and the concentrations used in toxicity testing ranged between 0.01 g/L to 100 g/L. At medium leachate concentrations (5 g/L, 15 g/L, and 35 g/L), both copepods responded to the leachate in a dose-dependent manner, with the smaller *Acartia* (48-hr LC50 of < 5 g/L) showing higher sensitivity than the larger *Calanus* (48-hr LC50 of 35 g/L).

Recently, it has been discovered that coho salmon, *Oncorhynchus kisutch*, returning from the ocean to spawn in urban watersheds in the Pacific Northwest die in large numbers from exposure to stormwater runoff after rain events (Peter et al. 2018, Tian et al. 2021, McIntyre et al. 2021). With analytical methods using UPLC-HRMS accompanied by intensive database

searches, a single compound in TWP leachate, 6PPD-quinone ($C_{18}H_{22}N_2O_2$), a degradation product of 6PPD which is used in tires as an antioxidant and protectant from ozone, was found to be the cause of this pre-spawn mortality syndrome in juvenile coho salmon (Tian et al. 2021).

In a study based out of Western Washington University, apical endpoint (i.e. mortality) *in vivo* 96-hr acute toxicity tests on *A. bahia* were conducted using a wide range of leachates from different types of TWPs and from two different weathering treatment groups (Roberts, 2021). The author used "weathered" and "un-weathered" TWPs from 6 different tire groups and calculated dose-response relationships and the resulting lethal concentrations for all leachate exposures. From these calculations, the author found that TWP leachates were more toxic than other microplastic leachates, based on mortality in *A. bahia* (Johnson 2021, Roberts 2021).

Although an apical endpoint has been measured in *A. bahia* exposed to TWP leachate (Roberts 2021), along with sublethal effects on general growth and swimming behavior in *A. bahia* exposed to TWP leachate (Siddiqui et al. 2022), there has been no work done on assessing a physiological activity associated with energy metabolism in response to TWP leachate exposure at a sublethal level, nor has there been work done measuring molecular effects to *A. bahia* exposed to TWP leachate. Respiration is one of the basic physiological activities associated with energy metabolism in animals, and it has been shown to be a sensitive indicator used to determine physiological responses of animals in response to varying environmental conditions (Bao et al. 2020). Respiration rate has been studied in crustaceans to elucidate the effects caused by a variety of toxic chemicals, as the amount of oxygen consumed over a period of time is indicative of the energy the animal spent during that time period to maintain its processes in the presence of chemical exposure (Barbieri et al. 2009, Barbieri and Paes 2011). Similarly, molecular investigations can help elucidate the mechanisms through which toxic

responses occur. The characterization of molecular responses in an organism after exposure to a toxicant is possible without prior knowledge of the specific mechanisms of toxicity due to technology advancements in recent years (Alcaraz et al. 2021). These next generation technologies include transcriptomics, which is a global analysis of all expressed transcripts in an organism (Alcaraz et al. 2021). My study will be the first of its kind measuring both respiration rate and transcriptomic responses in a marine organism exposed to TWP leachate; the combination of a general physiological endpoint and a broad view of potentially affected body processes at the molecular level will provide a more complete understanding of how *A. bahia* are impacted by TWP leachates and their associated chemicals.

1.5 – Test organism – background and use in toxicity testing

The test organism used in this study is *Americamysis bahia*. The species was first taxonomically described in 1969 by Joane Molenock and was originally given the name *Mysidopsis bahia* (Molenock 1969). In 1994, a new genus, *Americamysis*, was created, and several existing species were classified under the new genus, including *Mysidopsis bahia* (Price et al. 1994). According to the World List of Lophogastrica, Stygiomysida and Mysida, which is part of the World Register of Marine Species (WoRMS) (Meland et al. 2015), *A. bahia* ranges from 3 mm-10 mm in length, lives in marine/brackish habitats, and is distributed in estuaries from the east coast of South America up through the Gulf of Mexico, and from the west coast of South America up to the southern coast of California (Mees and Meland 2012/onwards).

In 1982, Nimmo and Hamaker reviewed the use of mysids, particularly *A. bahia*, in a variety of toxicity tests, and documented their previous work with the species and their first acknowledgement of *A. bahia*'s utility as a test organism (Nimmo et al. 1977). According to Nimmo and Hamaker (1982), *A. bahia* is an ideal organism for saltwater toxicity testing because

it has been shown to be as or more sensitive to toxic substances than other marine species, it is easily cultured and handled in the laboratory, it has a short life cycle, it is small, and its larval development is direct. Because of its acceptance and utility as a saltwater toxicity testing organism in the field of aquatic toxicology (USEPA 2002*a*, 2002*b*), and because of its previous use in toxicity testing with TWP leachates (Roberts 2021), *A. bahia* was used for this exploratory study of the sublethal and molecular responses of the shrimp exposed to TWP leachates.

1.6 – Objectives and hypotheses

The objectives of my research were to: *a)* determine how one weathered leachate and one un-weathered leachate using ground tire-wear particles (TWPs) from Roberts (2021), affect sublethal responses of *A. bahia* (with shrimp respiration rate as the measured endpoint), *b)* compare the transcriptomic responses (differential expression and pathway enrichment) of *A. bahia* exposed to the different weathering treatment groups of TWP leachate, and *c)* compare the chemical components of the weathered versus un-weathered TWP leachates and relate them to potential changes to the transcriptome and/or sublethal effects to respiration that may be observed.

In this study, differential expression or "dysregulation" was measured by differences in the expressed "contigs", or contiguous sequences of messenger RNA (mRNA), between treatment animals and control animals. Pathway enrichment was measured by the number of dysregulated contig sequences that are "overrepresented" in a specific TWP leachate exposure (e.g. leachate type and concentration) relative to a reference transcriptome, or the entire set of expressed contig sequences in *A. bahia*. This overrepresentation of dysregulated contigs in a specific treatment group relative to the reference transcriptome is defined by comparison to the

Gene Ontology (GO) database (Gene Ontology *a*, n.d.), which groups dysregulated contigs by their potential biological functionality in an organism.

It was hypothesized that there will be observable effects to *A. bahia* exposed to TWP leachate relative to control animals, both in the form of sublethal effects to respiration rate and in transcriptomic responses. It was also expected that there will be differences in the chemistry of the weathered versus un-weathered TWP leachates, given that Johnson (2021) found a difference in chemical composition between weathered and un-weathered microplastic particle and fiber leachates. This probable chemical difference between the two leachate types is expected to lead to observable differences in the sublethal respiration rates as well as in the transcriptomic responses of *A. bahia* depending on whether the shrimp were exposed to weathered or un-weathered TWP leachate.

2.0 – Methods

2.1 – The tires

Roberts (2021) conducted apical endpoint, whole-organism acute toxicity tests on *A. bahia* using weathered and un-weathered tire-wear-particle (TWP) leachates. In brief, used tires from 5 different cars were collected and separated into 6 treatment groups by year, from 2013-2018. The tires were the same brand and model and only differed by tire diameter and manufacture/production year. Tire particles were generated using an angle grinder with a tire shaping disc. The particles were dry sieved and divided into two different treatment groups: "weathered" and "un-weathered". The weathered particles were put into 25 μm nylon mesh bags, sewn shut, placed in Bellingham Bay at 2.5 ft below mean sea level, and left for 82 days from September to December 2020. The weathered tire particles were collected, sonicated to remove sediments, air-dried, and stored in the freezer at -20°C until their use in the acute toxicity tests.

The un-weathered particles were stored in a freezer at -20°C from the time of generation until use for toxicity testing and chemical analysis. Roberts (2021) created leachates from the tire particles, exposed *A. bahia* to the leachates for 96 hours, and calculated dose-response relationships for lethality and the corresponding LC50s. In my study, only the TWPs from the 2017 tires from Roberts (2021) were used; the 2017 weathered group and 2017 un-weathered group were classified by Roberts (2021) into different toxicity categories based on their LC50 values from a ratio test of the LC50 values. The LC50 for the weathered group was 5.19 g/L and the LC50 for the un-weathered group was 1.97 g/L.

2.2 – Leachate creation

In my study, tire-wear particle (TWP) leachates were created according to the methods presented in Johnson (2021) and Roberts (2021). The tire particles were weighed out to the appropriate stock concentration and then placed for 48 hours in 25 ppt seawater filtered to 0.2 μm. This allowed chemicals associated with the tire particles, either additive chemicals or sorbed chemicals, to leach into the seawater. For those 48-hrs, the leachates were on a rotary mixer table set to 100 rotations per minute in a 21°C ± 1°C, dark environmental chamber. After 48-hrs, the leachates were filtered through 25 and 10 μm acid-washed and acetone-rinsed mesh screens to separate tire particles from the leachate. The leachates were then diluted to 5 nominal concentrations per tire type (Table 1). The highest concentration for the weathered 2017 tire type was 52% of the LC50 calculated in Roberts (2021). The highest concentration for the un-weathered 2017 tire type was 55% of the LC50 calculated in Roberts (2021). For each of the two leachate types, 50% sequential dilutions were used to create the remaining four concentrations.

Table 1. For each of two tire leachates studied in Roberts (2021), "2017 weathered" and "2017 un-weathered", 5 nominal concentrations below the calculated LC50 were prepared. The LC50 for the weathered group was 5.19 g/L and the LC50 for the un-weathered group was 1.97 g/L (Roberts 2021). The concentrations that were used in sublethal respiration toxicity tests and/or in downstream transcriptomic analysis are marked with a check mark.

Leachate Treatment	Concentration (g/L)	% of LC50 from Roberts (2021)	Used in respiration tests?	Used in transcriptomic analysis?
Weathered 2017	2.68	51.54	✓	✓
	1.34	25.77	✓	✓
	0.67	12.89	✓	✓
	0.33	6.44	✓	
	0.17	3.22	✓	
Un-weathered 2017	1.08	54.82	✓	✓
	0.54	27.41	✓	✓
	0.27	13.71	✓	✓
	0.14	6.85	✓	
	0.07	3.43	✓	

2.3 – Chemical analysis of leachates

2.3.1 – Organics

The 14 weathered and un-weathered leachates previously studied in Roberts (2021) and four additional TWP leachates used in a different study (Sofield et al., unpublished), all created at a concentration 10 g TWP/L, along with a Nanopure blank and filtered 25 ppt seawater blank from Shannon Point Marine Center, were extracted and analyzed for organic chemicals via liquid chromatography-quadrupole time-of-flight mass spectrometry (LC-QTOF-MS) at the University of Washington, Tacoma Center for Urban Waters (CUW). Leachate samples were stored in the refrigerator or on ice until they were extracted, which occurred within 20 hours of leachate generation. 900 mL of the leachate samples and blanks were separated into three 300 mL replicates and extracted in pre-conditioned OASIS HLB Solid Phase Extraction (SPE) cartridges over a vacuum. Elutions were performed with 10 mL of methanol (Fisher Chemical, Optima LC/MS grade), transferred to autosampler vials, spiked with a QTOF Internal Standard Mix, and

analyzed in ESI+ mode. Individual molecular weights and retention times were identified in the samples via high-resolution mass spectrometry (HRMS), followed by identification of chemical features and hierarchical clustering with Euclidean distance and Ward's linkage. Chemical results from the Nanopure and seawater blanks were subtracted from the leachate sample results, so the leftover chemical features are unique to the leachates.

2.3.2 – Metals

The 14 TWP leachates previously studied in Roberts (2021), both weathered and un-weathered leachates all at a concentration of 10 g/L, along with four control 25 ppt seawater samples, were analyzed for dissolved metals at Western Washington University in Bellingham, WA using inductively coupled plasma mass spectrometry (ICP-MS; Agilent 7500ce). The seawater leachate samples were diluted 10x with Nanopure water to keep total dissolved solids below 0.5% and acidified to 5% trace metal grade nitric acid prior to ICP-MS analysis. Chemical analytes included the metals Be, Mg, Al, K, Ca, V, Cr, Mn, Fe, Co, Ni, Cu, Zn, As, Se, Mo, Ag, Cd, Sb, Ba, Tl, Pb, Th, and U. The identification of metal features in the leachates, along with the metals results from TWP leachates previously studied in Roberts (2021), were followed by multivariate principal component analysis (PCA) and hierarchical cluster analysis (HCA) with Ward's linkage. The principal components coefficients were used to develop clusters to identify TWP leachates with similar metal profiles according to the methods presented in Ben-Hur and Guyon (2003). The first four principal components created through PCA were chosen to be used in HCA because they explain 97.98% of the variance in the system. Cr, Cd, Sb, and Pb were excluded from the multivariate analyses *a priori*, as these metals were not detected in 100% of the samples; Cr and Sb were detected in 14% of tested leachate samples, Pb was detected in 7% of samples, and Cd was not detected in any of the samples.

2.4 – Sublethal toxicity tests (measuring respiration rate)

2.4.1 – Measurement of oxygen depletion

The five concentrations of the 2017 weathered and 2017 un-weathered TWP leachates, presented in Table 1, were tested in triplicate following the methods for toxicity testing outlined in USEPA (2016) using juvenile *A. bahia*, < 24-hrs old, bred, hatched, and delivered from Aquatic Biosystems (Fort Collins, Colorado). The only difference for these sublethal tests from the USEPA (2016) standard method was that my exposure was for 8-days instead of 4-days. Test chambers, in this case 400 mL high form beakers, were covered with acid-washed petri dishes and were indiscriminately placed into an environmental chamber set to a 16-hr light: 8-hr dark photoperiod between 540-1080 lux, at 25 °C ± 1 °C. Every 12-hrs, the mysids were fed with < 24-hr old *Artemia* nauplii at a rate of 5-8 nauplii per mysid. The leachate was not renewed for these tests due to limited tire particle material. Oxygen was measured with integrated oxygen sensor spots (type SP-PSt3-YOP) from PreSens Precision Sensing GmbH (PreSens; Regensberg, Germany).

A preliminary experiment was conducted to determine the duration for measuring oxygen depletion. A period of three-hours was chosen so that the dissolved oxygen used in shrimp respiration would be measurable with the PreSens system but would not be so long that organisms would be under oxygen stress. McKenney and Matthews (1990) used 50% pO2 as their minimum allowable oxygen concentration to avoid bias from low oxygen stress; in my experiments, the oxygen decrease in the vials fell between 5.5% - 34.3% reduction. The lower percent reductions were in vials measured towards the end of the exposure that had fewer

surviving shrimp; specifically, the 5.5% decrease was measured from a vial that contained two surviving shrimp after the sixth day of exposure (Appendix B).

Every 24 hours and for each replicate in each treatment group, the leachate (containing approximately 10 living shrimp depending on the dose and day) was poured from the 400 mL toxicity testing beaker, through a 300 μm circular mesh screen, into a secondary 400 mL beaker. The shrimp were retained by the screen and the leachate was collected in the secondary beaker. Shrimp were rinsed into a plastic weigh boat by rinsing the screen with leachate at the same concentration as the exposure. All living shrimp in a replicate were then gently poured from the weigh boat into a 20 mL vial that contained an integrated oxygen sensor spot from PreSens (Regensburg, Germany). The vial was filled to the brim to remove any headspace with leachate at the same concentration as the exposure; all air bubbles were removed using a plastic pipet before the vial cap was sealed. Once the cap was sealed, oxygen measurements were taken immediately, and approximately every 20 minutes thereafter for a three-hour period. Eight to fourteen measures at each time point were taken by placing a PreSens polymer optical fiber (POF) on the outer wall of the glass vial directly opposite the oxygen sensor spot, at a 90° angle. The POF transfers excitation light to the sensor and the sensor response back to the PreSens Fibox4 trace handheld oxygen meter, which communicates with the PreSens Measurement Studio 2 software to display the oxygen readings. Temperature during the test was at 25°C and was accounted for in the oxygen readings. After the three-hour monitoring period, the shrimp from each of the 20 mL vials were filtered through the 300 μm mesh screen and put back into their respective toxicity testing beaker with the solution retained in the secondary beaker and placed in the environmental chamber.

This entire process was repeated for the same shrimp three times during the sublethal toxicity test. Namely, respiration tests were conducted after two days of exposure to leachate (when the shrimp were ~3 days old), after four days of exposure (when the shrimp were ~5 days old), and after six days of exposure (when the shrimp were ~7 days old).

2.4.2 – Measuring respiration rate

In addition to all the vials that had shrimp in them, two 20 mL respiration vials were filled only with control 25 ppt seawater and monitored over the course of each three-hour respiration test to account for respiration by microorganisms in the test vials, as modeled by protocols in the literature (Toda et al. 1987, McKenney and Matthews 1990, Roast et al. 1999, Ogonowski et al. 2012). Respiration rate was calculated by filtering out all of the values with a POF light amplitude <20,000 µV, subtracting the average amount of oxygen lost via microbial respiration from all of the vials in which shrimp respiration was measured, calculating the rate at which oxygen decreased in a vial by including the eight to fourteen measurements taken with the POF cable at each time point in one regression, and then normalizing the amount of oxygen used per unit time to the volume of the respiration chamber and to the dry weight of shrimp in the vial, as modeled in a previous respiration study on *A. bahia* (McKenney and Matthews, 1990).

2.4.3 – Determination of dry weight

Every 24 hours for 8 days, dry weight of mysids was measured from 10 mysids from unexposed chambers (25 ppt filtered seawater). The shrimp were dried at 80°C for 1 hour, and weighed with a Metler AT261 Delta Range analytical balance to the nearest 0.01 mg. The average dry weight per individual was determined. This was conducted three times, and all data was used in one regression to determine the growth rate. The growth rate was used to estimate shrimp weight during the exposures and was used for normalization of respiration rate (Figure

1). The predicted weight of shrimp at 1.5 hours into the respiration measurements, which was the midpoint time of each respiration test, was used for the normalization.

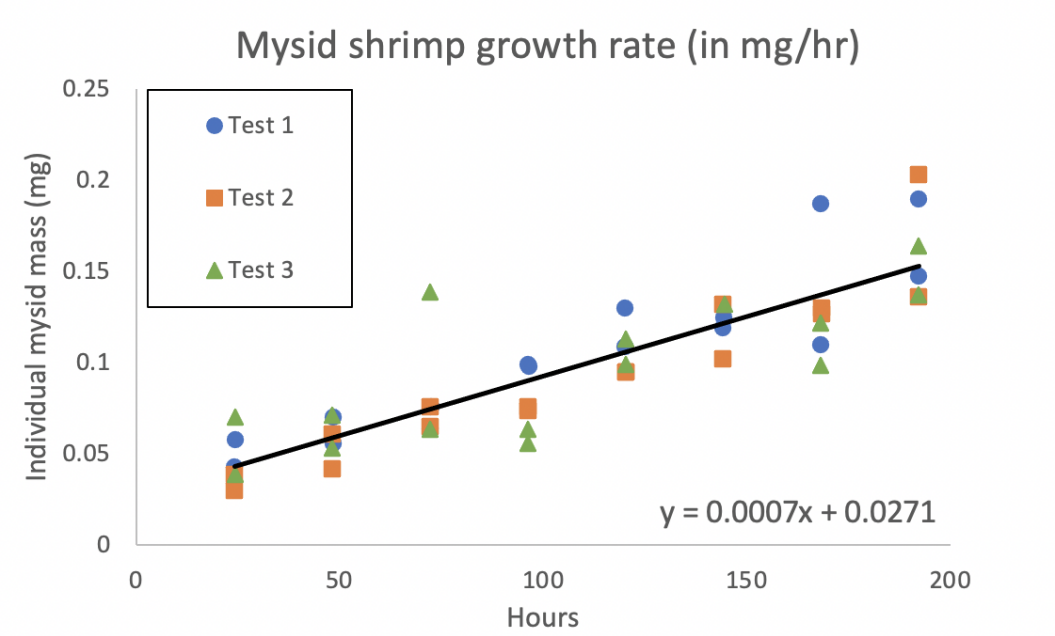

Figure 1. *Americamysis bahia* grow at a rate of 0.0007 mg/hr. Weight measurements were taken from unexposed organisms over the course of the 8-day sublethal toxicity test and are presented over time in decimal hours. The different tests (Test 1, Test 2, Test 3) represent different stand-alone tests (conducted during three consecutive months) for which the dry weights of shrimp were measured. Test 1 was conducted at the beginning of October 2021, Test 2 was conducted at the beginning of November 2021, and Test 3 was conducted at the beginning of December 2021. All tests were normalized to the same Time 0.

2.4.4 – Percent changes in respiration rates

Respiration rates of mysids exposed to both weathered and un-weathered TWP leachates, as well as respiration rates of control mysids, were calculated after two, four, and six days of exposure. The three control replicates for each exposure time (x) were averaged and used as a baseline respiration rate for that time (BRR_x); the results for leachate-exposed shrimp were compared to the BRR_x. At each leachate concentration, respiration rates normalized to mg of dry

body weight, were calculated for each of three replicate chambers; each replicate contained 2-11 surviving shrimp, with most containers having between 8-10 surviving shrimp (Appendix B). Respiration rates from the three replicates for each mysid were averaged for each concentration and exposure length (Appendix C). The percent change in respiration rates on one of the three days (ΔR_x%) of leachate-exposed shrimp relative to respiration rates of control shrimp were also calculated for each weathering treatment group according to the following equation:

$$\mathbf{\Delta R_x(\%) = ((BRR_x - TRR_x)/(BRR_x)) \times 100} \qquad \textit{[Equation 1]}$$

Where "BRR_x" represents the mean individual (per mysid) respiration rate for control shrimp on day x of exposure, and "TRR_x" represents the day x corresponding per mysid respiration rate of shrimp exposed to leachate for one replicate. The 95% confidence intervals were determined using a t-distribution around the standard error of the mean ΔR_x(%) calculated from the x3 ΔR_x(%) values from each replicate. The 95% confidence intervals were then compared to the mean change in the control respiration rate (ΔR_{Cx}(%)), as set to 0 in Equation 2.

$$\mathbf{\Delta R_{Cx}(\%) = ((BRR_x - BRR_x)/(BRR_x)) \times 100} \qquad \textit{[Equation 2]}$$

Significance was determined by a lack of overlap of the 95% confidence interval with the ΔR_{Cx}(%), or mean change in the control (line at y=0: Figure 4).

2.5 – 96-hr sub-lethal toxicity test

Juvenile *A. bahia* were divided into five control replicates as well as five replicates for each concentration used in transcriptomic analysis (Table 1): 0.67, 1.34, and 2.68 g/L for the weathered TWP leachate and 0.27, 0.54, and 1.08 g/L for the un-weathered TWP leachate. There were 10 mysids per replicate. Each of the treatments was dosed with a prepared TWP leachate (or 25 ppt control seawater) for a 96-hr, static-renewal toxicity test, according to USEPA (2016).

Test chambers, in this case 400 mL high form beakers, were covered with acid-washed petri dishes and were indiscriminately placed into an environmental chamber set to a 16-hr light : 8-hr dark photoperiod between 540-1080 lux, at 25 °C ± 1 °C. Every 12-hrs, the mysids were fed with < 24-hr old *Artemia* nauplii at a rate of 5-8 nauplii per mysid. After 97.5±1.5-hrs, surviving individuals in the leachates were removed from the leachate, flash-frozen on dry ice, and preserved in RNAlater®-ICE for subsequent RNA-Seq analysis.

2.6 – Total RNA extraction

Total RNA was extracted from the 35 samples preserved for RNA-Seq analysis with a Qiagen RNeasy Universal Plus Mini Kit (Qiagen, Germany) following the manufacturer's protocol. In brief, shrimp tissues (approximately 10 shrimp per replicate) were homogenized and exposed to a variety of solutions and wash buffers to extract total RNA. Total RNA samples from each replicate were stored in a -80°C freezer prior to RNA-Seq analysis.

2.7 – Next generation sequencing – RNA-Seq

2.7.1 – Library preparation and sequencing

Samples with RNA integrity number (RIN) ranging between 6.1 and 9.2 were sent to Génome Québec Innovation Centre (Génome Québec, Montreal, QB, Canada) for library preparation and next-generation sequencing (RNA-Seq). Briefly, libraries were prepared from 250 ng of total RNA per sample using NEBNext Ultra Directional kit with poly(A) magnetic isolation module (New England Biolabs Ltd, ON, Canada), double-stranded DNA was synthesized, and libraries were quantified using a KAPA Library Quantification kit with Revised Primers-SYBR Fast Universal kit (Kapa Biosystems) (Alcaraz et al. 2021). Paired-end libraries (100x2) were sequenced in a NovaSeq 6000 S4 lane (Illumina, CA, USA) at ~25 million reads per sample, for a total of ~875 million reads.

2.7.2 – Assembly and annotation of reference transcriptome, alignment of reads

The quality of reads was assessed using FastQC (version 0.72+galaxy1) (Andrews n.d.). The sequences were then trimmed to a minimum Phred score of 30 and a minimum length of 35 bases per paired-end using Trimmomatic (version 0.38.1) (Bolger et al. 2014). Quality assessment and trimming were done in the Galaxy Europe platform (Jalili et al. 2020).

Because the genome of *A. bahia* had not been sequenced previously, a transcriptome was assembled *de novo* from all the reads in this study. *De novo* transcriptome assembly was conducted by taking the above trimmed datasets and assembled using Trinity, set to all default parameters, which resulted in greater than 1 million contigs. The assembly was then clustered at 95% similarity, which resulted in >500k clusters. This set of contigs was then further filtered to a minimum of 300 nucleotides (310,860 contigs), then translated to amino acid sequences using the longest open reading frame (ORF) and subsequently filtered to only include proteins that had at least 100 amino acids. This resulted in 34,904 PROTEIN sequences.

This assembly was then annotated using the functional analysis module of OmicsBox v2.0.36 (BioBam Bioinformatics, 2019) using blastp (fast mode) in cloudblast under the non-redundant protein BLAST database (nr v.5), with all arthropods (taxonid 6656) as the taxon limit, with an Expectation value (e-value) of 1.0E-3, with word size set to 6, and with the highest scoring pair (HSP) length cut off at 33. All other settings were set to default.

The annotated contig (protein) IDs were then used to filter and extract nucleotide sequences from the *de novo* assembled transcriptome, which was subsequently used as reference for downstream analysis. The pseudo-alignment rates were tested using the Kallisto-quant tool (version 0.46.2+galaxy0; Bray et al. 2016) and ranged between 68.3 - 72.3%. The pseudo-

alignment rates for all replicates and samples that were used in the assembly and annotation are reported in Appendix A.

2.7.3 – Differential expression analysis

Differential expression of nucleotide sequences, or contigs, relative to the control were estimated in OmicsBox v2.0.36 (BioBam Bioinformatics, 2019) using edgeR v.3.28.0 (Robinson et al. 2010). A counts-per-million (CPM) filter was employed to filter out sequences with less than 5 CPM in at least 4 of the 5 replicates per concentration in each weathering treatment group. Trimmed Mean of M values (TMM) was used for the normalization of library sizes. A simple design was selected, which made a pairwise comparison between a single concentration condition and the control, repeated for all experimental concentrations in each of the two weathering treatment groups. An exact statistical test was used, which is based on quantile-adjusted conditional maximum likelihood (qCML) methods, and the test was robust, meaning estimation of differential expression was strengthened against potential outliers. The significance of differentially expressed contigs was scored with a cutoff false discovery rate (FDR; Benjamini and Hochberg, 1995) ≤ 0.05 and a minimum effect size threshold of the absolute value of log2 fold-change ($|\log2FC|$) ≥ 1. Venn diagrams that explored the intersections of differentially expressed contigs were constructed using InteractiVenn (Heberle et al. 2015).

2.7.4 – Pathway enrichment analysis

Pathway enrichment analysis of differentially expressed contigs was conducted separately for each concentration in each weathering treatment group in OmicsBox v2.0.36 (BioBam Bioinformatics, 2019). Each analysis was conducted by comparing a test set of contigs with respect to a reference set. For all analyses, the reference set was the functionally annotated *de novo* assembled transcriptome, described in section *2.7.2*. Separate analyses were run against

this reference set for both the up- versus down-regulated contigs that were differentially expressed at a FDR ≤ 0.05 for each of the 3 tested concentrations in each of the 2 weathering treatment groups, resulting in 12 separate analyses and therefore 12 different test sets. Fisher's Exact Test was used for each enrichment analysis, which finds GO terms that are over-represented in the test set with respect to the reference set. The GO term annotations used for enrichment were GO Molecular Functions (MF), Biological Processes (BP), and Cellular Components (CC). When the proportion of contigs annotated with a GO term in the test set was significantly higher than the proportion in the reference set, as determined by Fisher's Exact Test, the GO term was overrepresented, and the pathway was considered enriched.

3.0 – Results

3.1 – Leachate chemistry

3.1.1 – Organics

The organic chemical profiles for the 18 TWP leachates used in organic chemical analysis, 14 of which were studied in Roberts (2021) and four that were generated and analyzed in the same way (Sofield et al., unpublished), were organized by hierarchical clustering and the leachates clustered into four groups, with a clear separation by weathering treatment group (Figure 2). Cluster group #1 contained six of the nine un-weathered leachates, cluster group #2 contained all nine weathered leachates, cluster group #3 contained only the UltraPure water blank, and cluster group #4 contained the remaining three un-weathered leachates (Figure 2). The 2017 un-weathered leachate used in my study was within cluster group #1, while the 2017 weathered leachate was within cluster group #2 (Figure 2). Vertical comparison of the organic chemical profiles between cluster group #1 and cluster group #2 shows that some chemicals are

uniquely present in the un-weathered leachates that are not present in the weathered leachates and vice versa.

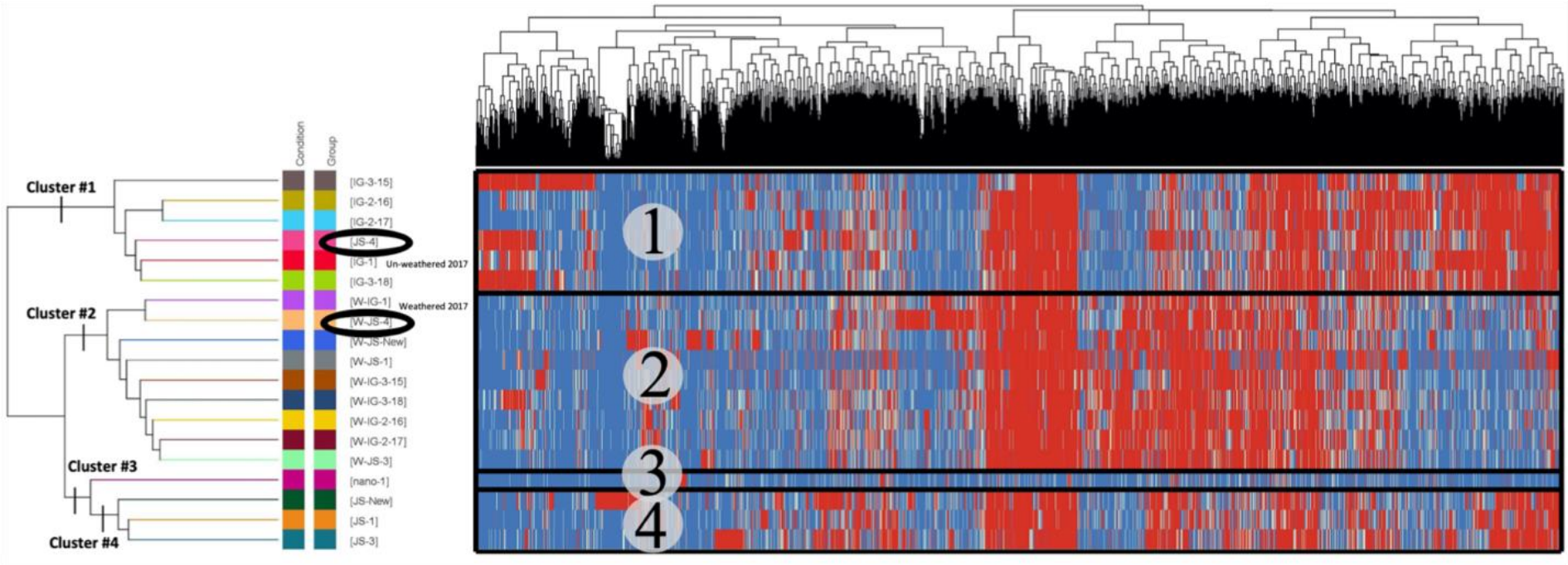

Figure 2. Hierarchical clustering (using Euclidean distances) of organic chemical features found in eighteen TWP leachates, all studied previously in Roberts (2021), analyzed via LC-QTOF-MS. Each row, marked by a different color, represents a different TWP leachate; the two circled leachates represent the 2017 un-weathered and 2017 weathered leachates that were investigated in my study. Each row represents the average of 3 replicate samples per leachate. In each row, the vertical lines (i.e. red or blue) represent a single chemical feature, all hierarchically clustered and denoted by the black dendrogram at the top of the figure. Blue indicates the absence of a chemical, while red indicates the presence of a chemical; darker red means that more of that chemical is present. The leachates cluster into 4 distinct groups based on their organic chemical profiles and are labeled on the far left dendrogram and on the chemical features themselves. Black boxes separating the 4 leachate cluster groups have been added for ease of visualization.

3.1.2 – Metals

The metal profiles for the 14 TWP leachates studied in Roberts (2021) were organized by hierarchical clustering and the leachates clustered into two groups. There were detectable amounts of Al, Co, Cu, Mn, Ni, and Zn in both leachate types, as well as a detectable level of Sb in the un-weathered leachate. At the highest concentration of each leachate type used in the current study, some of the detectable metals exceeded the Criterion Minimum Concentration (CMC) Water Quality Criteria for marine acute exposure and the Criterion Continuous Concentration (CCC) Water Quality Criteria for marine chronic exposure according to the EPA Water Quality Criteria (USEPA 2016b). In both the weathered and un-weathered treatment groups, both Cu and Zn exceeded the CMC and the CCC, while Ni exceeded only the CCC (Table 2). After 14 TWP leachate samples were organized via hierarchical clustering, cluster group #1 contained five of the un-weathered samples and cluster group #2 included all seven of the weathered leachate samples and two of the un-weathered samples. The “2017 un-weathered" and the “2017 weathered” leachates used in my study clustered into different groups (Figure 3); the 2017 un-weathered sample clustered with four other un-weathered samples, while the 2017 weathered sample clustered with six other weathered samples and two un-weathered samples.

Table 2. Concentrations of 10 different metals (in µg/L) for both the weathered and un-weathered leachates at their respective highest tested concentrations. Detection limits for the Agilent 7500ce ICP-MS are presented in µg/L, along with EPA Water Quality Criteria, including both the marine Criterion Minimum Concentration (CMC) for acute exposure and the marine Criterion Continuous Concentration (CCC) for chronic exposure.

Treatment	Concentration (g/L)	Al	Cr	Mn	Co	Ni	Cu	Zn	Cd	Sb	Pb
Weathered 2017	2.68	19.00	ND	0.49	0.42	43.95	26.75	307.65	ND	ND	ND
Un-weathered 2017	1.08	14.60	ND	0.25	0.35	26.83	11.64	402.80	ND	0.261	ND
Detection Limits		1.60	0.14	0.03	0.004	0.60	0.11	0.78	0.02	0.01	0.05
EPA Aquatic Life Criteria	CMC (acute)	NA	1100.00	NA	NA	74.00	4.80	90.00	33.00	NA	210.00
	CCC (chronic)	NA	50.00	NA	NA	8.20	3.10	81.00	7.90	NA	8.10

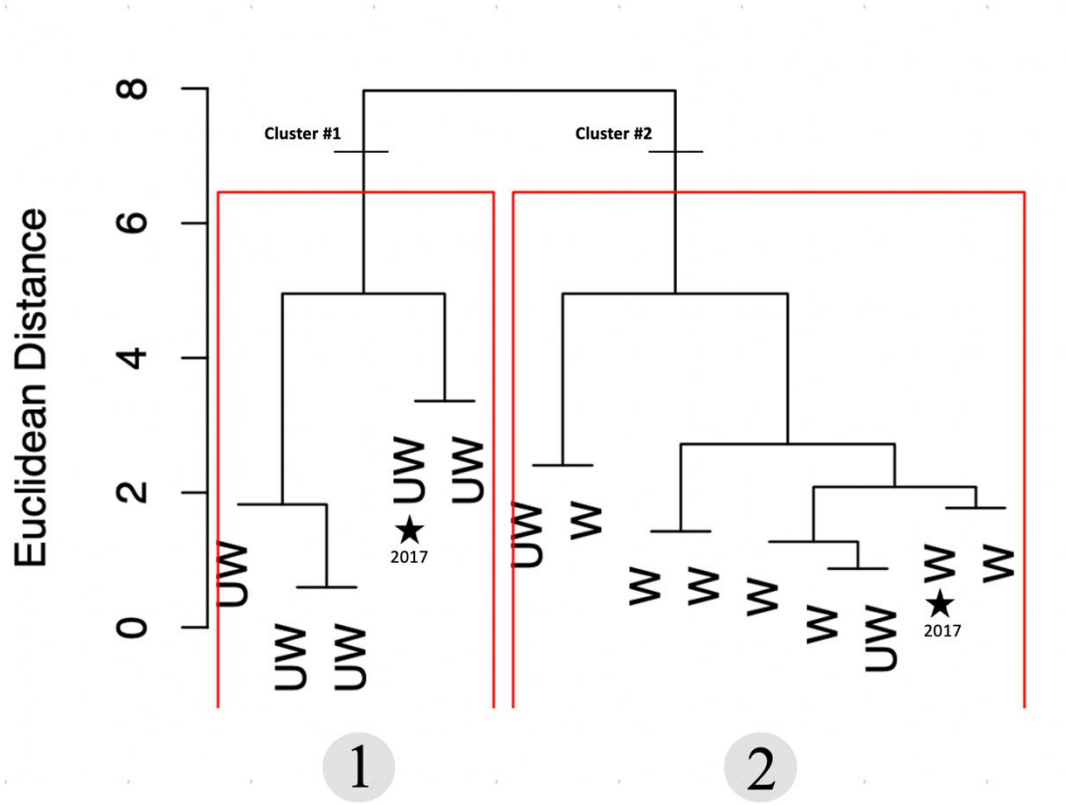

Figure 3. Hierarchical clustering (using Euclidean distances) of six metal features found in 14 TWP leachates, all studied previously in Roberts (2021), analyzed via ICP-MS. All metals in Table 2 were included in the cluster analysis except for Cr, Cd, Sb, and Pb; for those metals, less than 15% of the TWP leachate samples had detectable concentrations of metals, so were excluded from the multivariate analysis. The two starred leachates represent the 2017 un-weathered (UW) and the 2017 weathered (W) leachates that were investigated in my study. The leachates cluster into two distinct groups based on their metal profiles, and the cluster groups are marked by the red boxes, the numbered labels, and the cluster labels at the top of the dendrogram

3.2 – Respiration rates

Percent changes in respiration rates ($\Delta R_x\%$) of leachate-exposed shrimp compared to control shrimp were calculated for each concentration, day of exposure, and leachate type (Figure 4). Positive values for percent change in respiration indicate an inhibition in respiration rate relative to control animals, while negative values indicate a stimulation of respiration rate relative to control animals (Figure 4). For each leachate treatment and day of exposure, the mean individual respiration rates and the mean percent change in respiration rates, calculated across the three replicates at each exposure concentration, are reported in Appendix C.

After two days of exposure to the weathered leachate, significant stimulation in *A. bahia* respiration rates occurred at 0.67 and 2.68 g/L, with stimulation also observed at 1.34 g/L that was insignificant (Figure 4, Appendix C). After two days of exposure to the un-weathered leachate, there were no significant differences in any treatment concentration. After four and six days, there were no significant differences in any concentration in the weathered group, but there was a significant stimulation in respiration rate at 1.08 g/L in the un-weathered group (Figure 4, Appendix C).

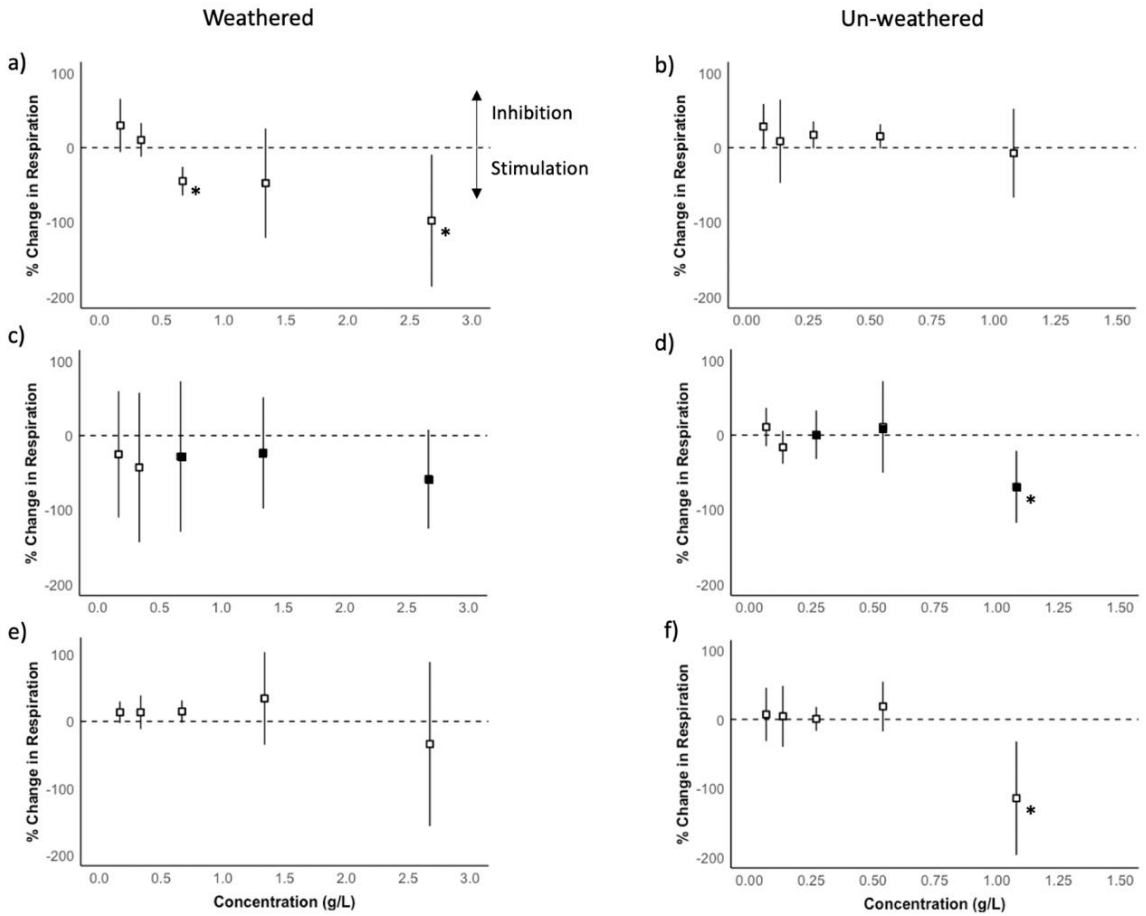

Figure 4. Mean percent change in respiration rate relative to the controls, across three replicates per concentration, for 2 days (*a,b*), 4 days (*c,d*), and 6 days (*e,f*) of exposure to leachate at concentrations ranging from 0.07 to 2.68 g/L (Table 1). Positive values indicate inhibition of respiration rate relative to the controls. Negative values indicate stimulation of respiration rate relative to the controls. The dashed line at y = 0 represents the $\Delta R_{Cx}(\%)$ as calculated in Equation 2. Error bars represent the 95% confidence interval; asterisks represent significant differences in respiration rate from the controls based on a lack of overlap with the $\Delta R_{Cx}(\%)$; and the solid squares at day 4 represent the three concentrations that were used for transcriptomic analysis (Table 1).

3.3 – Transcriptomic responses

Differentially expressed contigs (FDR ≤ 0.05; |log2FC| ≥ 1) compared to the control group, also referred to as "dysregulated contigs", in *A. bahia* were explored between the three concentrations used in the transcriptomic analyses and within each weathering treatment group (Table 1). This was followed by comparison between weathered and un-weathered leachates without consideration of the leachate concentrations.

Without consideration of specific leachate concentrations, there were a total of 80 differentially expressed contigs in the weathered group, 64 of which (80%) had orthologous gene descriptions in arthropods and were able to be annotated. There were 139 differentially expressed contigs in the un-weathered group, 112 of which (81%) had orthologous gene descriptions in arthropods and were able to be annotated (Appendix D). When leachate concentrations were considered, there were 86 dysregulations in the weathered group (with five contigs shared in common between multiple concentrations) and 152 dysregulations in the un-weathered group (with 12 contigs shared in common between multiple concentrations).

3.3.1 – Weathered leachate exposure

There were 86 differentially expressed contigs in the weathered leachate exposure. The 0.67 g/L concentration had a total of 14 dysregulated contigs with 12 unique contigs; the 1.34 g/L concentration had a total of five dysregulated contigs with only one unique contig; and the 2.68 g/L concentration had a total of 67 contigs with 62 unique contigs (Figure 5a). Of the 14 dysregulated contigs in the 0.67 g/L concentration, one contig was shared with only the 2.68 g/L concentration, and one contig was shared with both the 1.34 g/L and 2.68 g/L concentrations (Figure 5a, Appendix D). Of the five dysregulated contigs in the 1.34 g/L group, in addition to

the contig shared with the other two concentrations, there were three contigs shared only with the 2.68 g/L concentration (Figure 5a, Appendix D). No contigs were shared between the 0.67 g/L and 1.34 g/L concentrations (Figure 5a).

Of the 14 dysregulated contigs in the 0.67 g/L concentration, four were upregulated (log2FC > 1) relative to the control (only one of which had a gene description) and ten were downregulated (log2FC < 1) relative to the control (nine of which had a gene description) (Figure 6a, Appendix D). Of the five dysregulated contigs in the 1.34 g/L concentration, four were upregulated relative to the control (three of which had a gene description) and one was downregulated relative to the control, although it had no gene description (Figure 6a, Appendix D). Of the 67 dysregulated contigs in the 2.68 g/L concentration, 56 were upregulated relative to the control (48 of which had gene descriptions) and 11 were downregulated relative to the control (six of which had gene descriptions) (Figure 6a, Appendix D).

Only the 56 upregulated contig sequences in the 2.68 g/L concentration showed significant Gene Ontology (GO) enrichment compared to the functionally annotated *de novo* reference transcriptome; since only 48 of those contig sequences had annotated gene descriptions, only 85.7% of the dysregulated contigs at this concentration contributed toward significant GO-term enrichment and could be functionally inferred. Overrepresented GO terms, indicating enriched pathways, in the 2.68 g/L concentration included four molecular functions and one cellular component (Figure 6a).

3.3.2 – Un-weathered leachate exposure

There were 152 differentially expressed contig sequences in the un-weathered leachate exposure. The 0.27 g/L concentration had a total of four dysregulated contigs with two unique contigs; the 0.54 g/L concentration had a total of 15 dysregulated contigs with four unique

contigs; and the 1.08 g/L concentration had a total of 133 contigs with 121 unique contigs (Figure 5b). Of the four dysregulated contigs in the 0.27 g/L concentration, one contig was shared with only the 1.08 g/L concentration, and one contig was shared with both the 0.54 g/L and 1.08 g/L concentrations (Figure 5b, Appendix D). Of the 15 dysregulated contigs in the 0.54 g/L group, in addition to the contig shared with the other two concentrations, there were ten contigs shared only with the 1.08 g/L concentration (Figure 5b, Appendix D). No contigs were shared between the 0.27 g/L and 0.54 g/L concentrations (Figure 5b).

Of the four dysregulated contigs in the 0.27 g/L concentration, three were upregulated (log2FC > 1) relative to the control (two of which had a gene description) and one was downregulated (log2FC < 1) relative to the control, and it had a gene description (Figure 6b, Appendix D). Of the 15 dysregulated contigs in the 0.54 g/L concentration, 12 were upregulated relative to the control (nine of which had a gene description) and three were downregulated relative to the control (two of which had a gene description) (Figure 6b, Appendix D). Of the 133 dysregulated contigs in the 1.08 g/L concentration, 107 were upregulated relative to the control (87 of which had gene descriptions) and 26 were downregulated relative to the control (22 of which had gene descriptions) (Figure 6b, Appendix D).

Only the 107 upregulated contig sequences in the 1.08 g/L concentration showed significant Gene Ontology (GO) enrichment compared to the functionally annotated *de novo* reference transcriptome; since only 87 of those contig sequences had annotated gene descriptions, only 81.3% of the dysregulated contigs at this concentration contributed toward significant GO-term enrichment and could be functionally inferred. Overrepresented GO terms, indicating enriched pathways, in the 1.08 g/L concentration included eight molecular functions and two biological processes (Figure 6b)

3.3.3 – Between treatments – both weathered and un-weathered leachate exposures

The intersection between the contig sequences that were dysregulated in each leachate type was explored (Figure 7). The weathered leachate group had a total of 80 dysregulated contigs while the un-weathered leachate group had a total of 139 dysregulated contigs, 73.75% more than the weathered group. The weathered group had 23 unique contigs, the un-weathered group had 82 unique contigs, and there were 57 contigs shared between the treatment groups. Contig IDs, the type of dysregulation (up- or down-regulation), and orthologous gene descriptions for each of the contigs, as well as which treatment group they are part of are listed for Figure 7 in Appendix E. The weathered and un-weathered treatments shared three significantly enriched GO pathways (all GO molecular functions), all from upregulated contigs, at the highest leachate concentrations (2.68 g/L for the weathered leachate and 1.08 g/L for the un-weathered leachate): serine hydrolase activity, serine-type peptidase activity, and peptidase activity (Figure 6).

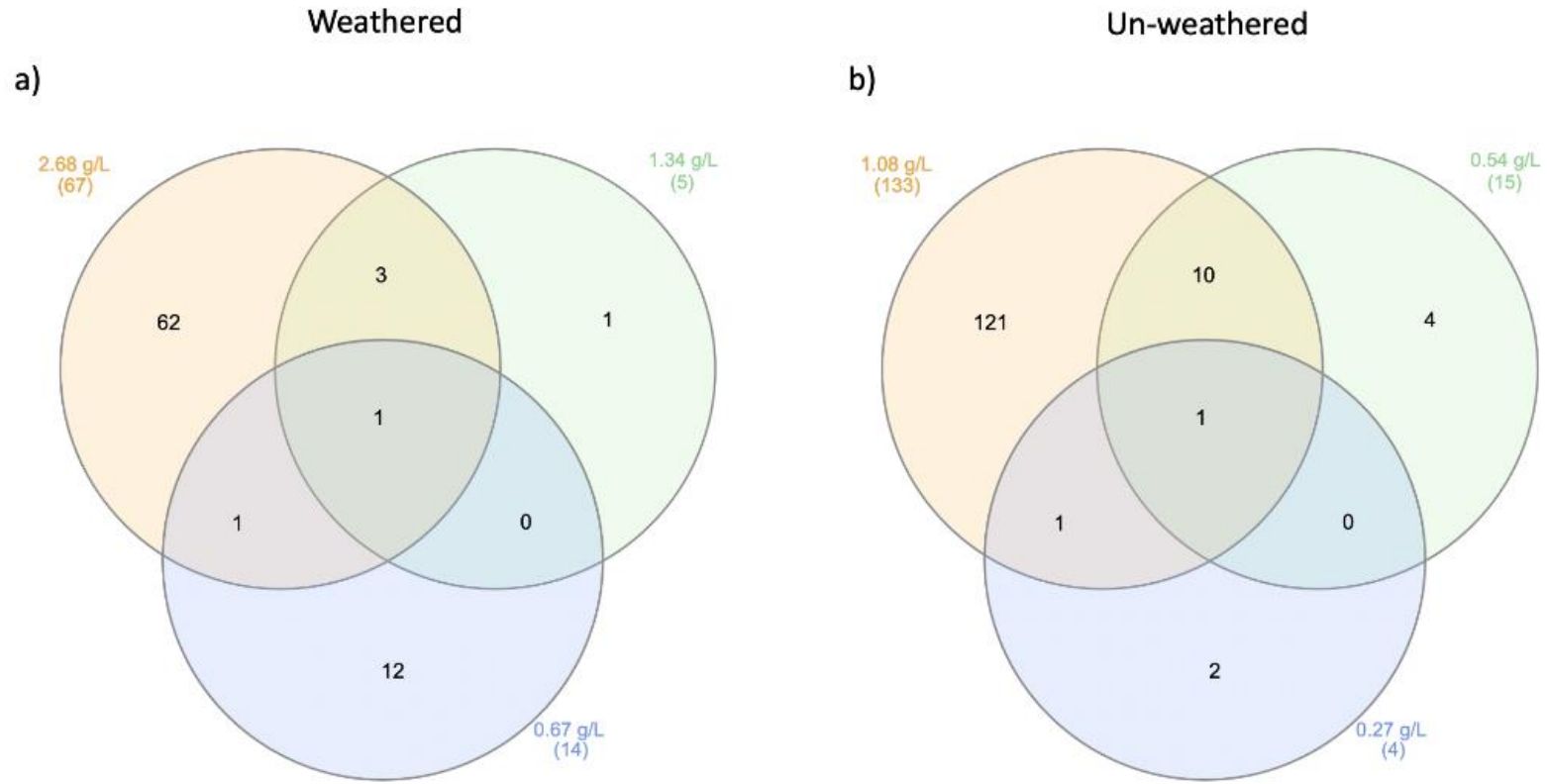

Figure 5. Venn diagrams of dysregulated contig sequences (FDR ≤ 0.05; |log2FC| ≥ 1) in *Americamysis bahia* exposed for four days in the three tested concentrations used in transcriptomic analyses (Table 1) in *a)* the weathered group and *b)* the un-weathered group. There were 86 unique dysregulated contigs in the weathered group and 152 unique dysregulated contigs in the un-weathered group. All dysregulated contig IDs, along with which concentration they were dysregulated in, whether they were up- or down- regulated, their level of expression, their counts, and the gene descriptions for orthologous genes in arthropods are listed in Appendix D.

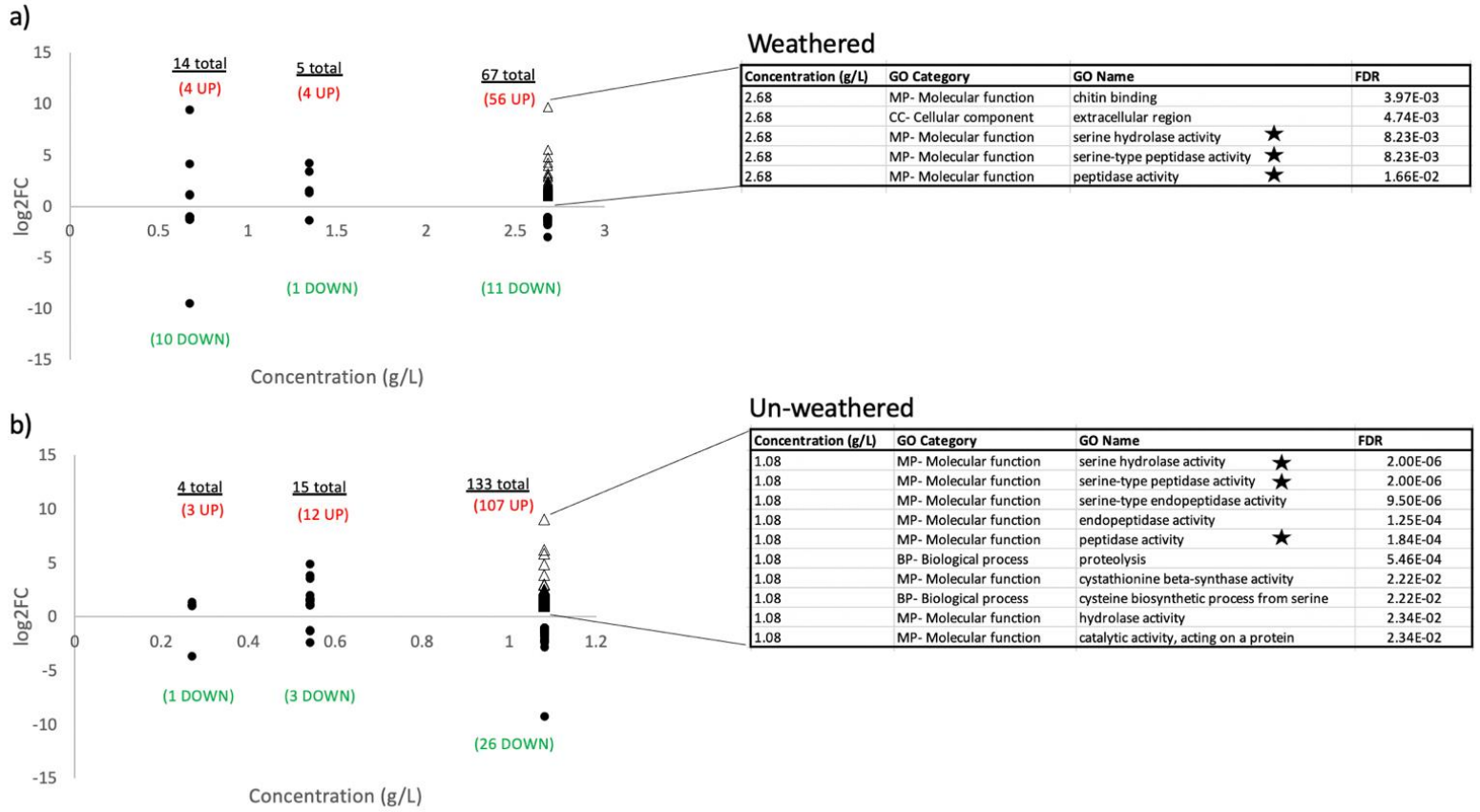

Weathered

Concentration (g/L)	GO Category	GO Name	FDR
2.68	MP- Molecular function	chitin binding	3.97E-03
2.68	CC- Cellular component	extracellular region	4.74E-03
2.68	MP- Molecular function	serine hydrolase activity ★	8.23E-03
2.68	MP- Molecular function	serine-type peptidase activity ★	8.23E-03
2.68	MP- Molecular function	peptidase activity ★	1.66E-02

Un-weathered

Concentration (g/L)	GO Category	GO Name	FDR
1.08	MP- Molecular function	serine hydrolase activity ★	2.00E-06
1.08	MP- Molecular function	serine-type peptidase activity ★	2.00E-06
1.08	MP- Molecular function	serine-type endopeptidase activity	9.50E-06
1.08	MP- Molecular function	endopeptidase activity	1.25E-04
1.08	MP- Molecular function	peptidase activity ★	1.84E-04
1.08	BP- Biological process	proteolysis	5.46E-04
1.08	MP- Molecular function	cystathionine beta-synthase activity	2.22E-02
1.08	BP- Biological process	cysteine biosynthetic process from serine	2.22E-02
1.08	MP- Molecular function	hydrolase activity	2.34E-02
1.08	MP- Molecular function	catalytic activity, acting on a protein	2.34E-02

Figure 6. Concentration-response portraying the level of expression of dysregulated contig sequences (FDR ≤ 0.05; |log2FC| ≥ 1) as a function of increasing concentration for *a)* the weathered group and *b)* the un-weathered group, along with a list of significantly overrepresented Gene Ontology (GO) terms (in decreasing order of significance) for each weathering treatment group. Total numbers of dysregulated contig sequences for each concentration are listed in black, the number of upregulated contigs are listed in red, and the number of downregulated contigs are listed in green. The open black triangles represent the only dysregulated contigs in which significant pathway enrichment was found. Gene Ontology (GO) terms are divided into Molecular Functions (MF), Biological Processes (BP), and Cellular Components (CC), and the black stars on the GO tables indicate shared enriched pathways between weathered and un-weathered leachate treatment.

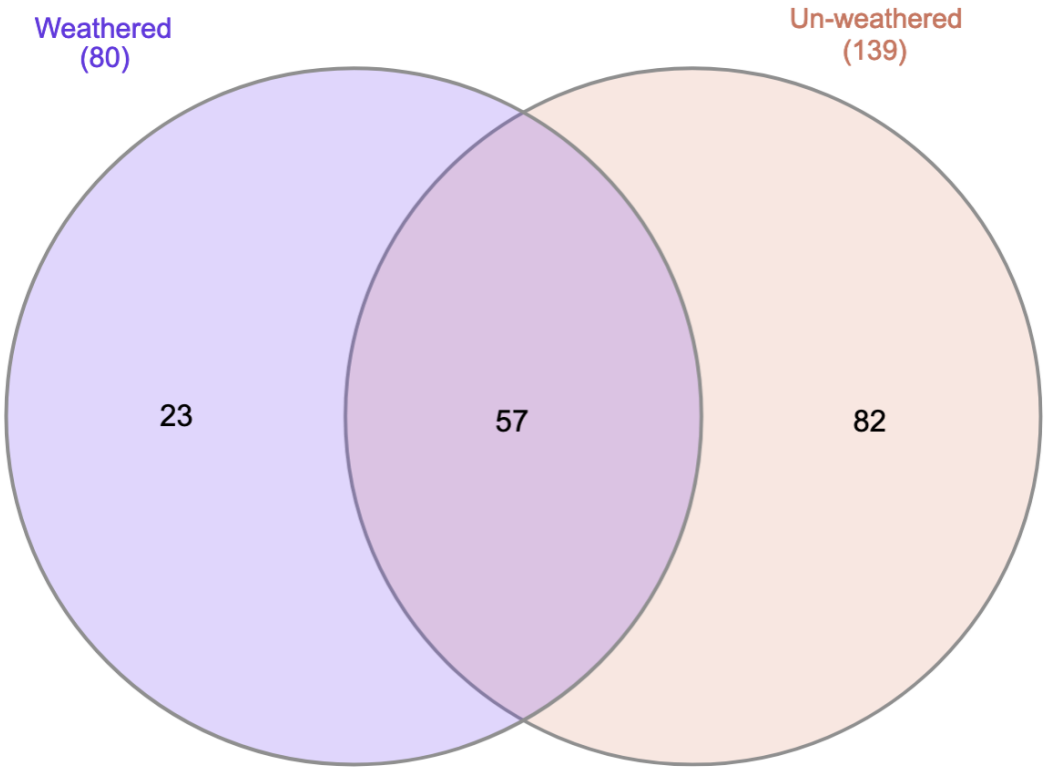

Figure 7. Venn diagram of dysregulated contig sequences (FDR ≤ 0.05; |log2FC| ≥ 1) in *Americamysis bahia* between weathered leachate and un-weathered leachate four-day exposures. The numbers included in this diagram are the unique contigs for all concentrations in that weathering treatment group (Figure 5). Contig IDs, type of dysregulation (up- or down-regulation), and orthologous gene descriptions are shown for this diagram in Appendix E.

4.0 – Discussion

In this study, the sublethal and molecular responses of *A. bahia* caused by exposure to two different TWP leachates were explored through sublethal acute toxicity tests (i.e. measuring respiration rate as the endpoint) and the analysis of overarching transcriptomic responses (i.e. differential expression and pathway enrichment analyses). The focus of my work was to see whether there were observable sublethal and/or molecular effects to *A. bahia* exposed to TWP leachates compared to the control shrimp, and to see whether there was a difference in these potential effects in treatment shrimp exposed to the weathered TWP leachate versus the un-weathered TWP leachate. To explore the potential drivers of TWP leachate toxicity, both metal and organic chemical compounds found in each of the TWP leachates were considered along with the observed sublethal and molecular effects to *A. bahia*.

4.1 – Sublethal responses – respiration rates of *A. bahia*

One sublethal response was measured in my study: the respiration rate of *A. bahia*. The hypotheses that there would be changes in respiration rate compared to the control shrimp and that there would be differences in respiration rate between the weathered versus un-weathered TWP leachates were both supported.

4.1.1 – Stimulation in respiration rate

According to Garnacho et al. (2001), the baseline respiration rates of mysid shrimp are dependent on a variety of factors, including variations in mysid weight, age, and reproductive status, and/or variations in environmental conditions such as season, salinity, or temperature. In my study, all these factors were either controlled for (i.e. age, reproductive status, season, temperature, and salinity) or randomized (i.e., mysid weight). Depending on the concentration and the length of exposure, after exposure to both the weathered and un-weathered TWP

leachates, *A. bahia* exhibited stimulation of respiration rate (Figure 4). This observed stimulation of *A. bahia* respiration rate relative to the controls is consistent with a respiratory uncoupler of phosphorylation, an acetylcholinesterase inhibitor, or potentially a respiratory irritant (McKim et al. 1987). Because the TWP leachates that *A. bahia* were exposed to in my study are composed of a complex mixture of chemicals, including hundreds of organic chemicals (Figure 2), it is difficult to ascertain which of those chemicals or chemical groups may have been responsible. However, the observed stimulation in respiration rate is consistent with past studies on the respiration rates of *A. bahia* after entire life-cycle exposures to organic pesticides. McKenney (2018) detailed the results of many of his previous studies measuring *A. bahia* respiration rates after exposure to a variety of pesticides: endrin, an organochlorine (McKenney 1982); thiobencarb, a carbamate (McKenney 1985); fenthion, an organophosphate insecticide (McKenney and Matthews 1990); and DEF, an organophosphate herbicide (McKenney et al. 1991). In all these separate studies, exposure to organic pesticides resulted in elevated respiration rates that were observable early in the exposure period for juvenile mysids (McKenney 2018). In younger juveniles, respiration rate increased linearly with increasing pesticide concentration, while in older juveniles and adults, the relationship between pesticide concentration and respiration displayed a curvilinear dose-response relationship (McKenney 2018), indicating that *A. bahia* can exhibit differences in respiration response depending on their age and time of exposure to organic pesticides. In a study exposing another species of mysid shrimp, *Neomysis integer*, to water soluble fractions of light fuel oil at various temperatures, the authors found that the respiration rates of the shrimp were temperature dependent; the authors modeled respiration rate as a function of temperature and oil concentration and found that above 10°C, the mysids generally increased their respiration rate with increasing oil concentration, although the trend

was subtle (Laughlin and Linden 1983). In contrast to the stimulation in mysid respiration rate reported in these previous studies, Capuzzo et al. (1984) exposed juvenile lobster, *Homarus americanus*, to Southern Louisiana Crude Oil and found that stage 1 larvae exposed for 24 hours and all stages of larvae exposed for 72 hours showed significant reductions in respiration rate compared to the controls. After analysis of the exposed animals via GC-MS, the authors found trace amounts of benzene, thiophene, toluene, alkylcyclohexane, and alkylbenzenes in the lobster tissue (Capuzzo et al. 1984). The results of these studies suggest that different organic chemicals can lead to different effects to crustacean respiration rates; this difference in response is likely reflective of these different organic chemicals having different mechanisms of action.

To my knowledge, there has been no work done on the effects of metals exposure on the respiration rates of *A. bahia* specifically. However, there are many studies that look at respiration rates of crustaceans in general; crustaceans generally exhibit a reduction in respiration rate after exposure to metals (Spicer and Weber 1991). This could be due to metal-induced pathological damage and interference with respiratory processes that can include a decrease in ventilation, impeded gas exchange at respiratory surfaces, disrupted perfusion, impaired respiratory gas transport to or from the tissues, or the direct inhibition of cellular respiration (Spicer and Weber 1971). The respiration rate of a variety of crustacean species have been tested, and in almost every case, there was a significant decrease in respiration rate compared to control animals reported by the authors. An exception was in one study where no significant change in the respiration rate of *Cancer pagurus* was found over the exposure period to Cu and Zn, and any respiratory impairment that was temporarily observed was due to an increase in the diffusion barrier thickness at the crab's respiratory surfaces and was reversible even during continued metal exposure (Spicer and Weber 1992). In another study, exposure to Cu decreased the

respiration rate of *Artemia* larvae by approximately 25% without significantly affecting motility (Corner and Sparrow 1956). The oxygen consumption rates of both adult and larval *Uca pugilator* were depressed after acute exposure to mercury (Vernberg and Vernberg 1971, DeCoursey and Vernberg 1972, Vernberg et al. 1973). Depledge (1984) found that after exposure to either 10 mg/L Cu ions or 1 mg/L mercury ions, the respiration rate of *Carcinus maenas* (L.) decreased relative to control animals, with the 10 mg/L Cu treatment suppressing crab respiration within 2 hours. Exposure of *Farfantepenaeus paulensis* to both 10 mg/L Zn and 2 mg/L cadmium inhibited the shrimps' oxygen consumption by 25% and 32.4% respectively, relative to control shrimp (Barbieri 2009). In another study by the same author, the oxygen consumption in cadmium-exposed *F. paulensis* was measured across different salinities; at a salinity of 5, the highest cadmium concentration used (2 mg/L) decreased oxygen consumption by 53.7% (Barbieri and Paes 2011). *Cambaroides dauricus* experienced respiratory inhibition after both 96-hr acute and 7 and 14-day sub-chronic exposures to Cu; for the acute exposure, the respiration rate decreased by 48.4% at 16.48 g/L Cu (50% of the 96-hr LC50), while for the sub-chronic exposures, the respiration rate decreased by 39.6% after 7 days and 52.4% after 14 days at 2.06 mg/L Cu (Bao et al. 2020). Spicer and Weber (1991) compiled the results of many of these studies, and they suggested that water-borne Cu and Zn disrupt gill function in crustaceans which results in a decrease in respiration rate leading to the development of internal hypoxia, although reparation can be accomplished at high sub-lethal concentrations.

Comparing the observed stimulation of *A. bahia* respiration rate after TWP leachate exposure in my study to the respiration responses of crustaceans exposed to both organic chemicals and metals (both components of TWP leachate) in these previous studies, it can be hypothesized that the largest contributor to the observed sublethal toxicity in both the weathered

and un-weathered TWP leachate exposures is the organic chemicals rather than the metals present in the leachate because stimulation was observed in every case (Figure 4). This is not to say that the metals in the leachate have no contribution to the observed toxicity in *A. bahia*, just that they do not likely contribute to the measured sublethal response of changes in respiration rate. In Roberts (2021), the author compared metal concentrations across weathered and un-weathered TWP leachates with the corresponding calculated LC50 values for the leachates. He found that Zn was a probable driver of inorganic TWP leachate toxicity that could lead to *A. bahia* mortality. The Cu and Ni concentrations in the leachates were inversely correlated with toxicity; as toxicity increased, the Cu and Ni concentrations decreased, indicating that those metals did not contribute to the observed toxicity. However, as the toxicity increased, the Zn concentrations stayed relatively constant, implying that Zn could be a contributor to the inorganic TWP leachate toxicity to *A. bahia*.

4.1.2 – Respiration response between weathered and un-weathered TWP leachate exposures

In addition to the significant stimulation in respiration rate compared to control animals for both leachate types, there were also differences in the patterns of respiration response in shrimp depending on whether they were exposed to weathered or un-weathered TWP leachate. In shrimp exposed to the weathered TWP leachate, the only significant effect was observed on the second day of exposure at the highest (2.68 g/L) and third highest (0.67 g/L) concentrations, after which point the respiration rate of the exposed shrimp was not significantly different from the control shrimp at the 95% confidence interval (Figure 4). In contrast, the shrimp exposed to the un-weathered TWP leachate only exhibited significant stimulation at the highest concentration (1.08 g/L) later in the exposure period (i.e., both on the fourth and sixth days), while the shrimp exhibited no significantly different effect compared to the controls early in the exposure period

(i.e., on the second day of exposure) (Figure 4). This supports that there are different mechanisms of action for toxicity for the weathered versus un-weathered TWP leachates. In Roberts (2021), the author found that the weathered and un-weathered TWP leachates were classified into different toxicity categories based on their LC50 values (5.19 g/L for the 2017 weathered leachate and 1.97 g/L for the 2017 un-weathered leachate).

According to the organic chemical analysis of the leachates, the weathered and the un-weathered TWP leachates have different organic chemical profiles, with some groups of organic chemicals only present in the weathered group and other groups of organic chemicals only present in the un-weathered group (Figure 2). In addition, the weathered and un-weathered leachates statistically clustered into separate groups based on the groups of organic chemicals present in each (Figure 2). Similarly, the weathered and un-weathered leachates used in my study statistically clustered into separate groups based on the metals present in each (Figure 3), even though in both leachates, concentrations of Cu and Zn exceeded both EPA Water Quality Criteria (CMC and CCC) and Ni concentrations exceeded the CCC (Table 2). Although the chemical profiles of the weathered versus un-weathered leachates are different both in organics and in metals (Figure 2, Figure 3), the differences between weathering treatment groups observed in their respiration response (Figure 4) is likely due to differences in organic chemicals, as the organics are likely the chemicals driving this sublethal respiration response, as discussed earlier.

Although specific metals were detected in the TWP leachates, individual organic chemical features were not able to be determined. Future chemical analyses on the leachates used in my study that further investigate the specific organic chemicals present in each one would help to infer which organic chemical or group of organic chemicals may be contributing to the

observed sublethal response of changes in respiration rate outlined in section 4.1.1. Halsband et al. (2020) tested both naturally weathered (from tire particles collected from an outdoor sports field) and un-weathered "crumb rubber granulate") leachates for both metals and organic compounds and found that the organic chemicals were different for the weathered versus un-weathered crumb rubber granulate leachates. The authors found that the weathered crumb rubber granulate leachates contained higher concentrations of phenanthrene, PAHs, and bisphenols, and phenols, while the un-weathered crumb rubber granulate leachates contained more phthalates, additives, phthalide, acetophenone, *n*-Cyclohexylformamide, and benzothiazole (Halsband et al. 2020). The differences in response of *A. bahia* between weathering treatment groups are further explored in my study at the molecular level of biological organization via the results of the differential expression and pathway enrichment analyses.

4.1.3 – Other potential sublethal responses

Only one sublethal response was measured in my study. Although an effect was observed for the sublethal endpoint of respiration rate, it is important to note that this is not the only possible sublethal response that *A. bahia* could have exhibited. Another recent study investigating the impacts of TWP leachates measured *A. bahia* growth and swimming behavior (i.e., freezing, movement, in-zone duration, frequency, meander, and turn angle) and found that in TWP leachate-exposed shrimp, growth was not significantly impacted, but all six swimming behaviors were significantly different from the control shrimp (Siddiqui et al. 2022). In future studies with *A. bahia* exposed to TWP leachate, measuring other types of sublethal responses will be important to get a more holistic picture of the range of responses that could occur in *A. bahia* in response to TWP leachate exposure. To inform what endpoints to assess in these future

studies, global transcriptomics was used to cast a broader net that could identify possible new or unknown biological functions in *A. bahia* that may be affected by the TWP leachates.

4.2 – Molecular responses – changes in differential expression and enriched pathways

The molecular responses of *A. bahia* after TWP leachate exposure were first explored within each weathering treatment group, followed by an exploration between weathering treatment groups. The hypotheses that there would be changes in the transcriptomic responses of leachate exposed shrimp compared to the control shrimp and that there would be differences in response between shrimp exposed to the weathered versus the un-weathered TWP leachate were both supported.

Within each of the leachate treatments, molecular responses were considered from multiple angles. First, the contigs that appeared in more than one concentration were explored (Table 3), as they are dysregulated at the lowest concentrations and are therefore likely the first processes to be impacted in *A. bahia* in response to TWP leachate exposure. Second, the levels of expression of contig sequences were investigated (Figure 6), along with contigs that had comparatively large levels of expression (Table 4) or had high counts (Table 5). The majority of dysregulated contigs had a 2-3 fold-change (FC) relative to the control (Appendix D), so contigs with a cutoff level of expression of $|FC| > 5$ were further investigated as potentially highly dysregulated (Table 4). In addition, contigs with a counts per million (CPM) > 100 were further investigated, as they had high counts compared to the majority of contig sequences (Table 5, Appendix D). Finally, the overrepresented Gene Ontology (GO) terms that appeared within each leachate treatment were investigated (Figure 6). GO terms are the result of grouping contig sequences based on their potential functionality; they are meant to reflect the most up-to-date view of the contig sequences' role in biology (Gene Ontology *b*, n.d.). The association of a

contig sequence with a GO term falls into three categories: Molecular Functions (MF), or the molecular activities of individual contig sequences; Cellular Components (CC), or where in the body the contigs are active; and Biological Processes (BP), or to which pathways and larger processes a specific contig sequence's activity contributes (Gene Ontology *b*, n.d.).

Between leachate weathering treatment groups, contigs that appeared in both treatments were explored further, along with the GO terms that were overrepresented in both the weathered and un-weathered leachate treatments.

4.2.1 – Weathered group

In the weathered leachate group, there were five upregulated contigs found in more than one weathered leachate concentration (Figure 5). Three of those five contigs were upregulated in both the highest (2.68 g/L) and middle (1.34 g/L) weathered leachate concentrations and were mapped to orthologous gene descriptions in arthropods: one contig sequence is associated with a lysosomal protective protein, one is associated with an uncharacterized protein (LOC119576313), and one is associated with a proton-coupled folate transporter (PCFT)-like gene object (Table 3). It is important to note that uncharacterized proteins do not currently have a known function, and they are marked with an LOC identifier number. The two of the five remaining contigs shared among the three weathered leachate concentrations did not have orthologous gene descriptions, so their functionality could not be meaningfully inferred from the *de novo* annotation (Table 3). However, one of those contigs was shared among all three concentrations (Figure 5, Table 3); it was upregulated with a 17.5 FC and 6 CPM at the lowest tested concentration (0.67 g/L) and is likely a sequence for a gene that is one of the first to be impacted in *A. bahia* after exposure to weathered TWP leachate. The other contig was highly upregulated with an 851 FC in the 2.68 g/L concentration and a 689 FC in the 0.67 g/L

concentration, but it was not dysregulated at all in the 1.34 g/L concentration (Table 3). This is a similar pattern to the day 2 % change in respiration results (Figure 4a), suggesting that this unknown contig sequence may contribute to early-juvenile respiratory processes in *A. bahia*. Future studies and an annotated *A. bahia* genome would be helpful to understand what processes this contig sequence may or may not contribute to. Even though there are very high fold changes in this contig sequence in shrimp exposed to weathered TWP leachate relative to control shrimp, there are only 2.66 CPM, meaning that this particular contig sequence has a large expression change but does not appear very often when considering all reads. In all ~250 million reads that this contig sequence was upregulated in within the weathered treatment group, this contig only appeared 665 times, indicating that it is a holistically lowly expressed contig sequence (Table 3).

All dysregulated contigs in the weathered treatment group were plotted as a function of concentration (Figure 6a). For all contigs that appear in more than one concentration in the weathered treatment, their FC levels of expression increased with increasing concentration (Table 3). It was expected that the lowest concentration would have the fewest and most lowly expressed contigs while the highest concentration would have the most numerous and the most highly expressed contigs, but this is not what was found. The lowest concentration (0.67 g/L) had 14 dysregulated contigs, whereas the middle concentration (1.34 g/L) had five dysregulated contigs and the highest concentration (2.68 g/L) had 67 dysregulated contigs (Figure 6a). There were some highly expressed dysregulated contigs at the 0.67 g/L concentration that did not follow the expected pattern (Figure 6a), one of which is the above-mentioned contig sequence with 689 FC, the positive value signifying upregulation. Another is a contig sequence with an FC of –721.96, signifying downregulation; this contig sequence was not mapped to an ortholog description, so its function is currently unknown, and it also had a low CPM of 2.70 (Table 4).

All contigs in the weathered treatment group with |FC| > 5 were considered as highly dysregulated (Table 4). Within these results, contigs that also had a CPM > 25 were considered, as this means that the contig is both highly expressed relative to the control and that it has a high enough count to imply that it may contribute to a biological process that is affected in *A. bahia.* Only one contig that has an |FC| > 5 as well as a CPM > 25 and is mapped to an orthologous gene description in arthropods was unique to the weathered treatment group. This contig was upregulated at the 2.68 g/L leachate concentration and is a proton-coupled folate transporter (PCFT)-like gene object (Table 4). The PCFT is a proton symporter and is the mechanism by which folates are transported across cell membranes (Zhao et al. 2017). Its upregulation indicates that the affected mysids are increasing their folate transport to counter the stress they are under from weathered TWP leachate exposure. In addition, contigs with CPM > 100, but a |FC| < 5, that were unique to the weathered leachate group at the 2.68 g/L leachate concentration included upregulation of an obstructor of the F2 gene, an uncharacterized protein (LOC119573628), and a fibrocystin-L-like gene (Table 5). Fibrocystin is a gene that has been shown to control cellular structure and adhesion, with its deficiency linked to deformities in epithelial structure (Ziegler et al. 2020). Its upregulation suggests that shrimp are attempting to maintain their cellular structure despite stress from the weathered TWP leachate.

The highest concentration of weathered leachate, 2.68 g/L, was the only concentration in the weathered leachate group that showed significant GO-term enrichment compared to the *de novo* annotated reference transcriptome, and all enrichment came from upregulated contig sequences. All of these upregulated contigs were grouped together by their potential function, and it was found that there were five significant GO-terms; three molecular functions and one cellular component (Figure 6a). The cellular component enrichment suggests that the molecular

functions occur in the extracellular regions (Figure 6a). Of the four molecular functions, only one was unique to the weathered group: chitin binding, and it was the most significantly overrepresented (Figure 6a). Chitin binding proteins are located in the cuticle, a protective barrier covering the outer surface of the shrimp's body and regions of the gastrointestinal tract, and in the peritrophic membrane, a vital physical barrier unique to invertebrates located in the gut (Yang et al. 2018, Xu et al. 2021). These protective barriers guard against physical injuries, chemical injuries, and pathogen infections (Yang et al. 2018, Xu et al. 2021). Xu et al. (2021) studied chitin binding proteins in shrimp (*Marsupenaeus japonicus*), and found that the proteins served as an opsonin, or pattern recognition receptor to achieve antibacterial immune response in the shrimp; the proteins were able to identify and tag foreign substances that allowed the shrimp's immune system to target harmful bacteria (Xu et al. 2021). Although in my study *A. bahia* were exposed to chemicals, the enrichment of upregulated contigs associated with chitin binding makes sense, as the route of chemical exposure from the leachate was through the seawater in which they lived. The mysids may have been able to recognize the chemicals in the leachate as foreign substances, and their bodies increased the production of chitin-binding proteins to thicken or enhance their protective barriers. These overrepresented GO terms that appear only in the weathered leachate group indicate that the chemical or group of chemicals that contribute to these observed transcriptomic responses in *A. bahia* are unique to the weathered TWP leachate, and are likely organic chemicals, as the organic chemical profiles between weathering treatment groups have clear differences (Figure 2), whereas most metals appear in both weathering treatment groups (Table 2).

4.2.2 – Un-weathered group

In the un-weathered leachate group, there were 12 upregulated contigs found in more than one un-weathered leachate concentration (Figure 5). Ten of those contigs had orthologous gene descriptions, and of those ten, three contig sequences were for uncharacterized proteins (Table 3). It is important to note that two of the contig sequences mapped to the same uncharacterized protein description with the same LOC identifier (Table 3). This is one of the downfalls of using an organism for which not much is known of the genome; since there is no annotated genome for *A. bahia*, we had to use contig sequences mapped to ortholog gene descriptions for all arthropods instead of specific gene IDs and descriptions for *A. bahia*. If I had been able to use gene IDs and descriptions for our specific organism, we would have been able to make much more informative conclusions about the effect of TWP leachate to *A. bahia* and what genes and processes were dysregulated. Mapping contig sequences to orthologous gene descriptions means that there is inherent uncertainty and duplication; two different contig sequences mapped to the same orthologous description means that they could potentially share the same function or be a part of the same gene. All results reported in my study and all inference of function from the contig sequences reported in the *de novo A. bahia* transcriptome assembly and annotation are generalized to all arthropods (taxonid 6656). The remaining seven contig sequences that had orthologous gene descriptions included the upregulation of a lysosomal protective protein in all three un-weathered leachate concentrations; an upregulation of a PCFT - like gene object, a pentraxin-related PTX3 - like protein, and a putative ankyrin repeat protein RF_0381 isoform X4 in the 1.08 g/L and 0.54 g/L leachate concentrations; an upregulation of a glycine N-methyltransferase in the 1.08 g/L and 0.27 g/L leachate concentrations; and a downregulation of a chitinase-3-like protein and a protein obstructor-E-like isoform X1 in the 1.08 g/L and the 0.54 g/L leachate concentrations (Figure 5, Table 3). The PTX3 protein is made

in many different types of cells in response to primary inflammatory signals (Mantovani et al. 2003); its upregulation suggests that the shrimp were responding to inflammation resulting from un-weathered TWP leachate exposure starting at a concentration of 0.54 g/L. The protein obstructor-E like isoform X1 had high counts, with a CPM of 1401.93, and is a chitin-binding protein associated with maintaining body shape by controlling the mechanical properties of the exoskeleton (Tajiri et al. 2017). Its downregulation starting at a concentration of 0.54 g/L indicates that the shrimp may start to experience physical deformation of their exoskeletons after exposure to un-weathered leachate.

For all contigs that appear in more than one concentration in the un-weathered treatment, their FC levels of expression increased with increasing concentration (Table 3). The un-weathered group showed a more expected pattern in how the level of expression changed with concentration; in general, the lowest concentration (0.27 g/L) had the fewest dysregulated contigs (four) and the lowest levels of expression, the middle concentration (0.54 g/L) had 15 dysregulated contigs and a larger level of expression, and the highest concentration (1.08 g/L) had the most numerous dysregulated contigs (133) and the largest levels of expression (Figure 6b). There were some highly expressed dysregulated contigs at the 1.08 g/L concentration that are notable (Figure 6b). First, there was a contig sequence with a 540.80 FC, signifying upregulation; this contig does not have a known function and has low counts at 2.66 CPM (Table 4). Second, there was a contig sequence with a –599.62 FC, signifying downregulation; this contig is associated with xylulose kinase and has a low CPM of 2.51 (Table 4). In humans, xylulose kinase is an enzyme that catalyzes the reaction that produces a key regulator of lipogenesis and carbohydrate metabolism, xylulose 5-phosphate (Bunker et al. 2013). The downregulation of xylulose kinase in *A. bahia* suggests that there is an imbalance in their

metabolic regulation after exposure to un-weathered TWP leachate at a concentration of 1.08 g/L.

All contigs in the un-weathered treatment group with |FC| > 5 were considered as highly dysregulated (Table 4). Within these results, contigs that also had a CPM > 25 were considered, as this means that the contig is both highly expressed relative to the control and that it has a high enough count to imply that it may contribute to a biological process that is affected in *A. bahia.* Only one contig that has a |FC| > 5 as well as a CPM > 25 and is mapped to an orthologous gene description in arthropods was unique to the un-weathered treatment group. This contig was upregulated at the 1.08 g/L leachate concentration and is mapped to a papilin isoform X4 gene (Table 4). Papilin is an extracellular matrix glycoprotein that has been found to inhibit a specific metalloproteinase; its presence influences cell rearrangements, especially during arthropod early embryonic development (Kramerova et al. 2000). Excess expression of papilin in *Drosophila* causes lethal abnormalities in muscle, Malpighian tubule, and trachea formation during early development (Kramerova et al. 2000), so its upregulation in juvenile *A. bahia* could result in developmental abnormalities. In addition, contigs with CPM > 100, but an |FC| < 5, that were unique to the un-weathered leachate group at the 1.08 g/L leachate concentration include upregulation of a contig sequence associated with a low-density lipoprotein receptor (LDLR) -like gene object and an uncharacterized protein (LOC113806809), along with a downregulation of a contig sequence associated with a hemocyanin A chain and an oplophorus-luciferin 2-monooxygenase non-catalytic subunit-like gene object (Table 5). LDLR is a receptor that binds lipoproteins in both mammals and insects and transports these lipoproteins into cells by endocytosis to replenish fat (Rodenburg and Van der Horst 2005). Upregulation of LDLR has been found to be concurrent with critical periods where endocytosis of lipoprotein is needed

(Rodenburg and Van der Horst 2005). It can be assumed that *A. bahia* were under stress from the TWP leachate and therefore were increasing their expression of LDLR to replenish energy stores. Hemocyanin is a metalated protein responsible for the sensing, transport, and storage of oxygen, and is freely dissolved in the hemolymph plasma of arthropods and molluscs (Coates and Decker 2017). Originally thought to be primarily a respiratory protein, its synthesis was expected to be related to respiratory system stress (Senkbeil and Wriston 1981). Senkbeil and Wriston (1981) studied hemocyanin in the lobster, *H. americanus*, and found that although hemocyanin was produced when under hypoxic stress, only a small fraction of the hemocyanin appeared to be essential for respiratory function. Rather, hemocyanin has recently been found to be an integral component of biological defense systems in arthropods, combating infection, parasitism, viremia and physical damages (Coates and Decker 2017). The downregulation of hemocyanin at 1.08 g/L (Table 5) was not consistent with the observed stimulation of respiration rate in *A. bahia* at 1.08 g/L (Figure 4 d,f), which indicates that the downregulation of hemocyanin may instead be related to the impairment of defense systems in *A. bahia* rather than to respiratory stress.

The highest concentration of un-weathered leachate, 1.08 g/L, was the only concentration in the un-weathered leachate group that showed significant GO-term enrichment compared to the *de novo* annotated reference transcriptome, and all enrichment came from upregulated contig sequences. All of these upregulated contigs were grouped together by their potential function, and it was found that there were ten significant GO-terms; eight molecular functions and two biological processes (Figure 6b). Of these ten significant GO terms, the two biological processes and five of the molecular functions were unique to the un-weathered leachate group. The significant biological processes indicate that the upregulated contigs in the 1.08 g/L un-

weathered leachate concentration significantly disrupted both proteolysis and cysteine biosynthetic process from serine pathways in *A. bahia* (Figure 6b). Contributing to these disrupted biological processes, the molecular functions of catalytic activity acting on a protein, hydrolase activity, cystathionine beta-synthase activity, endopeptidase activity, and serine-type endopeptidase activity were all significantly overrepresented (Figure 6b).

Overall, after exposure to 1.08 g/L of un-weathered TWP leachate, many different enzymes in *A. bahia* that catalyze reactions that contribute to proteolysis, or the breakdown of proteins or peptides into their component amino acids, were overrepresented. Hydrolase is an enzyme that catalyzes hydrolysis reactions, endopeptidase is an enzyme that catalyzes the cleavage of peptide bonds within a polypeptide or protein. Serine-type endopeptidase is a specific type of endopeptidase that has been found to be essential to the functions of various physiological and pathological processes, including survival, developmental processes, digestion, fertilization, blood coagulation, apoptosis, fibrinolysis, and immune defense (Park and Kwak 2020). In addition, cystathionine beta-synthase, an enzyme that is involved in the reaction converting serine to cysteine, was overrepresented (Kitabatake et al. 2000). Cysteine is an essential amino acid unique in its ability to form disulfide linkages that greatly contribute to protein structure (Kitabatake et al. 2000). In one study, a cysteine-rich protein called stablin stabilized the hemolymph clotting mesh in arthropods and was able to immobilize bacteria at injury sites, suggesting that cysteine could play a role in the initial stages of defense and healing (Matsuda et al. 2007). The overrepresentation of the biological process creating cysteine from serine in *A. bahia* exposed to un-weathered TWP leachate could be an attempt to increase defense mechanisms. These overrepresented GO terms that appear only in the un-weathered

leachate group indicates that the chemical or group of chemicals that contribute to these observed transcriptomic responses in *A. bahia* are unique to the un-weathered TWP leachate.

4.2.3 – Between treatments – both weathered and un-weathered groups

Without considering leachate concentrations, there were 23 differentially expressed contigs that appeared only in shrimp exposed to weathered leachate, 82 differentially expressed contigs that appeared only in shrimp exposed to un-weathered leachate, and 57 differentially expressed contigs that appeared in shrimp regardless of if they were exposed to weathered or un-weathered TWP leachate (Figure 7, Appendix E). The un-weathered TWP leachate disrupted more molecular processes in *A. bahia* than its weathered leachate counterpart, and this signifies that the un-weathered TWP leachate was more toxic overall, which is also evidenced by its lower LC50 value (Roberts 2021). Although there were differences in transcriptomic response between the leachates, in this section the contigs that were dysregulated in both weathering treatment groups are further explored, as these contigs are more generally representative of TWP leachate impacts to *A. bahia* regardless of the whether the tire particles were weathered or not.

Of the dysregulated contigs that appear in more than one leachate concentration within a weathering treatment group (Figure 5), four contig sequences were dysregulated in both weathering treatment groups and were upregulated relative to the control in every case (Table 3). These include one sequence that has an unknown function (does not have an orthologous gene description) and three sequences that map to orthologous gene descriptions in arthropods: a lysosomal protective protein, an uncharacterized protein (LOC119576313), and a proton-coupled folate transporter (PCFT) - like gene object, in decreasing order of significance (Table 3). The lysosomal protective protein was more highly upregulated with a larger FC in the un-weathered group, and it occurred at all three concentrations (e.g., 0.27, 0.54, and 1.08 g/L) instead of just in

the middle (1.34 g/L) and high (2.68 g/L) concentrations in the weathered group. The uncharacterized protein (LOC119576313) had a higher FC in the un-weathered group as well. The PCFT- like gene object was more highly dysregulated in the un-weathered group at the middle leachate concentration but was more highly dysregulated in the weathered group at the highest leachate concentration, with the 2.68 g/L weathered leachate concentration showing a $|FC| > 5$ (Table 3). This is an important set of contigs, because they are dysregulated at multiple concentrations tested in each weathering treatment group, and they occurred in shrimp exposed to TWP leachate regardless of whether the tire particles were weathered or un-weathered. This suggests that these individual contig sequences could potentially be biomarkers for TWP leachate exposure in *A. bahia.* If I had used a stricter log2FC filter of $\log2FC \geq 1.5$, which would make it statistically more difficult for a contig sequence to be dysregulated compared to the control, all of these contigs would have still been dysregulated except for the lysosomal protective protein at the 1.34 g/L weathered leachate concentration and at the 0.27 g/L un-weathered leachate concentration (Appendix D). Because the results are close to the same with a stricter log2FC cutoff employed, and because the lysosomal protective protein remains dysregulated at the highest leachate concentrations under this stricter cutoff, I can be more confident in these contigs' potential utility as general TWP biomarkers in *A. bahia*. Future studies could be directed towards discovering specific TWP biomarkers in *A. bahia*, and the above findings may be a good place to start.

The contigs with $|FC| > 5$ as well as a CPM > 25 that were mapped to orthologous gene descriptions in arthropods and that appeared in both the weathered and the un-weathered leachate treatments include an upregulation of a hypothetical protein Anas_12497, a putative ankyrin repeat protein RF_0381 isoform X4, and an uncharacterized protein (LOC119576313) (Table 4).

Most of these are hypothetical or uncharacterized proteins that do not yet have known functions, but ankyrin repeat proteins have a specific repeated amino acid sequence and have been linked to functions including cell-cell signaling, cytoskeleton integrity, transcription and cell-cell regulation, inflammatory response, development, and various transport phenomena, all of which mediate specific protein-protein interactions (Mosavi et al. 2004). Additionally, there was downregulation of a chitinase-3 like protein with $|FC| > 5$ and $CPM > 25$ in both the weathered and un-weathered groups (Table 4). The chitinase-3-like protein binds to chitin, heparin, and hyaluronic acid, is regulated by many factors including stress, and plays a large role in tissue injury, inflammation, tissue repair, and remodeling responses (Zhao et al. 2020). The downregulation of this protein would not allow the affected organism to successfully repair its tissues or fight inflammation when under stress, and this is a shared effect between the two weathering treatment groups, indicating that the chemical or group of chemicals that contribute to this response in *A. bahia* appear in both leachate types (Figure 2, Table 2). In addition, the previously discussed downregulation of the protein obstructor E-like isoform in the un-weathered group at both the 1.08 g/L and the 0.54 g/L concentrations with a CPM of 1401.93 also appears in the weathered group with a CPM of 1401.93, but only at the 2.68 g/L concentration (Table 5). This suggests that there may be an element of deformation of body shape that occurs in the cuticle in shrimp exposed to both weathered and un-weathered TWP leachate (Tajiri et al. 2017).

The highest concentrations of both weathered and un-weathered TWP leachate (2.68 g/L and 1.08 g/L respectively), were the only concentrations that showed significant GO-term enrichment compared to the *de novo* annotated reference transcriptome, and in both weathering treatment groups all enrichment came from upregulated contig sequences. The un-weathered

group had five more GO terms overrepresented than the weathered group (Figure 6). Of the five significant GO terms found in the weathered group and the ten significant GO terms found in the un-weathered group, only three GO terms were shared between treatment groups, and all three were molecular functions: serine hydrolase activity, serine-type peptidase activity, and peptidase activity (Figure 6). Although these molecular functions were impacted in shrimp exposed to both leachates, it is important to note that the relative significance of these overrepresented GO terms was higher in the un-weathered group than in the weathered group (Figure 6). Similar to the GO terms that appeared uniquely in the un-weathered group, the three GO terms shared between weathering treatment groups mainly involve the breakdown of proteins and polypeptides.

Serine hydrolases are a broad superfamily of enzymes that catalyze a variety of important hydrolysis reactions in a two-step process with all enzymes in the superfamily unified by the presence of a serine residue in the active site. They consist of proteases and peptidases, lipases, and carboxylesterases, and are considered one of the largest functional enzyme classes in all forms of life (Kumar et al. 2021). Peptidases are enzymes that catalyze the cleavage of peptide bonds; they are also known as proteases and are further divided into endopeptidase and exopeptidase enzymes (Barrett and McDonald 1986); endopeptidase enzymes (overrepresented in the un-weathered leachate group only) cleave bonds internal to a protein, while exopeptidase enzymes cleave bonds on the terminal end of a protein. Serine-type peptidase falls under the broader serine hydrolase enzyme family. Serine peptidases have been found to be important in physiological processes related to immune response and embryonic development and body patterning in *Drosophila* (Kumar et al. 2021). Lysosomal protective proteins, dysregulated in multiple leachate concentrations in both weathered and un-weathered groups, are a type of serine peptidase that forms a complex with beta-galactosidase and neuraminidase hydrolase enzymes,

exerting a protective function necessary for their stability and activity (Galjart et al. 1991, Bonten et al. 1995). The upregulation of lysosomal protective proteins in *A. bahia* would allow specific hydrolases in the lysosomes to continue to function properly.

Table 3. The five contig IDs that are dysregulated in more than one concentration in the weathered leachate, and the 12 contig IDs that are dysregulated in more than one concentration in the un-weathered leachate group. The first four contig IDs in each leachate treatment are marked with an asterisk to indicate that they appear in both leachate treatments. The "Concentration Overlap" column details which concentrations the contig ID is dysregulated in. The type of dysregulation (up- or down- regulated relative to the control), along with the fold-change (FC) level of expression, counts per million reads (CPM), false discovery rate (FDR) adjusted p-value, orthologous gene descriptions in arthropods, and whether the contig ID had a |FC| > 5 or a CPM > 100 are included. The intersections of these contigs are visualized in Figure 5 and their levels of expression are included in Figure 6.

Leachate Treatment	Contig ID found in *A. bahia* (from *de novo* assembly)	Concentration Overlap	Concentration (g/L)	Dysregulation	FC	CPM	FDR	Gene description - orthologous genes in arthropods (from annotation file)	|FC| > 5?	CPM > 100?
Weathered	TRINITY_DN6462_c0_g1_i1 *	Highest, Middle	2.68	Upregulated	3.44	189.78	5.01E-15	Lysosomal protective protein		✓
			1.34	Upregulated	2.48	189.78	5.90E-07			✓
	TRINITY_DN734_c0_g1_i20 *	Highest, Middle	2.68	Upregulated	46.53	38.73	1.63E-07	uncharacterized protein LOC119576313	✓	
			1.34	Upregulated	10.87	38.73	1.60E-02		✓	
	TRINITY_DN6949_c6_g1_i5 *	Highest, Middle	2.68	Upregulated	5.10	47.15	1.41E-06	proton-coupled folate transporter-like	✓	
			1.34	Upregulated	2.95	47.15	3.93E-02			
	TRINITY_DN24816_c0_g2_i5 *	Highest, Middle, Lowest	2.68	Upregulated	18.85	6.13	1.07E-03	---NA---	✓	
			1.34	Upregulated	18.56	6.13	1.13E-02		✓	
			0.67	Upregulated	17.51	6.13	8.66E-03		✓	
	TRINITY_DN11122_c0_g1_i13	Highest, Lowest	2.68	Upregulated	851.90	2.66	2.34E-02	---NA---	✓	
			0.67	Upregulated	689.83	2.66	4.29E-02		✓	
Un-weathered	TRINITY_DN6462_c0_g1_i1 *	Highest, Middle, Lowest	1.08	Upregulated	3.77	189.78	3.16E-17	Lysosomal protective protein		✓
			0.54	Upregulated	2.83	189.78	6.59E-10			✓
			0.27	Upregulated	2.14	189.78	3.70E-04			✓
	TRINITY_DN734_c0_g1_i20 *	Highest, Middle	1.08	Upregulated	76.13	38.73	1.77E-09	uncharacterized protein LOC119576313	✓	
			0.54	Upregulated	29.90	38.73	1.12E-05		✓	
	TRINITY_DN6949_c6_g1_i5 *	Highest, Middle	1.08	Upregulated	4.49	47.15	6.26E-06	proton-coupled folate transporter-like		
			0.54	Upregulated	3.01	47.15	1.63E-02			
	TRINITY_DN24816_c0_g2_i5 *	Highest, Middle	1.08	Upregulated	14.91	6.13	1.57E-03	---NA---	✓	
			0.54	Upregulated	14.52	6.13	1.48E-02		✓	
	TRINITY_DN13160_c0_g1_i5	Highest, Middle	1.08	Downregulated	-6.90	83.10	5.87E-09	chitinase-3-like protein 1	✓	
			0.54	Downregulated	-5.15	83.10	1.06E-05		✓	
	TRINITY_DN2594_c0_g1_i5	Highest, Middle	1.08	Upregulated	4.31	10.65	4.97E-05	pentraxin-related protein PTX3-like		
			0.54	Upregulated	2.95	10.65	3.33E-02			
	TRINITY_DN2935_c0_g1_i11	Highest, Middle	1.08	Upregulated	58.76	32.06	1.68E-07	putative ankyrin repeat protein RF_0381 isoform X4	✓	
			0.54	Upregulated	11.87	32.06	1.48E-02		✓	
	TRINITY_DN5090_c4_g2_i3	Highest, Middle	1.08	Upregulated	3.63	435.55	1.77E-09	PREDICTED: uncharacterized protein LOC108673189		✓
			0.54	Upregulated	2.32	435.55	4.06E-03			✓
	TRINITY_DN672_c0_g1_i29	Highest, Middle	1.08	Upregulated	5.82	8.91	2.84E-06	---NA---	✓	
			0.54	Upregulated	3.22	8.91	3.11E-02			
	TRINITY_DN734_c0_g1_i13	Highest, Middle	1.08	Upregulated	5.25	4.90	1.84E-05	uncharacterized protein LOC119576313	✓	
			0.54	Upregulated	3.96	4.90	7.04E-03			
	TRINITY_DN9575_c0_g2_i1	Highest, Middle	1.08	Downregulated	-4.69	1401.93	3.78E-12	protein obstructor-E-like isoform X1		✓
			0.54	Downregulated	-2.33	1401.93	7.04E-03			✓
	TRINITY_DN736_c0_g1_i15	Highest, Lowest	1.08	Upregulated	2.10	4.18	3.39E-02	Glycine N-methyltransferase		
			0.27	Upregulated	2.62	4.18	4.34E-02			

Table 4. All dysregulated contig sequences from Appendix D with a |FC| > 5. Contigs IDs are generally grouped by increasing level of expression (FC) within each leachate treatment group; some exceptions are where one contig ID is expressed across multiple concentrations; these were kept together. There are 12 dysregulated contig IDs in the weathered leachate group and 16 dysregulated contig IDs in the un-weathered leachate group with |FC| > 5. The gene descriptions for which specific contig IDs are unique to a treatment group are colored in gray.

Leachate Treatment	Contig ID found in *A. bahia* (from *de novo* assembly)	Concentration (g/L)	Dysregulation	FC	CPM	FDR	Gene description - orthologous genes in arthropods (from annotation file)
Weathered	TRINITY_DN6949_c6_g1_i5	2.68	Upregulated	**5.10**	47.15	1.41E-06	proton-coupled folate transporter-like
	TRINITY_DN6098_c0_g1_i1	2.68	Upregulated	**5.47**	26.63	1.79E-05	hypothetical protein Anas_12496
	TRINITY_DN7665_c0_g1_i1	2.68	Upregulated	**7.32**	9.10	6.26E-03	Fatty acid amide hydrolase 1
	TRINITY_DN13160_c0_g1_i5	2.68	Downregulated	**-7.83**	83.10	1.68E-09	chitinase-3-like protein 1
	TRINITY_DN8241_c0_g1_i2	2.68	Upregulated	**7.91**	21.77	5.90E-06	hypothetical protein Anas_12496
	TRINITY_DN5071_c0_g1_i1	2.68	Upregulated	**9.15**	3.56	1.09E-02	---NA---
	TRINITY_DN2935_c0_g1_i12	2.68	Upregulated	**15.76**	11.46	2.27E-03	putative ankyrin repeat protein RF_0381 isoform X4
	TRINITY_DN24816_c0_g2_i5	0.67	Upregulated	**17.51**	6.13	8.66E-03	---NA---
		1.34	Upregulated	**18.56**	6.13	1.13E-02	
		2.68	Upregulated	**18.85**	6.13	1.07E-03	
	TRINITY_DN2935_c0_g1_i11	2.68	Upregulated	**27.68**	32.06	3.19E-05	putative ankyrin repeat protein RF_0381 isoform X4
	TRINITY_DN734_c0_g1_i20	1.34	Upregulated	**10.87**	38.73	1.60E-02	uncharacterized protein LOC119576313
		2.68	Upregulated	**46.53**	38.73	1.63E-07	
	TRINITY_DN8131_c0_g1_i18	0.67	Downregulated	**-721.96**	2.70	1.77E-02	---NA---
	TRINITY_DN11122_c0_g1_i13	0.67	Upregulated	**689.83**	2.66	4.29E-02	---NA---
		2.68	Upregulated	**851.90**	2.66	2.34E-02	
Un-weathered	TRINITY_DN6098_c0_g1_i1	1.08	Upregulated	**5.14**	26.63	2.08E-05	hypothetical protein Anas_12496
	TRINITY_DN22786_c0_g1_i1	1.08	Downregulated	**-5.17**	7.49	3.73E-16	delta(24)-sterol reductase-like
	TRINITY_DN672_c0_g1_i20	1.08	Upregulated	**5.21**	27.07	2.18E-08	papilin isoform X4
	TRINITY_DN734_c0_g1_i13	1.08	Upregulated	**5.25**	4.90	1.84E-05	uncharacterized protein LOC119576313
	TRINITY_DN7237_c0_g1_i3	1.08	Upregulated	**5.45**	3.79	1.38E-02	Apolipoprotein D
	TRINITY_DN672_c0_g1_i29	1.08	Upregulated	**5.82**	8.91	2.84E-06	---NA---
	TRINITY_DN13160_c0_g1_i5	0.54	Downregulated	**-5.15**	83.10	1.06E-05	chitinase-3-like protein 1
		1.08	Downregulated	**-6.90**	83.10	5.87E-09	
	TRINITY_DN5071_c0_g1_i1	1.08	Upregulated	**7.76**	3.56	1.15E-02	---NA---
	TRINITY_DN8241_c0_g1_i2	1.08	Upregulated	**7.99**	21.77	2.23E-06	hypothetical protein Anas_12496
	TRINITY_DN11720_c0_g1_i12	0.27	Downregulated	**-12.56**	6.85	4.68E-02	glycine-rich cell wall structural protein 1-like
	TRINITY_DN24816_c0_g2_i5	0.54	Upregulated	**14.52**	6.13	1.48E-02	---NA---
		1.08	Upregulated	**14.91**	6.13	1.57E-03	
	TRINITY_DN2935_c0_g1_i12	1.08	Upregulated	**29.81**	11.46	4.14E-05	putative ankyrin repeat protein RF_0381 isoform X4
	TRINITY_DN2935_c0_g1_i11	0.54	Upregulated	**11.87**	32.06	1.48E-02	putative ankyrin repeat protein RF_0381 isoform X4
		1.08	Upregulated	**58.76**	32.06	1.68E-07	
	TRINITY_DN734_c0_g1_i20	0.54	Upregulated	**29.90**	38.73	1.12E-05	uncharacterized protein LOC119576313
		1.08	Upregulated	**76.13**	38.73	1.77E-09	
	TRINITY_DN11122_c0_g1_i13	1.08	Upregulated	**540.80**	2.66	1.77E-02	---NA---
	TRINITY_DN11999_c0_g1_i10	1.08	Downregulated	**-599.62**	2.51	3.21E-03	Xylulose kinase

Table 5. All dysregulated contigs from Appendix D that have a CPM > 100. Contig IDs are ordered by increasing CPM within each leachate treatment group. There are 13 dysregulated contig IDs in the weathered leachate group and 14 dysregulated contig IDs in the un-weathered leachate group with CPM > 100. The gene descriptions for which specific contig IDs are unique to a treatment group are colored in gray.

Leachate Treatment	Contig ID found in *A. bahia* (from *de novo* assembly)	Concentration (g/L)	Dysregulation	FC	CPM	FDR	Gene description - orthologous genes in arthropods (from annotation file)
Weathered	TRINITY_DN11316_c0_g1_i17	2.68	Downregulated	-2.63	**143.30**	1.99E-04	probable deoxycytidylate deaminase
	TRINITY_DN1613_c0_g1_i15	2.68	Upregulated	2.31	**181.88**	1.13E-02	obstructor F2
	TRINITY_DN2003_c0_g2_i1	2.68	Upregulated	3.05	**183.18**	3.18E-08	juvenile hormone binding protein 7
	TRINITY_DN19891_c0_g1_i1	2.68	Upregulated	2.46	**183.73**	1.21E-07	peritrophin-44-like protein
	TRINITY_DN6462_c0_g1_i1	2.68	Upregulated	3.44	**189.78**	5.01E-15	Lysosomal protective protein
		1.34	Upregulated	2.48	**189.78**	5.90E-07	
	TRINITY_DN15559_c0_g1_i10	2.68	Upregulated	2.94	**191.68**	8.10E-05	apolipoprotein D-like
	TRINITY_DN4854_c0_g1_i1	2.68	Upregulated	2.07	**192.43**	6.76E-04	uncharacterized protein LOC119573628
	TRINITY_DN6695_c0_g2_i4	2.68	Upregulated	2.77	**309.97**	4.71E-04	uncharacterized protein LOC119573322
	TRINITY_DN5399_c0_g1_i1	2.68	Upregulated	2.17	**322.20**	8.39E-16	fibrocystin-L-like
	TRINITY_DN22896_c0_g1_i3	2.68	Upregulated	2.75	**362.66**	2.66E-05	C-type lectin 3
	TRINITY_DN5090_c4_g2_i3	2.68	Upregulated	3.64	**435.55**	3.93E-09	PREDICTED: uncharacterized protein LOC108673189
	TRINITY_DN3295_c0_g1_i10	2.68	Upregulated	3.17	**453.27**	4.45E-05	C-type lectin
	TRINITY_DN9575_c0_g2_i1	2.68	Downregulated	-3.43	**1401.93**	1.63E-07	protein obstructor-E-like isoform X1
Un-weathered	TRINITY_DN11316_c0_g1_i17	1.08	Downregulated	-4.30	**143.30**	2.26E-10	probable deoxycytidylate deaminase
	TRINITY_DN2003_c0_g2_i1	1.08	Upregulated	2.89	**183.18**	8.67E-08	juvenile hormone binding protein 7
	TRINITY_DN19891_c0_g1_i1	1.08	Upregulated	2.10	**183.73**	1.80E-05	peritrophin-44-like protein
	TRINITY_DN6462_c0_g1_i1	1.08	Upregulated	3.77	**189.78**	3.16E-17	Lysosomal protective protein
		0.54	Upregulated	2.83	**189.78**	6.59E-10	
		0.27	Upregulated	2.14	**189.78**	3.70E-04	
	TRINITY_DN9238_c0_g1_i6	1.08	Upregulated	2.76	**190.72**	2.15E-08	low-density lipoprotein receptor-like
	TRINITY_DN15559_c0_g1_i10	1.08	Upregulated	3.07	**191.68**	1.80E-05	apolipoprotein D-like
	TRINITY_DN6710_c3_g1_i5	1.08	Upregulated	2.01	**196.18**	4.23E-02	uncharacterized protein LOC113806809
	TRINITY_DN6695_c0_g2_i4	1.08	Upregulated	2.47	**309.97**	1.75E-03	uncharacterized protein LOC119573322
	TRINITY_DN22896_c0_g1_i3	1.08	Upregulated	2.19	**362.66**	1.76E-03	C-type lectin 3
	TRINITY_DN13699_c0_g1_i8	1.08	Downregulated	-2.18	**368.34**	2.59E-04	Hemocyanin A chain
	TRINITY_DN5090_c4_g2_i3	1.08	Upregulated	3.63	**435.55**	1.77E-09	PREDICTED: uncharacterized protein LOC108673189
		0.54	Upregulated	2.32	**435.55**	4.06E-03	
	TRINITY_DN3295_c0_g1_i10	1.08	Upregulated	2.51	**453.27**	1.64E-03	C-type lectin
	TRINITY_DN2231_c1_g3_i1	1.08	Downregulated	-2.03	**859.52**	8.23E-05	oplophorus-luciferin 2-monooxygenase non-catalytic subunit-like
	TRINITY_DN9575_c0_g2_i1	1.08	Downregulated	-4.69	**1401.93**	3.78E-12	protein obstructor-E-like isoform X1
		0.54	Downregulated	-2.33	**1401.93**	7.04E-03	

4.3 – Connecting effects through levels of biological organization

Connecting molecular effects to apical effects or adverse outcomes in whole organisms is an identified data gap for traditional microplastics (Jeong and Choi 2019, Gunaalan et al. 2020) as well as for TWPs. The connections are important because apical effects are traditionally more relevant to environmental risk assessments (Ankley et al. 2010), yet the molecular responses can be detected sooner, they may give clues as to what the specific biological processes are that may be the target of TWPs, and they may help explain why apical responses occurred. One conceptual framework that connects these levels of biological organization is the adverse outcome pathway (AOP) framework (Ankley et al. 2010, Villeneuve et al. 2014a, Villeneuve et al. 2014b). My study is the first to look at the molecular and sublethal responses in marine organisms exposed to TWP leachate for which there was previously observed mortality of the same organism using the same TWP materials (Roberts 2021). While my study presented a unique opportunity to connect molecular effects to apical effects via the AOP framework, this was not possible due to the lack of interoperability between omics databases and the AOP Wiki (AOP-Wiki, n.d., Martens et al. 2018) and the fact that AOPs are usually constructed after exposure to a single chemical, or "stressor", while TWP leachates are a complex mixture of chemicals containing metals and organic compounds (Table 2, Figure 2).

4.4 – Conclusions and future directions

This was an exploratory study investigating both the sublethal and molecular responses of a marine organism to TWP leachate, the first of its kind. We found that *A. bahia* experienced significant stimulation in respiration rate after exposure to TWP leachate, which is consistent with previous studies exposing *A. bahia* to organic chemicals, and in contrast to previously observed responses of crustaceans to metals exposure. This indicates that the organic chemicals in the TWP leachate are likely driving the observed sublethal respiration response in *A. bahia*, although the specific chemicals responsible were not able to be determined. In addition, differences in patterns of respiration rate were observed after exposure to the weathered versus un-weathered leachates, which could be due to the differences in either the metals or the organic chemicals present in each leachate; the leachates statistically clustered into different groups based on differences in their metal and organic chemical profiles respectively.

It was also found that there was significant dysregulation of contig sequences in *A. bahia* in both weathering treatment groups. In my study, dysregulated contig sequences are contigs that were significantly differentially expressed in the treatment group compared to the control group at the cutoff filters I employed (i.e. FDR ≤ 0.05 and $|\log2FC| \geq 1$). Dysregulated contigs include upregulated contigs, or those sequences that appear more often in the treatment group compared to the control group ($|\log2FC| > 1$), and down-regulated contigs, or those sequences that appear less often in the treatment group compared to the control group ($|\log2FC| < 1$). Exposure of shrimp to the un-weathered leachate resulted in more dysregulated contig sequences overall (Figure 7) and more overrepresented GO term enrichment at the highest concentration (i.e., 1.08 g/L) than resulted from exposure to the weathered leachate (Figure 6). Chitin binding in extracellular regions was significantly overrepresented and upregulated in the weathered

treatment group (Figure 6). Catalytic activity acting on a protein, hydrolase activity, cystathionine beta-synthase activity, endopeptidase activity, and serine-type endopeptidase activity molecular functions were overrepresented and upregulated in the un-weathered treatment group, which impacted two biological processes: proteolysis and cysteine biosynthetic process from serine (Figure 6). Serine hydrolase activity, serine-type peptidase activity, and peptidase activity were significantly overrepresented and upregulated in both treatment groups (Figure 6). Many contig sequences mapped to orthologous gene descriptions that regulated physical body structure, inflammatory response, and mediated protein-protein interactions, signifying that TWP leachate exposure disrupts many internal molecular processes in *A. bahia.* The transcriptomics results taken together – both the types of dysregulated contigs with orthologous gene descriptions (Table 3) and the enriched pathways (Figure 6) – indicate that the leachates are non-specific in their mechanism of toxic action; they induced generalized responses in the shrimp. Three important dysregulated contig sequences appear in more than one concentration in both leachate types and map to the following orthologous gene descriptions: a lysosomal protective protein, an uncharacterized protein (LOC119576313), and a proton-coupled folate transporter (PCFT) - like gene object (Table 3). These could be potential general biomarkers of TWP leachate exposure in *A. bahia*, but future studies are needed to strengthen this theory, and to determine what this uncharacterized protein's function is.

The results of my study and Roberts' (2021) study imply that the un-weathered TWP leachate is more toxic overall, disrupting more molecular processes in *A. bahia* than its weathered counterpart at similarly toxic sublethal concentrations and resulting in a lower LC50 value. This implies that the additive chemicals associated with the tire particles and the chemicals picked up by the tire particles from the roadside are more toxic to marine organisms

than the chemicals sorbed from the marine environment. This suggests that the time where TWPs are immediately released into the marine environment is the time where the chemicals associated with TWPs will have the greatest effect on marine organisms, as is observed by the occurrence of urban stormwater runoff mortality syndrome in coho salmon directly after large rain events (Peter et al. 2018, McIntyre et al. 2021).

The impacts of TWP leachate to *A. bahia*, an estuarine organism commonly used in toxicity testing, suggest that the chemicals associated with TWPs can have effects that cascade through levels of biological organization at sublethal concentrations, despite the current inability to link these effects through the AOP framework. It is important to note that the concentrations used in my study, although sublethal, are not at known environmentally relevant concentrations, although there is much uncertainty to what actual TWP concentrations are in the environment. Wik and Dave (2009) suggest that environmentally relevant concentrations of TWPs in surface waters range between 0.03 - 56 mg/L, which is between 3 and 5,666 times less than the lowest concentration used in the weathered leachate exposures (0.17 g/L) and 1.25 to 2,333 less than the lowest concentration used in the un-weathered leachate exposures (0.07 g/L). The concentrations used in my study (Table 1) were selected based on the calculated LC50 values in Roberts (2021) and because of my study's exploratory nature and the uncertainty surrounding whether there would be observable responses in *A. bahia* at the sublethal and/or molecular levels and at what leachate concentrations those responses would be evident. There was no observable effect on respiration rate at the lowest leachate concentrations for either the weathered or un-weathered leachate exposures (Figure 4). As for molecular effects at the filters employed (FDR ≤ 0.05 and $|\log2FC| \geq 1$), there were only 12 dysregulated contigs at the lowest tested concentration in the weathered leachate exposure (0.67 g/L) and 4 dysregulated contigs at the lowest tested

concentration in the un-weathered leachate (0.27 g/L) (Table 1, Figure 5). If the TWP leachate concentrations used had been lower, it is hard to predict how much lower the level of dysregulation would have been, or if there would have been any dysregulation. It is accepted in the literature that TWPs are an environmentally relevant problem (Peter et al. 2018, McIntyre et al. 2021, Tian et al. 2021), I just cannot say for certain, given the results of my study, that that is true for *A. bahia*.

Because of the lack of information currently available in the literature on *A. bahia* (its genome has not been sequenced), approximately 20% of the dysregulated contigs found in this study did not have an orthologous gene description in arthropods (Appendix D), making it so that the functionality of those dysregulated contigs could not be inferred in any meaningful way. Future studies will be necessary to build up knowledge about the specific genes and pathways that are disrupted in *A. bahia* after TWP leachate exposure, along with what function they may perform. The first assembled and annotated transcriptome for *A. bahia* was generated from this work and will be published in an upcoming manuscript, serving as an important launchpad for those future studies.

5.0 - Works Cited

Alamo-Nole LA, Perales-Perez O, Roman-Velazquez FR. 2011. Sorption study of toluene and xylene in aqueous solutions by recycled tires crumb rubber. Journal of Hazardous Materials. 185(1):107–111. doi:10.1016/j.jhazmat.2010.09.003.

Alcaraz AJG, Mikulášek K, Potěšil D, Park B, Shekh K, Ewald J, Burbridge C, Zdráhal Z, Schneider D, Xia J, et al. 2021. Assessing the toxicity of 17α-ethinylestradiol in rainbow trout using a 4-day transcriptomics Benchmark Dose (BMD) embryo assay. Environ Sci Technol. 55(15):10608–10618. doi:10.1021/acs.est.1c02401.

Alimi OS, Farner Budarz J, Hernandez LM, Tufenkji N. 2018. Microplastics and nanoplastics in aquatic environments: Aggregation, deposition, and enhanced contaminant transport. Environ Sci Technol. 52(4):1704–1724. doi:10.1021/acs.est.7b05559.

Andrews, S. (n.d.). FastQC A Quality Control tool for High Throughput Sequence Data. [accessed 2021 Sep 9]. Retrieved from http://www.bioinformatics.babraham.ac.uk/projects/fastqc/

Ankley, G. T., R. S. Bennett, R. J. Erickson, D. J. Hoff, M. W. Hornung, R. D. Johnson, D. R. Mount, J. W. Nichols, C. L. Russom, P. K. Schmieder, J. A. Serrrano, J. E. Tietge, and D. L. Villeneuve. 2010. Adverse outcome pathways: A conceptual framework to support ecotoxicology research and risk assessment. Environmental Toxicology and Chemistry 29:730–741.

AOP Wiki. n.d. https://aopwiki.org/. [accessed 2022 Jun 16]

Auta HS, Emenike CU, Fauziah SH. 2017. Distribution and importance of microplastics in the marine environment: A review of the sources, fate, effects, and potential solutions. Environment International. 102:165–176. doi:10.1016/j.envint.2017.02.013.

Balbi, T., S. Franzellitti, R. Fabbri, M. Montagna, E. Fabbri, and L. Canesi. 2016. Impact of bisphenol A (BPA) on early embryo development in the marine mussel *Mytilus galloprovincialis*: Effects on gene transcription. Environmental Pollution 218:996–1004.

Bao J, Xing Y, Feng C, Kou S, Jiang H, Li X. 2020. Acute and sub-chronic effects of copper on survival, respiratory metabolism, and metal accumulation in *Cambaroides dauricus*. Sci Rep. 10(1):16700. doi:10.1038/s41598-020-73940-1.

Barbieri E. 2009. Effects of zinc and cadmium on oxygen consumption and ammonium excretion in pink shrimp (*Farfantepenaeus paulensis*, Pérez-Farfante, 1967, Crustacea). Ecotoxicology. 18(3):312–318. doi:10.1007/s10646-008-0285-y.

Barbieri E, Paes ET. 2011. The use of oxygen consumption and ammonium excretion to evaluate the toxicity of cadmium on *Farfantepenaeus paulensis* with respect to salinity. Chemosphere. 84(1):9–16. doi:10.1016/j.chemosphere.2011.02.092.

Barrett AJ, McDonald JK. 1986. Nomenclature: protease, proteinase and peptidase. Biochemical Journal. 237(3):935–935. doi:10.1042/bj2370935.

Ben-Hur A. and Guyon I. 2003. Detecting stable clusters using principal component analysis. In: Methods in molecular biology. In: Functional genomics: methods and protocols. p.159-182. Brownstein M.J., Khodursky A.B. Eds., Humana Press, Totowa, N.J.

Benjamini Y, Hochberg Y. 1995. Controlling the False Discovery Rate: A practical and powerful approach to multiple testing. Journal of the Royal Statistical Society Series B (Methodological). 57(1):289–300.

BioBam Bioinformatics. 2019. OmicsBox: bioinformatics made easy (version 2.0.36). BioBam Bioinformatics, Valencia, Spain.

Bocca B, Forte G, Petrucci F, Costantini S, Izzo P. 2009. Metals contained and leached from rubber granulates used in synthetic turf areas. Science of The Total Environment. 407(7):2183–2190. doi:10.1016/j.scitotenv.2008.12.026.

Bolger AM, Lohse M, Usadel B. 2014. Trimmomatic: a flexible trimmer for Illumina sequence data. Bioinformatics. 30(15):2114–2120. doi:10.1093/bioinformatics/btu170.

Bonten EJ, Galjart NJ, Willemsen R, Usmany M, Vlak JM, d'Azzo A. 1995. Lysosomal protective protein/cathepsin A. Role of the "linker" domain in catalytic activation. J Biol Chem. 270(44):26441–26445. doi:10.1074/jbc.270.44.26441.

Bray NL, Pimentel H, Melsted P, Pachter L. 2016. Near-optimal probabilistic RNA-seq quantification. Nat Biotechnol. 34(5):525–527. doi:10.1038/nbt.3519.

Bunker RD, Bulloch EMM, Dickson JMJ, Loomes KM, Baker EN. 2013. Structure and function of human xylulokinase, an enzyme with important roles in carbohydrate metabolism. Journal of Biological Chemistry. 288(3):1643–1652. doi:10.1074/jbc.M112.427997.

Capolupo M, Sørensen L, Jayasena KDR, Booth AM, Fabbri E. 2020. Chemical composition and ecotoxicity of plastic and car tire rubber leachates to aquatic organisms. Water Research. 169:115270. doi:10.1016/j.watres.2019.115270.

Capuzzo JM, Lancaster BA, Sasaki GC. 1984. The effects of petroleum hydrocarbons on lipid metabolism and energetics of larval development and metamorphosis in the American lobster (*Homarus americanus* Milne Edwards). Marine Environmental Research. 14(1–4):201–228. doi:10.1016/0141-1136(84)90079-5.

Chibwe L, Parrott JL, Shires K, Khan H, Clarence S, Lavalle C, Sullivan C, O'Brien AM, De Silva AO, Muir DCG, et al. 2021. A deep dive into the complex chemical mixture and toxicity of tire wear particle leachate in fathead minnow. Environmental Toxicology and Chemistry. 00(00):1–10. doi:10.1002/etc.5140.

Coates CJ, Decker H. 2017. Immunological properties of oxygen-transport proteins: hemoglobin, hemocyanin and hemerythrin. Cell Mol Life Sci. 74(2):293–317. doi:10.1007/s00018-016-2326-7.

Corner EDS, Sparrow BW. 1956. The modes of action of toxic agents I. Observations on the poisoning of certain crustaceans by copper and mercury. J Mar Biol Ass. 35(3):531–548. doi:10.1017/S0025315400010390.

Cunningham B, Harper B, Brander S, Harper S. 2022. Toxicity of micro and nano tire particles and leachate for model freshwater organisms. Journal of Hazardous Materials. 429:128319. doi:10.1016/j.jhazmat.2022.128319.

Day KE, Holtze KE, Metcalfe-Smith JL, Bishop CT, Dutka BJ. 1993. Toxicity of leachate from automobile tires to aquatic biota. Chemosphere. 27(4):665–675. doi:10.1016/0045-6535(93)90100-J.

DeCoursey PJ, Vernberg WB. 1972. Effect of mercury on survival, metabolism and behaviour of larval *Uca pugilator* (Brachyura). Oikos. 23(2):241. doi:10.2307/3543412.

Degaffe FS, Turner A. 2011. Leaching of zinc Ffrom tire wear particles under simulated estuarine conditions. Chemosphere. 85(5):738–743. doi:10.1016/j.chemosphere.2011.06.047.

Depledge MH. 1984. Disruption of circulatory and respiratory activity in shore crabs (*Carcinus maenas* (L.)) exposed to heavy metal pollution. Comparative Biochemistry and Physiology Part C: Comparative Pharmacology. 78(2):445–459. doi:10.1016/0742-8413(84)90113-0.

Fried JR. 2003. Polymer Science and Technology. 2nd edition. Pearson Education.

Galgani, F., G. Hanke, and T. Maes. 2015. Global distribution, composition and abundance of marine litter. Pages 29–56 *in* M. Bergmann, L. Gutow, and M. Klages, editors. Marine anthropogenic litter. Springer International Publishing, Cham

Galjart NJ, Morreau H, Willemsen R, Gillemans N, Bonten EJ, d'Azzo A. 1991. Human lysosomal protective protein has cathepsin A-like activity distinct from its protective function. J Biol Chem. 266(22):14754–14762.

Gene Ontology *a*. (n.d.) The Gene Ontology resource. [accessed 2022 Aug 5]. http://geneontology.org/

Gene Ontology *b*. (n.d.) Introduction to GO annotations. [accessed 2022 Jun 7]. http://geneontology.org/docs/go-annotations/.

GIA, Inc. Tires – Global market trajectory & analytics. 2022. [accessed 2022 Mar 14]. https://www.strategyr.com/market-report-tires-forecasts-global-industry-analysts-inc.asp

Gunaalan, K., E. Fabbri, and M. Capolupo. 2020. The hidden threat of plastic leachates: A critical review on their impacts on aquatic organisms. Water Research 184:116170.

Gunasekara AS, Donovan JA, Xing B. 2000. Ground discarded tires remove naphthalene, toluene, and mercury from water. Chemosphere. 41(8):1155–1160. doi:10.1016/S0045-6535(00)00016-3.

Halle LL, Palmqvist A, Kampmann K, Khan FR. 2020. Ecotoxicology of micronized tire rubber: Past, present and future considerations. Science of The Total Environment. 706:135694. doi:10.1016/j.scitotenv.2019.135694.

Halsband C, Sørensen L, Booth AM, Herzke D. 2020. Car tire crumb rubber: does leaching produce a toxic chemical cocktail in coastal marine systems? Front Environ Sci. 8:125. doi:10.3389/fenvs.2020.00125.

Hansen E, Nilsson N, Lithner D, Lassen C. 2013. Hazardous substances in plastic materials. [accessed 2022 March 2]. https://www.miljodirektoratet.no/publikasjoner/publikasjoner-fra-klif/2013/februar/hazardous-substances-in-plastic-materials/.

Hartmann NB, Hüffer T, Thompson RC, Hassellöv M, Verschoor A, Daugaard AE, Rist S, Karlsson T, Brennholt N, Cole M, et al. 2019. Are we speaking the same language? Recommendations for a definition and categorization framework for plastic debris. Environ Sci Technol. 53(3):1039–1047. doi:10.1021/acs.est.8b05297.

Heberle H, Meirelles GV, da Silva FR, Telles GP, Minghim R. 2015. InteractiVenn: a web-based tool for the analysis of sets through Venn diagrams. BMC Bioinformatics. 16(1):169. doi:10.1186/s12859-015-0611-3.

Hirata Y, Kondo H, Ozawa Y. 2014. Natural rubber (NR) for the tyre industry. In: Chemistry, Manufacture and Applications of Natural Rubber. Elsevier. p. 325–352. [accessed 2022 Mar 1]. https://linkinghub.elsevier.com/retrieve/pii/B9780857096838500124.

Hüffer T, Wagner S, Reemtsma T, Hofmann T. 2019. Sorption of organic substances to tire wear materials: Similarities and differences with other types of microplastic. TrAC trends in analytical chemistry. 113:392–401. doi:10.1016/j.trac.2018.11.029.

Hüffer T, Wehrhahn M, Hofmann T. 2020. The molecular interactions of organic compounds with tire crumb materials differ substantially from those with other microplastics. Environmental Science: Processes & Impacts. 22(1):121–130. doi:10.1039/C9EM00423H.

ISO, 2012. Rubber - vocabulary. [WWW Document]. 1382:2012. URL. https://www.iso.org/standard/68018.html Accessed date: 1 March 2022.

Jalili V, Afgan E, Gu Q, Clements D, Blankenberg D, Goecks J, Taylor J, Nekrutenko A. 2020. The Galaxy platform for accessible, reproducible and collaborative biomedical analyses: 2020 update. Nucleic Acids Research. 48(W1):W395–W402. doi:10.1093/nar/gkaa434.

Johnson, Allie, "Effects of Environmental Aging on the Acute Toxicity and Chemical Composition of Various Microplastic Leachates" (2021). *WWU Graduate School Collection*. 1064. https://cedar.wwu.edu/wwuet/1064

Khan FR, Halle LL, Palmqvist A. 2019. Acute and long-term toxicity of micronized car tire wear particles to *Hyalella azteca*. Aquatic Toxicology. 213:105216. doi:10.1016/j.aquatox.2019.05.018.

Kitabatake M, So MW, Tumbula DL, Söll D. 2000. Cysteine biosynthesis pathway in the Archaeon *Methanosarcina barkeri* encoded by acquired bacterial genes? Journal of Bacteriology. 182(1):143–145. doi:10.1128/JB.182.1.143-145.2000.

Knocke W, Hemphill W. 1981. Mercury(II) sorption by waste rubber. Water Research. 15(2):275–282. doi:10.1016/0043-1354(81)90121-4.

Kole PJ, Löhr AJ, Van Belleghem FGAJ, Ragas AMJ. 2017. Wear and tear of tyres: A stealthy source of microplastics in the environment. International Journal of Environmental Research and Public Health. 14(10):1265. doi:10.3390/ijerph14101265.

Kramerova IA, Kawaguchi N, Fessler LI, Nelson RE, Chen Y, Kramerov AA, Kusche-Gullberg M, Kramer JM, Ackley BD, Sieron AL, et al. 2000. Papilin in development; a pericellular protein with a homology to the ADAMTS metalloproteinases. Development. 127(24):5475–5485. doi:10.1242/dev.127.24.5475.

Kreider ML, Panko JM, McAtee BL, Sweet LI, Finley BL. 2010. Physical and chemical characterization of tire-related particles: Comparison of particles generated using different methodologies. Science of The Total Environment. 408(3):652–659. doi:10.1016/j.scitotenv.2009.10.016.

Kumar K, Mhetre A, Ratnaparkhi GS, Kamat SS. 2021. A superfamily-wide activity atlas of serine hydrolases in *Drosophila melanogaster*. Biochemistry. 60(16):1312–1324. doi:10.1021/acs.biochem.1c00171.

Laughlin F, Linden O. 1983. Oil pollution and Baltic mysids: acute and chronic effects of the water soluble fractions of light fuel oil on the mysid shrimp *Neomysis integer*. Mar Ecol Prog Ser. 12:29–41. doi:10.3354/meps012029.

Li X, Berger W, Musante C, Mattina MI. 2010. Characterization of substances released from crumb rubber material used on artificial turf fields. Chemosphere. 80(3):279–285. doi:10.1016/j.chemosphere.2010.04.021.

Mantovani A, Garlanda C, Bottazzi B. 2003. Pentraxin 3, a non-redundant soluble pattern recognition receptor involved in innate immunity. Vaccine. 21:S43–S47. doi:10.1016/S0264-410X(03)00199-3.

Martens M, Verbruggen T, Nymark P, Grafström R, Burgoon LD, Aladjov H, Torres Andón F, Evelo CT, Willighagen EL. 2018. Introducing WikiPathways as a data-source to support Adverse Outcome Pathways for regulatory risk assessment of chemicals and nanomaterials. Front Genet. 9:661. doi:10.3389/fgene.2018.00661.

Matsuda Y, Osaki T, Hashii T, Koshiba T, Kawabata S. 2007. A cysteine-rich protein from an arthropod stabilizes clotting mesh and immobilizes bacteria at injury sites. Journal of Biological Chemistry. 282(46):33545–33552. doi:10.1074/jbc.M705854200.

McIntyre JK, Prat J, Cameron J, Wetzel J, Mudrock E, Peter KT, Tian Z, Mackenzie C, Lundin J, Stark JD, et al. 2021. Treading Water: Tire wear particle leachate recreates an urban runoff mortality syndrome in coho but not chum salmon. Environ Sci Technol. 55(17):11767–11774. doi:10.1021/acs.est.1c03569.

McKenney, CL. 1982. Interrelationships between energy metabolism, growth dynamics, and reproduction during the life cycle of *Mysidopsis bahia* as influenced by sublethal endrin exposure. In: Physiological Mechanisms of Marine Pollutant Toxicity. p. 447-476. Vernberg W.B., Calabrese A., Thurberg F.P., and Vernberg F.J. Eds., Academic Press, New York.

McKenney C.L. 1985. Associations between physiological alterations and population changes in an estuarine mysid during chronic exposure to a pesticide. In: Marine Pollution and Physiology, Recent Advances. p. 397-418. Vernberg F.J., Thurberg F.P., Calabrese A., and Vernberg W.B. Eds., University of South Carolina Press, Columbia.

McKenney CL, Matthews E. 1990. Alterations in the energy metabolism of an estuarine mysid (*Mysidopsis bahia*) as indicators of stress from chronic pesticide exposure. Marine Environmental Research. 30(1):1–19. doi:10.1016/0141-1136(90)90007-B.

McKenney CL, Hamaker TL, Matthews E. 1991. Changes in the physiological performance and energy metabolism of an estuarine mysid (*Mysidopsis bahia*) exposed in the laboratory through a complete life cycle to the defoliant DEF. Aquatic Toxicology. 19(2):123–135. doi:10.1016/0166-445X(91)90032-5.

McKenney CL. 2018. Physiological dysfunction in estuarine mysids and larval decapods with chronic pesticide exposure. In: Microscale Testing in Aquatic Toxicology. 1st ed. p. 465–476. Wells PG, Lee K, Blaise C, editors. CRC Press. [accessed 2022 May 25].

McKim JM, Bradbury SP, Niemi GJ. 1987. Fish acute toxicity syndromes and their use in the QSAR approach to hazard assessment. Environ Health Perspect. 71:171–186. doi:10.1289/ehp.8771171.

Mees J, Meland K. (Eds) (2012 onwards). World List of Lophogastrida, Stygiomysida and Mysida. Accessed at https://www.marinespecies.org/mysidacea on 2022-01-12. doi:10.14284/369

Meland K, Mees J, Porter M, Wittmann KJ. 2015. Taxonomic Review of the Orders Mysida and Stygiomysida (Crustacea, Peracarida). PLOS ONE. 10(4):e0124656. doi:10.1371/journal.pone.0124656.

Molenock J. 1969. *Mysidopsis bahia*, a new species of mysid (Crustacea: Mysidacea) from Galveston Bay, Texas. Tulane studies in zoology and botany. 15(3):113–116.

Mosavi LK, Cammett TJ, Desrosiers DC, Peng Z. 2004. The ankyrin repeat as molecular architecture for protein recognition. Protein Sci. 13(6):1435–1448. doi:10.1110/ps.03554604.

Netzer A, Norman JD. 1973. Removal of trace metals from wastewater by activated carbon. Water Quality Research Journal. 8(1):110–121. doi: 10.2166/wqrj.1973.009

Netzer A, Wilkinson P. 1974. Removal of heavy metals from wastewater utilizing discarded automotive tires. Water Quality Research Journal. 9(1):62–66. doi:10.2166/wqrj.1974.007.

Nguyen B, Claveau-Mallet D, Hernandez LM, Xu EG, Farner JM, Tufenkji N. 2019. Separation and analysis of microplastics and nanoplastics in complex environmental samples. Acc Chem Res. 52(4):858–866. doi:10.1021/acs.accounts.8b00602.

Nimmo DR, Bahner LH, Rigby RA, Sheppard JM, Wilson AJJr. 1977. *Mysidopsis bahia*: An Estuarine Species Suitable for Life-Cycle Toxicity Tests to Determine the Effects of a Pollutant. Aquatic Toxicology and Hazard Evaluation.:109–116.

Nimmo DR, Hamaker TL. 1982. Mysids in toxicity testing - a review. Hydrobiologia. 93:171–178. doi:https://doi-org.offcampus.lib.washington.edu/10.1007/BF00008110.

Ogonowski, M., K. Andersson, and S. Hansson. 2012. A weight- and temperature-dependent model of respiration in *Praunus flexuosus* (Crustacea, Mysidacea). Journal of Plankton Research 34:642–645.

Ozaki H, Watanabe I, Kuno K. 2004. Investigation of the heavy metal sources in relation to automobiles. Water, Air, & Soil Pollution. 157(1):209–223. doi:10.1023/B:WATE.0000038897.63818.f7.

Park K, Kwak I-S. 2020. Cadmium-induced developmental alteration and upregulation of serine-type endopeptidase transcripts in wild freshwater populations of *Chironomus plumosus*. Ecotoxicology and Environmental Safety. 192:110240. doi:10.1016/j.ecoenv.2020.110240.

Peter KT, Tian Z, Wu C, Lin P, White S, Du B, McIntyre JK, Scholz NL, Kolodziej EP. 2018. Using high-resolution mass spectrometry to identify organic contaminants linked to urban stormwater mortality syndrome in coho salmon. Environ Sci Technol. 52(18):10317–10327. doi:10.1021/acs.est.8b03287.

Price WW, Heard RW, Stuck L. 1994. Observations on the genus *Mysidopsis* Sars, 1864 with the designation of a new genus, *Americamysis*, and the descriptions of *Americamysis alleni* and *A. stucki* (Peracarida: Mysidacea *Mysidae*), from the Gulf of Mexico. 107(4):680–698.

Rhodes EP, Ren Z, Mays DC. 2012. Zinc leaching from tire crumb rubber. Environ Sci Technol. 46(23):12856–12863. doi:10.1021/es3024379.

Roast, S. D., J. Widdows, and M. B. Jones. 1999. Respiratory responses of the estuarine mysid *Neomysis integer* (Peracarida: Mysidacea) in relation to a variable environment. Marine Biology 133:643–649.

Roberts, P. Matt, "Effects of environmental weathering on the acute toxicity of tire wear particle eluate to the mysid shrimp, *Americamysis bahia*" (2021). *WWU Graduate School Collection*. 1072. https://cedar.wwu.edu/wwuet/1072

Robinson MD, McCarthy DJ, Smyth GK. 2010. edgeR: a Bioconductor package for differential expression analysis of digital gene expression data. Bioinformatics. 26(1):139–140. doi:10.1093/bioinformatics/btp616.

Rodenburg KW, Van der Horst DJ. 2005. Lipoprotein-mediated lipid transport in insects: analogy to the mammalian lipid carrier system and novel concepts for the functioning of LDL receptor family members. Biochim Biophys Acta. 1736(1):10–29. doi:10.1016/j.bbalip.2005.07.002.

Rowley A. 1984. Mechanisms of metal adsorption from aqueous solutions by waste tyre rubber. Water Research. 18(8):981–984. doi:10.1016/0043-1354(84)90248-3.

Sadiq M, Alam I, El-Mubarek A, Al-Mohdhar HM. 1989. Preliminary evaluation of metal pollution from wear of auto tires. Bull Environ Contam Toxicol. 42(5):743–748. doi:10.1007/BF01700397.

Senkbeil EG, Wriston JC. 1981. Hemocyanin synthesis in the American lobster, *Homarus americanus*. Comparative Biochemistry and Physiology Part B: Comparative Biochemistry. 68(1):163–171. doi:10.1016/0305-0491(81)90198-X.

Siddiqui S, Dickens JM, Cunningham BE, Hutton SJ, Pedersen EI, Harper B, Harper S, Brander SM. 2022. Internalization, reduced growth, and behavioral effects following exposure to micro and nano tire particles in two estuarine indicator species. Chemosphere.:133934. doi:10.1016/j.chemosphere.2022.133934.

Sommer F, Dietze V, Baum A, Sauer J, Gilge S, Maschowski C, Gieré R. 2018. Tire abrasion as a major source of microplastics in the environment. Aerosol Air Qual Res. 18(8):2014–2028. doi:10.4209/aaqr.2018.03.0099.

Spicer JI, Weber RE. 1991. Respiratory impairment in crustaceans and molluscs due to exposure to heavy metals. Comparative Biochemistry and Physiology Part C: Comparative Pharmacology. 100(3):339–342. doi:10.1016/0742-8413(91)90005-E.

Spicer JI, Weber RE. 1992. Respiratory impairment by water-borne copper and zinc in the edible crab *Cancer pagurus* (L.) (Crustacea: Decapoda) during hypoxic exposure. Marine Biology. 112(3):429–435. doi:10.1007/BF00356288.

Tajiri R, Ogawa N, Fujiwara H, Kojima T. 2017. Mechanical control of whole body shape by a single cuticular protein obstructor-E in *Drosophila melanogaster*. PLOS Genetics. 13(1):e1006548. doi:10.1371/journal.pgen.1006548.

Tian Z, Zhao H, Peter KT, Gonzalez M, Wetzel J, Wu C, Hu X, Prat J, Mudrock E, Hettinger R, et al. 2021. A ubiquitous tire rubber–derived chemical induces acute mortality in coho salmon. Science. 371(6525):185–189. doi:10.1126/science.abd6951.

Toda, H., T. Arima, M. Takahashi, and S. Ichimura. 1987. Physiological evaluation of temperature effect on the growth processes of the mysid, *Neomysis intermedia* Czerniawsky. Journal of Plankton Research 9:51–63.

United Nations Environment Programme (2018). Mapping of global plastics value chain and plastics losses to the environment (with a particular focus on marine environment). Ryberg, M., Laurent, A., Hauschild, M. United Nations Environment Programme. Nairobi, Kenya

USEPA. 2002*a*. Methods for measuring the acute toxicity of effluents and receiving waters to freshwater and marine organisms. [accessed 2022 Jun 29]. https://www.epa.gov/sites/default/files/2015-08/documents/acute-freshwater-and-marine-wet-manual_2002.pdf.

USEPA. 2002*b*. Method 1007.0: Mysid, *Mysidopsis bahia*, survival, growth, and fecundity test; chronic toxicity. Office of Water, Washington D.C. p 1-80. [accessed 2022 June 29]. https://www.epa.gov/sites/default/files/2015-12/documents/method_1007_2002.pdf

USEPA. 2016. Office of Chemical Safety and Pollution Prevention. OCSPP 850.1035 Mysid acute toxicity test. USEPA. EPA 712-C-16-011. https://beta.regulations.gov/document/EPA-HQ-OPPT-2009-0154-0038

USEPA. 2016*b*. National Recommended Water Quality Criteria - Aquatic Life Criteria Table. https://www.epa.gov/wqc/national-recommended-water-quality-criteria-aquatic-life-criteria-table, accessed 2/23/22.

Veith GD, Broderius SJ. 1990. Rules for distinguishing toxicants that cause type I and type II narcosis syndromes. Environ Health Perspect. 87:207–211. doi:10.1289/ehp.9087207

Vernberg WB, Vernberg J. 1971. The synergistic effects of temperature, salinity, and mercury on survival and metabolism of the adult fiddler crab, *Uca pugilator*. Fishery Bulletin. 70:415–420.

Vernberg WB, DeCoursey PJ, Padgett WJ. 1973. Synergistic effects of environmental variables on larvae of Uca pugilator. Mar Biol. 22(4):307–312. doi:10.1007/BF00391386.

Verschoor A, de Poorter L, Dröge R, Kuenen J, de Valk E. 2016. Emission of microplastics and potential mitigation measures: Abrasive cleaning agents, paints and tyre wear. National Institute for Public Health and the Environment. RIVM Report 2016-0026.

Villeneuve, D. L., D. Crump, N. Garcia-Reyero, M. Hecker, T. H. Hutchinson, C. A. LaLone, B. Landesmann, T. Lettieri, S. Munn, M. Nepelska, M. A. Ottinger, L. Vergauwen, and M. Whelan. 2014a. Adverse outcome pathway (AOP) development I: Strategies and principles. Toxicological Sciences 142:312–320.

Villeneuve, D. L., D. Crump, N. Garcia-Reyero, M. Hecker, T. H. Hutchinson, C. A. LaLone, B. Landesmann, T. Lettieri, S. Munn, M. Nepelska, M. A. Ottinger, L. Vergauwen, and M. Whelan. 2014b. Adverse outcome pathway development II: Best practices. Toxicological Sciences 142:321–330.

Wachtendorf V, Kalbe U, Krüger O, Bandow N. 2017. Influence of weathering on the leaching behaviour of zinc and PAH from synthetic sports surfaces. Polymer Testing. 63:621–631. doi:10.1016/j.polymertesting.2017.09.021.

Wagner S, Hüffer T, Klöckner P, Wehrhahn M, Hofmann T, Reemtsma T. 2018. Tire wear particles in the aquatic environment - A review on generation, analysis, occurrence, fate and effects. Water Research. 139:83–100. doi:10.1016/j.watres.2018.03.051.

Wik A, Dave G. 2006. Acute toxicity of leachates of tire wear material to *Daphnia magna*—Variability and toxic components. Chemosphere. 64(10):1777–1784. doi:10.1016/j.chemosphere.2005.12.045.

Wik A, Dave G. 2009. Occurrence and effects of tire wear particles in the environment – A critical review and an initial risk assessment. Environmental Pollution. 157(1):1–11. doi:10.1016/j.envpol.2008.09.028.

Xu S, Jing M, Kong D-M, Wang Y-R, Zhou Q, Liu W-Y, Jiao F, Li Y-J, Xie S-Y. 2021. Chitin binding protein from the kuruma shrimp *Marsupenaeus japonicus* facilitates the clearance of *Vibrio anguillarum*. Dev Comp Immunol. 117:103981. doi:10.1016/j.dci.2020.103981.

Yang F, Li S, Li F, Xiang J. 2018. A cuticle protein from the Pacific white shrimp *Litopenaeus vannamei* involved in WSSV infection. Developmental & Comparative Immunology. 81:303–311. doi:10.1016/j.dci.2017.12.018.

Zhao R, Aluri S, Goldman ID. 2017. The proton-coupled folate transporter (PCFT-SLC46A1) and the syndrome of systemic and cerebral folate deficiency of infancy: Hereditary folate malabsorption. Mol Aspects Med. 53:57–72. doi:10.1016/j.mam.2016.09.002.

Zhao T, Su Z, Li Y, Zhang X, You Q. 2020. Chitinase-3 like-protein-1 function and its role in diseases. Sig Transduct Target Ther. 5(1):1–20. doi:10.1038/s41392-020-00303-7.

Ziegler WH, Soetje B, Marten LP, Wiese J, Burute M, Haffner D. 2020. Fibrocystin is essential to cellular control of adhesion and epithelial morphogenesis. IJMS. 21(14):5140. doi:10.3390/ijms21145140.

Appendix A

Number of input read pairs, number of reads both surviving after being trimmed, number of reads pseudo-aligned to the *de novo* assembled reference transcriptome, percent of reads both surviving, and the percent pseudo-alignment rates of every replicate sample in the *de novo* assembled reference transcriptome.

Treatment	Concentration (g/L)	Replicate	# Input Read Pairs	# Reads Both Surviving	# Reads pseudo-aligned	% Reads both surviving	% Reads pseudo-aligned
Control	0.00	1	44745153	38020554	26636832	84.97	70.10
	0.00	2	39274966	33719164	23604386	85.85	70.00
	0.00	3	40290216	34766298	24682350	86.29	71.00
	0.00	4	30668655	25492272	18081326	83.12	70.90
	0.00	5	40755006	34192035	24033343	83.90	70.30
Weathered	0.67	1	40036970	33103970	23793190	82.68	71.90
	0.67	2	36024135	30212251	21127377	83.87	69.90
	0.67	3	38032799	32321821	22964831	84.98	71.10
	0.67	4	41844633	35595693	24905343	85.07	70.00
	0.67	5	39214286	33897663	23989433	86.44	70.80
	1.34	1	33677956	28616510	20098353	84.97	70.20
	1.34	2	44928693	38393216	27041420	85.45	70.40
	1.34	3	40909262	34424897	23604333	84.15	68.60
	1.34	4	38063954	32637992	23300436	85.75	71.40
	1.34	5	43996037	37627845	26599681	85.53	70.70
	2.68	1	44065714	36649402	25725956	83.17	70.20
	2.68	2	36332398	30669400	21541998	84.41	70.20
	2.68	3	47203128	39522310	27765099	83.73	70.30
	2.68	4	44446019	37318670	25480912	83.96	68.30
	2.68	5	36232479	31246795	21963458	86.24	70.30
Un-weathered	0.27	1	38018418	31790196	22301911	83.62	70.20
	0.27	2	45140338	38011046	27161000	84.21	71.50
	0.27	3	34363826	29520320	20837234	85.91	70.60
	0.27	4	47269346	40541483	28390588	85.77	70.00
	0.27	5	33512159	28840504	20342087	86.06	70.50
	0.54	1	38476943	32857555	23741620	85.40	72.30
	0.54	2	37849023	31841353	22402649	84.13	70.40
	0.54	3	46629407	39503392	27533170	84.72	69.70
	0.54	4	36390397	30963608	21898475	85.09	70.70
	0.54	5	35278865	29686362	21200672	84.15	71.40
	1.08	1	43384343	36984812	26035944	85.25	70.40
	1.08	2	36997524	31540755	22235260	85.25	70.50
	1.08	3	37106569	31372641	21768326	84.55	69.40
	1.08	4	37993905	30478673	21275297	80.22	69.80
	1.08	5	44169520	37483234	26206777	84.86	69.90

Appendix B

The number of shrimp in each respiration chamber replicate for each concentration, day of exposure, and leachate type. The range is between 2-11 surviving shrimp, with the majority of chambers containing between 8-10 surviving shrimp, and the number of shrimp in each chamber was used to calculate mean individual respiration rates reported in Appendix C.

Leachate Treatment	Days of exposure	Concentration (g/L)	Replicate	#Shrimp in respiration chamber
Weathered	2 days	0.00	R1	10
			R2	10
			R3	10
		0.17	R1	10
			R2	10
			R3	10
		0.33	R1	10
			R2	10
			R3	11
		0.67	R1	10
			R2	9
			R3	11
		1.34	R1	10
			R2	10
			R3	10
		2.68	R1	10
			R2	9
			R3	10
	4 days	0.00	R1	10
			R2	10
			R3	10
		0.17	R1	10
			R2	9
			R3	10
		0.33	R1	10
			R2	10
			R3	10
		0.67	R1	10
			R2	10
			R3	9
		1.34	R1	8
			R2	9
			R3	9
		2.68	R1	5
			R2	2
			R3	8
	6 days	0.00	R1	10
			R2	9
			R3	10
		0.17	R1	8
			R2	9
			R3	10
		0.33	R1	9
			R2	10
			R3	9
		0.67	R1	8
			R2	8
			R3	9
		1.34	R1	7
			R2	7
			R3	8
		2.68	R1	2
			R2	2
			R3	3

Un-weathered	2 days	0.00	R1	10
			R2	10
			R3	9
		0.07	R1	10
			R2	10
			R3	10
		0.14	R1	10
			R2	10
			R3	10
		0.27	R1	9
			R2	11
			R3	10
		0.54	R1	10
			R2	10
			R3	10
		1.08	R1	10
			R2	10
			R3	10
	4 days	0.00	R1	10
			R2	10
			R3	9
		0.07	R1	10
			R2	10
			R3	10
		0.14	R1	10
			R2	9
			R3	10
		0.27	R1	8
			R2	10
			R3	9
		0.54	R1	10
			R2	10
			R3	10
		1.08	R1	9
			R2	8
			R3	8
	6 days	0.00	R1	10
			R2	10
			R3	9
		0.07	R1	10
			R2	10
			R3	10
		0.14	R1	10
			R2	9
			R3	9
		0.27	R1	8
			R2	10
			R3	9
		0.54	R1	10
			R2	10
			R3	8
		1.08	R1	3
			R2	5
			R3	6

Appendix C

Mean mysid respiration rates (µg O2 mg d.w.-1 hr -1) and mean % changes in respiration rates relative to control animals are reported after 2 days, 4 days, and 6 days of exposure to leachate for each of two leachate types, "weathered" and "un-weathered". The mean individual respiration rate for the control (0.00 g/L), marked with an asterisk for each day of exposure and leachate treatment, represents the respective BRR_x used in Equation 1 to calculate the % change in respiration rate in shrimp exposed to leachate for each of 3 replicates. The mean % change respiration rates reported here are the average of the 3 replicates at each concentration. Positive mean % change values indicate inhibition in respiration rates relative to the controls, while negative mean % change values indicate stimulation relative to the controls.

Leachate Treatment	Days of exposure	Concentration (g/L)	Mean individual respiration rate (µg O_2 mg d.w.$^{-1}$ hr $^{-1}$)	Mean % change in respiration (relative to control)
Weathered	2 days	0.00	8.25*	NA
		0.17	5.78	29.89
		0.33	7.38	10.48
		0.67	11.93	-44.73
		1.34	12.16	-47.51
		2.68	16.31	-97.79
	4 days	0.00	4.05*	NA
		0.17	5.07	-25.17
		0.33	5.79	-42.86
		0.67	5.19	-28.12
		1.34	4.99	-23.16
		2.68	6.42	-58.42
	6 days	0.00	6.26*	NA
		0.17	5.40	13.72
		0.33	5.41	13.65
		0.67	5.33	14.93
		1.34	4.12	34.28
		2.68	8.38	-33.75
Un-weathered	2 days	0.00	6.74*	NA
		0.07	4.83	28.36
		0.14	6.16	8.69
		0.27	5.58	17.19
		0.54	5.72	15.24
		1.08	7.23	-7.23
	4 days	0.00	5.38*	NA
		0.07	4.80	10.92
		0.14	6.26	-16.23
		0.27	5.35	0.52
		0.54	4.80	10.92
		1.08	9.11	-69.18
	6 days	0.00	4.77*	NA
		0.07	4.43	7.18
		0.14	4.55	4.62
		0.27	4.73	0.92
		0.54	3.87	18.87
		1.08	10.21	-114.01

Appendix D

Dysregulated contig sequences (represented by the "Contig ID" column) in *Americamysis bahia* exposed to TWP leachates. There are 80 contig IDs in the weathered group and 139 contig IDs in the un-weathered group. The "Concentration Overlap" column details which concentrations a certain contig ID was dysregulated in; some contig IDs are dysregulated in more than one concentration; there are a total of 86 dysregulated contigs in the weathered group (including those shared in common between concentrations) and 152 dysregulated contigs in the un-weathered group (including those shared in common between concentrations). For each contig ID and for each concentration in which it was dysregulated, whether it was up-regulated or down-regulated relative to the control was specified, and the level of expression (measured in fold change (FC) and log2foldchange (log2FC)), counts (measured in counts per million (CPM) and log2counts per million (log2CPM)), and the false discovery rate adjusted p-value (FDR) was included. Finally, the gene description of orthologous genes (in all arthropods) was included, where possible, for each dysregulated contig ID. In the weathered group, 64 out of the 80 contig IDs had a gene description (~80%), leaving 16 out of 80 (~20%) without a description. In the un-weathered group, 112 out of the 139 contig IDs had a gene description (~81%), leaving 27 out of 139 (~19%) without a description. Rows with $|FC| \geq 5$ and CPM > 100 are indicated.

Treatment	Contig ID found in *A. bahia* (from *de novo* assembly)	Concentration Overlap	Concentration (g/L)	Dysregulation	FC	log2FC	CPM	log2CPM	FDR	Gene description - orthologous genes in arthropods (from annotation file)	|FC| > 5?	CPM > 100?
Weathered	TRINITY_DN11316_c0_g1_i17	Highest	2.68	Downregulated	-2.625972829	-1.392851989	143.2995464	7.162890233	0.000199	probable deoxycytidylate deaminase	No	Yes
	TRINITY_DN11355_c0_g1_i1	Highest	2.68	Upregulated	2.748297716	1.458538296	14.37980371	3.845972077	0.013597	uncharacterized protein LOC113805697	No	No
	TRINITY_DN11617_c0_g1_i3	Highest	2.68	Upregulated	2.606659504	1.382202142	7.31071537	2.870012584	0.033979016	rhomboid-related protein 2-like isoform X1	No	No
	TRINITY_DN11842_c0_g1_i11	Highest	2.68	Upregulated	2.083429217	1.058960087	19.42878222	4.280123572	0.023304102	---NA---	No	No
	TRINITY_DN12572_c0_g1_i10	Highest	2.68	Upregulated	2.248914711	1.169228948	9.754434554	3.286058245	0.007363927	Dual specificity protein phosphatase 14	No	No
	TRINITY_DN13160_c0_g1_i5	Highest	2.68	Downregulated	-7.833276679	-2.969615917	83.10495887	6.37686266	1.68E-09	chitinase-3-like protein 1	Yes	No
	TRINITY_DN1475_c1_g1_i1	Highest	2.68	Upregulated	2.605339311	1.381471277	13.64761213	3.770576645	0.000388	peritrophin-48-like isoform X1	No	No
	TRINITY_DN1475_c1_g1_i13	Highest	2.68	Upregulated	2.193617169	1.133311768	58.28845949	5.865138368	0.000358	peritrophin-48-like isoform X1	No	No
	TRINITY_DN15559_c0_g1_i10	Highest	2.68	Upregulated	2.944039315	1.557796937	191.67777	7.582539219	8.10E-05	apolipoprotein D-like	No	Yes
	TRINITY_DN15803_c0_g1_i3	Highest	2.68	Upregulated	3.279348662	1.713409298	59.74975263	5.900860835	0.000112	oplophorus-luciferin 2-monooxygenase non-catalytic subunit-like	No	No
	TRINITY_DN1613_c0_g1_i15	Highest	2.68	Upregulated	2.308303832	1.206833132	181.8828849	7.506865982	0.011331598	obstructor F2	No	Yes
	TRINITY_DN16678_c0_g1_i2	Highest	2.68	Upregulated	2.34929355	1.232226993	18.24185746	4.189180733	0.012013415	sequestosome-1 isoform X1	No	No
	TRINITY_DN19142_c0_g1_i5	Highest	2.68	Upregulated	2.68519649	1.425027662	14.6876141	3.876528154	0.003024442	acetylcholinesterase-like precursor	No	No
	TRINITY_DN19212_c0_g1_i2	Highest	2.68	Downregulated	-2.547831448	-1.349269839	18.75050667	4.228857675	1.79E-05	---NA---	No	No
	TRINITY_DN19891_c0_g1_i1	Highest	2.68	Upregulated	2.463806091	1.300888716	183.7310776	7.521451865	1.21E-07	peritrophin-44-like protein	No	Yes
	TRINITY_DN2003_c0_g2_i1	Highest	2.68	Upregulated	3.050954936	1.609260871	183.1815391	7.517130307	3.18E-08	juvenile hormone binding protein 7	No	Yes
	TRINITY_DN22786_c0_g1_i1	Highest	2.68	Downregulated	-2.591248228	-1.373647225	7.487691922	2.904521077	1.50E-05	delta(24)-sterol reductase-like	No	No
	TRINITY_DN22848_c0_g1_i1	Highest	2.68	Upregulated	2.81925261	1.495312752	59.51047892	5.895071823	0.002398607	Hemocyanin A chain	No	No
	TRINITY_DN22896_c0_g1_i3	Highest	2.68	Upregulated	2.746494996	1.457591663	362.660646	8.50247639	2.66E-05	C-type lectin 3	No	Yes
	TRINITY_DN2376_c0_g1_i7	Highest	2.68	Upregulated	2.1563704	1.108605011	59.96197584	5.905976018	0.003237425	Acyl-coenzyme A thioesterase 1	No	No
	TRINITY_DN2594_c0_g1_i5	Highest	2.68	Upregulated	3.003517626	1.58665313	10.65061695	3.412865097	0.010930361	pentraxin-related protein PTX3-like	No	No
	TRINITY_DN2668_c0_g1_i5	Highest	2.68	Upregulated	2.454185789	1.295244469	85.27756097	6.414094271	0.000199	prophenoloxidase 2	No	No
	TRINITY_DN27246_c0_g1_i19	Highest	2.68	Upregulated	2.972649331	1.571749286	3.447927256	1.785729337	0.029856268	microsomal glutathione S-transferase 1-like	No	No
	TRINITY_DN28702_c0_g1_i8	Highest	2.68	Downregulated	-2.057281557	-1.040739253	13.58864165	3.764329343	1.41E-05	---NA---	No	No
	TRINITY_DN2935_c0_g1_i11	Highest	2.68	Upregulated	27.67957249	4.790749755	32.06365237	5.002866867	3.19E-05	putative ankyrin repeat protein RF_0381 isoform X4	Yes	No
	TRINITY_DN2935_c0_g1_i12	Highest	2.68	Upregulated	15.75552812	3.977786209	11.46117016	3.518682442	0.002268794	putative ankyrin repeat protein RF_0381 isoform X4	Yes	No
	TRINITY_DN3120_c0_g1_i35	Highest	2.68	Upregulated	3.104972966	1.634580707	64.33524417	6.007537387	3.19E-05	carboxypeptidase B	No	No
	TRINITY_DN3295_c0_g1_i10	Highest	2.68	Upregulated	3.172561125	1.66564796	453.2709867	8.824230009	4.45E-05	C-type lectin	No	Yes
	TRINITY_DN3295_c12_g1_i5	Highest	2.68	Upregulated	2.722847944	1.445116418	12.2715112	3.617241019	9.22E-07	serine protease 1	No	No
	TRINITY_DN3592_c3_g1_i1	Highest	2.68	Upregulated	2.009458398	1.00680671	9.472490041	3.243743718	0.003237425	putative zinc metalloproteinase	No	No
	TRINITY_DN4099_c0_g1_i6	Highest	2.68	Upregulated	2.27444501	1.185514555	54.82342991	5.776720685	0.005634874	Glutathione peroxidase	No	No
	TRINITY_DN4191_c0_g1_i4	Highest	2.68	Upregulated	2.12297898	1.086090087	35.71922249	5.158628772	0.016889115	prophenoloxidase activating factor	No	No
	TRINITY_DN4318_c5_g1_i2	Highest	2.68	Downregulated	-3.323095589	-1.732527793	11.82403605	3.563650668	0.035449265	---NA---	No	No
	TRINITY_DN4367_c0_g1_i2	Highest	2.68	Downregulated	-2.813720996	-1.492479281	17.05966659	4.092517546	0.02824576	---NA---	No	No
	TRINITY_DN4548_c0_g1_i1	Highest	2.68	Upregulated	4.3569919	2.123332431	15.45061246	3.949592122	7.10E-06	Anti-lipopolysaccharide factor	No	No
	TRINITY_DN4854_c0_g1_i1	Highest	2.68	Upregulated	2.074165036	1.052530691	192.4307038	7.5881952	0.000676	uncharacterized protein LOC119573628	No	Yes
	TRINITY_DN500_c0_g1_i12	Highest	2.68	Upregulated	4.303975989	2.10567003	7.709729734	2.946680287	0.000266	---NA---	No	No
	TRINITY_DN504_c0_g1_i5	Highest	2.68	Upregulated	2.003301255	1.002379389	61.86644679	5.951085272	0.030083839	sarcosine dehydrogenase, mitochondrial-like	No	No
	TRINITY_DN5071_c0_g1_i1	Highest	2.68	Upregulated	9.152409731	3.194151639	3.556835449	1.830594232	0.010930361	---NA---	Yes	No
	TRINITY_DN5090_c4_g2_i3	Highest	2.68	Upregulated	3.638131078	1.863197523	435.550561	8.766696394	3.93E-09	PREDICTED: uncharacterized protein LOC108673189	No	Yes
	TRINITY_DN5399_c0_g1_i1	Highest	2.68	Upregulated	2.165607826	1.114772006	322.2026729	8.331824652	8.39E-16	fibrocystin-L-like	No	Yes
	TRINITY_DN58469_c0_g1_i3	Highest	2.68	Upregulated	2.037779434	1.026997905	50.571353	5.660248472	2.46E-07	Gamma-interferon-inducible lysosomal thiol reductase	No	No
	TRINITY_DN5963_c0_g1_i3	Highest	2.68	Upregulated	4.480617815	2.163697674	50.58487847	5.660634274	0.004133451	CUB domain	No	No
	TRINITY_DN6098_c0_g1_i1	Highest	2.68	Upregulated	5.474313285	2.452678	26.63128505	4.73505014	1.79E-05	hypothetical protein Anas_12496	Yes	No
	TRINITY_DN6257_c0_g1_i10	Highest	2.68	Upregulated	2.63395227	1.397229203	15.78095993	3.98011306	0.009314187	chymotrypsin-like proteinase	No	No

TRINITY_DN6589_c0_g1_i1	Highest	2.68	Upregulated	2.234243385	1.159786353	7.135511667	2.835016885	1.89E-06	molt-inhibiting hormone	No	No
TRINITY_DN6598_c0_g2_i1	Highest	2.68	Downregulated	-2.311533589	-1.208850326	21.13884478	4.401824632	0.006931989	gamma-butyrobetaine dioxygenase-like isoform X1	No	No
TRINITY_DN6695_c0_g2_i4	Highest	2.68	Upregulated	2.76869423	1.469205734	309.9650782	8.275961875	0.000471	uncharacterized protein LOC119573322	No	Yes
TRINITY_DN6695_c0_g2_i5	Highest	2.68	Upregulated	3.869926458	1.952306151	79.41365914	6.311315267	0.000463	uncharacterized protein LOC119573322	No	No
TRINITY_DN672_c0_g1_i20	Highest	2.68	Upregulated	3.876427491	1.954727679	27.07247447	4.758754853	1.77E-05	papilin isoform X4	No	No
TRINITY_DN672_c0_g1_i29	Highest	2.68	Upregulated	4.268972945	2.093889019	8.907240901	3.154978613	0.000433	—NA—	No	No
TRINITY_DN672_c0_g1_i8	Highest	2.68	Upregulated	4.090324453	2.032215285	20.0928035	4.328606969	1.19E-05	—NA—	No	No
TRINITY_DN6849_c3_g1_i4	Highest	2.68	Downregulated	-2.264170476	-1.178982587	167.4208128	7.387335076	0.012013415	oplophorus-luciferin 2-monooxygenase non-catalytic subunit-like	No	No
TRINITY_DN734_c0_g1_i13	Highest	2.68	Upregulated	4.014034081	2.005052866	4.901837498	2.293322658	0.001303859	uncharacterized protein LOC119576313	No	No
TRINITY_DN736_c0_g1_i15	Highest	2.68	Upregulated	2.264526048	1.179209134	4.176009654	2.062125047	0.028675613	Glycine N-methyltransferase	No	No
TRINITY_DN7493_c0_g1_i1	Highest	2.68	Upregulated	2.279066615	1.188443094	32.11325945	5.005097199	5.99E-05	trypsin 3A1-like	No	No
TRINITY_DN7665_c0_g1_i1	Highest	2.68	Upregulated	7.315351137	2.870927115	9.101726966	3.186140309	0.006259507	Fatty acid amide hydrolase 1	Yes	No
TRINITY_DN8241_c0_g1_i2	Highest	2.68	Upregulated	7.907695936	2.983257398	21.76563694	4.443980334	5.90E-06	hypothetical protein Anas_12496	Yes	No
TRINITY_DN8283_c0_g1_i8	Highest	2.68	Upregulated	2.174355065	1.120587547	3.567304749	1.834834468	0.01137243	—NA—	No	No
TRINITY_DN9177_c0_g1_i1	Highest	2.68	Upregulated	2.717698473	1.442385399	31.62409044	4.982952081	0.001337631	MAP kinase-interacting serine/threonine-protein kinase 1	No	No
TRINITY_DN9575_c0_g2_i1	Highest	2.68	Downregulated	-3.431845128	-1.778984449	1401.926424	10.45319492	1.63E-07	protein obstructor-E-like isoform X1	No	Yes
TRINITY_DN993_c1_g1_i2	Highest	2.68	Downregulated	-2.061450404	-1.043659752	63.61538029	5.991303703	0.000222	—NA—	No	No
TRINITY_DN4509_c11_g1_i1	Middle	1.34	Downregulated	-2.55044136	-1.35074693	4.999443718	2.321767577	0.039335036	—NA—	No	No
TRINITY_DN1069_c0_g1_i5	Lowest	0.67	Downregulated	-2.474774075	-1.307296826	4.31695453	2.110013897	0.02205352	proteoglycan 4-like	No	No
TRINITY_DN11818_c0_g1_i5	Lowest	0.67	Downregulated	-2.022758006	-1.016323732	22.02431335	4.461025136	0.033918348	uncharacterized protein LOC119575634	No	No
TRINITY_DN16133_c0_g1_i9	Lowest	0.67	Downregulated	-2.052800068	-1.037593123	10.09130641	3.335041051	0.031824755	Glycogen-binding subunit 76A	No	No
TRINITY_DN16423_c0_g1_i1	Lowest	0.67	Downregulated	-2.070587371	-1.05004008	21.43421216	4.421843485	0.019229479	nucleoprotein TPR-like	No	No
TRINITY_DN1676_c0_g2_i2	Lowest	0.67	Downregulated	-2.357527733	-1.237274743	5.770778796	2.528766031	0.01417003	Protein wos2	No	No
TRINITY_DN18080_c0_g2_i1	Lowest	0.67	Downregulated	-2.04617698	-1.032930933	4.130771805	2.046411364	0.045560063	protein broad-minded-like	No	No
TRINITY_DN1952_c0_g1_i5	Lowest	0.67	Downregulated	-2.199045756	-1.136877623	3.33498526	1.737680385	0.019229479	nucleolar protein 9	No	No
TRINITY_DN29156_c0_g1_i2	Lowest	0.67	Upregulated	2.160461081	1.111339242	6.078375542	2.603685812	0.000912	—NA—	No	No
TRINITY_DN37484_c0_g1_i1	Lowest	0.67	Downregulated	-2.434748886	-1.283772984	3.289335308	1.717796081	0.02205352	Molybdenum cofactor sulfurase	No	No
TRINITY_DN4654_c0_g1_i11	Lowest	0.67	Downregulated	-2.06931596	-1.049153944	28.29844622	4.822650936	0.011408008	pre-mRNA-processing factor 40 homolog B-like isoform X3	No	No
TRINITY_DN8131_c0_g1_i18	Lowest	0.67	Downregulated	-721.9597661	-9.495774629	2.701475419	1.433747555	0.017666959	—NA—	Yes	No
TRINITY_DN9383_c0_g1_i1	Lowest	0.67	Upregulated	2.282867227	1.190846954	7.30466697	2.8688185	0.039635457	calcium homeostasis endoplasmic reticulum protein-like isoform X2	No	No
TRINITY_DN6462_c0_g1_i1	Highest, Middle	2.68	Upregulated	3.438984542	1.781982631	189.7761161	7.568154626	5.01E-15	Lysosomal protective protein	No	Yes
		1.34	Upregulated	2.476658171	1.308394761	189.7761161	7.568154626	5.90E-07		No	Yes
TRINITY_DN6949_c6_g1_i5	Highest, Middle	2.68	Upregulated	5.101117149	2.350813233	47.15184095	5.559242194	1.41E-06	proton-coupled folate transporter-like	Yes	No
		1.34	Upregulated	2.954495396	1.562911751	47.15184095	5.559242194	0.039335036		No	No
TRINITY_DN734_c0_g1_i20	Highest, Middle	2.68	Upregulated	46.52648882	5.539980411	38.7308291	5.27541048	1.63E-07	uncharacterized protein LOC119576313	Yes	No
		1.34	Upregulated	10.86507074	3.441625663	38.7308291	5.27541048	0.015977669		Yes	No
TRINITY_DN11122_c0_g1_i13	Highest, Lowest	2.68	Upregulated	851.9044192	9.734547764	2.664291171	1.413751758	0.023445187	—NA—	Yes	No
		0.67	Upregulated	689.8264813	9.430089702	2.664291171	1.413751758	0.042940512		Yes	No
TRINITY_DN24816_c0_g2_i5	Highest, Middle, Lowest	2.68	Upregulated	18.84517205	4.236123061	6.127385448	2.615271608	0.001066569	—NA—	Yes	No
		1.34	Upregulated	18.56263453	4.214329577	6.127385448	2.615271608	0.011286531		Yes	No
		0.67	Upregulated	17.51299637	4.130354036	6.127385448	2.615271608	0.008655266		Yes	No

	TRINITY_DN10614_c0_g1_i10	Highest	1.08	Upregulated	2.453703681	1.294961034	8.589364983	3.102551476	1.46E-06	PREDICTED: elastin-like	No	No
	TRINITY_DN11122_c0_g1_i13	Highest	1.08	Upregulated	540.8037025	9.078961219	2.664291171	1.413751758	0.017738328	---NA---	Yes	No
	TRINITY_DN11316_c0_g1_i10	Highest	1.08	Downregulated	-3.223452209	-1.688606594	36.35927615	5.184251573	0.010694359	probable deoxycytidylate deaminase	No	No
	TRINITY_DN11316_c0_g1_i17	Highest	1.08	Downregulated	-4.300806944	-2.104607373	143.2995464	7.162890233	2.26E-10	probable deoxycytidylate deaminase	No	Yes
	TRINITY_DN11316_c0_g1_i7	Highest	1.08	Downregulated	-2.811696804	-1.491441031	3.452942905	1.787826479	0.001697934	deoxycytidylate deaminase	No	No
	TRINITY_DN11355_c0_g1_i1	Highest	1.08	Upregulated	2.97626636	1.573503646	14.37980371	3.845972077	0.002358264	uncharacterized protein LOC113805697	No	No
	TRINITY_DN11842_c0_g1_i11	Highest	1.08	Upregulated	3.161708797	1.660704497	19.42878222	4.280123572	2.63E-06	---NA---	No	No
	TRINITY_DN11999_c0_g1_i10	Highest	1.08	Downregulated	-599.6170618	-9.227897625	2.513415366	1.32964911	0.003208034	Xylulose kinase	Yes	No
	TRINITY_DN12171_c0_g3_i1	Highest	1.08	Upregulated	2.50823758	1.326674007	3.645996858	1.866313318	0.000858	serine protease 1	No	No
	TRINITY_DN12572_c0_g1_i10	Highest	1.08	Upregulated	4.438506284	2.15007424	9.754434554	3.286058245	3.34E-10	Dual specificity protein phosphatase 14	No	No
	TRINITY_DN12572_c0_g1_i8	Highest	1.08	Upregulated	3.864371015	1.950233613	5.814092426	2.539554006	9.46E-06	Dual specificity protein phosphatase 14	No	No
	TRINITY_DN1264_c0_g1_i4	Highest	1.08	Downregulated	-2.131974358	-1.092190086	61.35468023	5.939101494	0.031281917	transient-receptor-potential-like protein	No	No
	TRINITY_DN12717_c0_g1_i6	Highest	1.08	Upregulated	2.002387448	1.001721153	82.45434514	6.365523617	0.007824475	---NA---	No	No
	TRINITY_DN12772_c0_g1_i7	Highest	1.08	Upregulated	2.247523319	1.168336085	65.76861946	6.039327482	0.004766886	pancreatic lipase-related protein 2-like	No	No
	TRINITY_DN12999_c0_g1_i11	Highest	1.08	Downregulated	-2.924213559	-1.548048677	6.03146097	2.592507501	0.014940252	betaine--homocysteine S-methyltransferase 1-like	No	No
	TRINITY_DN13160_c3_g1_i1	Highest	1.08	Upregulated	2.147498339	1.102657015	5.529005424	2.467019987	0.000858	---NA---	No	No
	TRINITY_DN1328_c2_g1_i3	Highest	1.08	Upregulated	2.511902323	1.328780365	15.28594388	3.934133734	0.001763142	Serine proteases trypsin domain	No	No
	TRINITY_DN13699_c0_g1_i8	Highest	1.08	Downregulated	-2.179644037	-1.124092544	368.3434134	8.524907635	0.000259	Hemocyanin A chain	No	Yes
	TRINITY_DN1409_c1_g1_i7	Highest	1.08	Downregulated	-2.379099255	-1.250415462	13.1767789	3.719925837	0.000986	carotenoid isomerooxygenase	No	No
	TRINITY_DN1452_c1_g1_i19	Highest	1.08	Upregulated	2.415692218	1.272436654	3.61674312	1.854691134	0.000363	---NA---	No	No
	TRINITY_DN1475_c1_g1_i13	Highest	1.08	Upregulated	2.050734282	1.036140571	58.28845949	5.865138368	0.000858	peritrophin-48-like isoform X1	No	No
	TRINITY_DN14779_c0_g1_i17	Highest	1.08	Upregulated	2.754024727	1.461541513	41.30329906	5.368185115	0.002654728	serine-rich adhesin for platelets-like isoform X15	No	No
	TRINITY_DN15085_c0_g1_i1	Highest	1.08	Upregulated	2.07395458	1.052384299	12.41453857	3.633958734	1.53E-07	Ankyrin repeat, SAM and basic leucine zipper domain-containing protein 1	No	No
	TRINITY_DN15559_c0_g1_i10	Highest	1.08	Upregulated	3.06903542	1.617785296	191.67777	7.582539219	1.80E-05	apolipoprotein D-like	No	Yes
	TRINITY_DN15803_c0_g1_i3	Highest	1.08	Upregulated	3.073768855	1.62000868	59.74975263	5.900860835	0.000174	oplophorus-luciferin 2-monooxygenase non-catalytic subunit-like	No	No
	TRINITY_DN16120_c0_g1_i5	Highest	1.08	Upregulated	2.236129189	1.16100354	4.388771194	2.133817058	0.036748814	venom protease-like	No	No
	TRINITY_DN1660_c3_g1_i1	Highest	1.08	Downregulated	-2.012564605	-1.009035095	15.64550732	3.967676535	0.000779	protein croquemort-like	No	No
	TRINITY_DN16678_c0_g1_i2	Highest	1.08	Upregulated	4.158716717	2.056138415	18.24185746	4.189180733	1.11E-07	sequestosome-1 isoform X1	No	No
	TRINITY_DN17832_c0_g1_i4	Highest	1.08	Upregulated	2.546541209	1.348539064	35.17413792	5.13644316	0.002149829	uncharacterized protein LOC113799941 isoform X1	No	No
	TRINITY_DN1879_c2_g1_i6	Highest	1.08	Upregulated	2.040483126	1.02891078	78.68732401	6.298059341	0.04745477	serine protease-like protein 3	No	No
	TRINITY_DN19142_c0_g1_i5	Highest	1.08	Upregulated	2.472664165	1.306066307	14.6876141	3.876528154	0.004571197	acetylcholinesterase-like precursor	No	No
	TRINITY_DN1955_c0_g1_i3	Highest	1.08	Upregulated	2.080848972	1.057172258	32.09041362	5.00407048	0.012159613	serine protease 2	No	No
	TRINITY_DN19891_c0_g1_i1	Highest	1.08	Upregulated	2.096972337	1.06830783	183.7310776	7.521451865	1.80E-05	peritrophin-44-like protein	No	Yes
	TRINITY_DN2003_c0_g2_i1	Highest	1.08	Upregulated	2.887504825	1.529823357	183.1815391	7.517130307	8.67E-08	juvenile hormone binding protein 7	No	Yes
	TRINITY_DN20289_c0_g1_i12	Highest	1.08	Upregulated	2.288139648	1.194175104	46.58168158	5.541690816	0.030992771	Cystathionine beta-synthase	No	No
	TRINITY_DN20289_c0_g1_i15	Highest	1.08	Upregulated	2.187987125	1.129604249	11.23434534	3.489844152	9.82E-05	Cystathionine beta-synthase	No	No
	TRINITY_DN20635_c0_g1_i1	Highest	1.08	Upregulated	2.551276498	1.351219261	4.85369221	2.279082625	0.002224861	Anti-lipopolysaccharide factor	No	No
	TRINITY_DN2077_c3_g2_i3	Highest	1.08	Upregulated	2.62280887	1.391112679	13.52507906	3.757565122	0.017007166	---NA---	No	No
	TRINITY_DN21273_c0_g1_i5	Highest	1.08	Upregulated	2.187476489	1.129267511	36.44382582	5.187602514	0.003281394	SCYLA-like protein	No	No
	TRINITY_DN2138_c0_g1_i17	Highest	1.08	Upregulated	2.022119008	1.015867907	73.39480636	6.197606072	0.004016168	---NA---	No	No
	TRINITY_DN2231_c1_g3_i1	Highest	1.08	Downregulated	-2.034869005	-1.024935924	859.5208039	9.747388749	8.23E-05	oplophorus-luciferin 2-monooxygenase non-catalytic subunit-like	No	Yes
	TRINITY_DN22402_c0_g1_i11	Highest	1.08	Upregulated	2.712135191	1.439429094	3.870280822	1.95243825	0.002668578	cuticle protein 8-like	No	No
	TRINITY_DN2261_c4_g1_i1	Highest	1.08	Downregulated	-2.642773424	-1.402052742	69.66186908	6.122297277	6.48E-07	zinc proteinase Mpc1	No	No
	TRINITY_DN22786_c0_g1_i1	Highest	1.08	Downregulated	-5.166922542	-2.369305256	7.487691922	2.904521077	3.73E-16	delta(24)-sterol reductase-like	Yes	No
	TRINITY_DN22848_c0_g1_i1	Highest	1.08	Upregulated	3.204186315	1.679958039	59.51047892	5.895071823	0.000147	Hemocyanin A chain	No	No
	TRINITY_DN22896_c0_g1_i3	Highest	1.08	Upregulated	2.186382217	1.12854631	362.660646	8.50247639	0.001763142	C-type lectin 3	No	Yes
	TRINITY_DN2376_c0_g1_i7	Highest	1.08	Upregulated	2.290584244	1.195715624	59.96197584	5.905976018	0.00045	Acyl-coenzyme A thioesterase 1	No	No
	TRINITY_DN2382_c0_g1_i16	Highest	1.08	Upregulated	2.243954793	1.166043612	47.55135167	5.571414446	0.004411837	rhythmically expressed gene 5 protein-like	No	No
	TRINITY_DN2496_c0_g1_i2	Highest	1.08	Upregulated	2.031401037	1.022475083	5.389535605	2.430160967	0.000655	---NA---	No	No
	TRINITY_DN25116_c0_g1_i2	Highest	1.08	Upregulated	2.420845345	1.275510916	6.28888992	2.652805383	6.74E-07	uncharacterized protein LOC113805499	No	No
	TRINITY_DN25454_c0_g1_i7	Highest	1.08	Upregulated	2.801320913	1.486107265	30.4204102	4.926967702	1.11E-07	uncharacterized protein LOC113804027	No	No
	TRINITY_DN2620_c0_g1_i13	Highest	1.08	Upregulated	2.012281634	1.008832236	10.37952322	3.375668271	0.030979489	---NA---	No	No
	TRINITY_DN2668_c0_g1_i5	Highest	1.08	Upregulated	2.485912595	1.313775572	85.27756097	6.414094271	7.70E-05	prophenoloxidase 2	No	No
	TRINITY_DN27_c0_g1_i2	Highest	1.08	Upregulated	2.522792238	1.3350214	4.251218945	2.087876562	0.031711316	putative inorganic phosphate cotransporter	No	No
	TRINITY_DN2821_c0_g1_i4	Highest	1.08	Downregulated	-2.574741748	-1.364427734	3.585019828	1.841981098	0.042256819	7,8-dihydro-8-oxoguanine triphosphatase-like	No	No
	TRINITY_DN2934_c0_g1_i15	Highest	1.08	Upregulated	2.737480269	1.452848566	50.46632647	5.657249169	0.000629	phenoloxidase-activating factor 2-like	No	No
	TRINITY_DN2935_c0_g1_i12	Highest	1.08	Upregulated	29.80935367	4.89769319	11.46117016	3.518682442	4.14E-05	putative ankyrin repeat protein RF_0381 isoform X4	Yes	No
	TRINITY_DN30383_c0_g1_i13	Highest	1.08	Upregulated	2.099995523	1.070386253	10.51867272	3.394880767	7.89E-06	ERAD-associated E3 ubiquitin-protein ligase HRD1B-like	No	No
	TRINITY_DN309913_c0_g1_i2	Highest	1.08	Downregulated	-2.021495937	-1.015423304	22.26456344	4.476677419	3.72E-07	phosphatidylserine decarboxylase proenzyme, mitochondrial-like isoform	No	No
	TRINITY_DN3120_c0_g1_i35	Highest	1.08	Upregulated	2.935298835	1.553507388	64.33524417	6.007537387	5.19E-05	carboxypeptidase B	No	No
	TRINITY_DN3295_c0_g1_i10	Highest	1.08	Upregulated	2.506350954	1.325588444	453.2709867	8.824230009	0.00163838	C-type lectin	No	Yes
	TRINITY_DN3295_c12_g1_i5	Highest	1.08	Upregulated	3.698706153	1.887020689	12.2715112	3.617241019	3.78E-12	serine protease 1	No	No
	TRINITY_DN3318_c0_g1_i15	Highest	1.08	Upregulated	2.328086721	1.219144799	24.02123763	4.586238579	2.17E-05	tolloid-like protein 2	No	No
	TRINITY_DN3387_c0_g1_i1	Highest	1.08	Downregulated	-3.284298324	-1.715585178	8.886706837	3.151648896	0.045900198	Laminin subunit alpha	No	No
	TRINITY_DN3431_c0_g1_i11	Highest	1.08	Upregulated	2.248210871	1.16877736	39.07735178	5.288260796	0.003225118	---NA---	No	No
	TRINITY_DN3592_c3_g1_i1	Highest	1.08	Upregulated	2.029825164	1.021355468	9.472490041	3.243743718	0.001217229	putative zinc metalloproteinase	No	No
	TRINITY_DN3666_c0_g1_i12	Highest	1.08	Downregulated	-3.782019105	-1.919156651	27.38329827	4.775224322	8.67E-08	D-3-phosphoglycerate dehydrogenase	No	No
	TRINITY_DN3720_c0_g1_i4	Highest	1.08	Downregulated	-2.01884908	-1.013533065	4.57572281	2.195212861	0.027110437	---NA---	No	No
	TRINITY_DN3747_c1_g1_i3	Highest	1.08	Upregulated	2.364955813	1.241813229	14.37560483	3.845550751	0.027658019	DNA topoisomerase 2-alpha	No	No
	TRINITY_DN3753_c5_g1_i2	Highest	1.08	Upregulated	2.196351416	1.135108904	8.72265159	3.124766765	0.000567	---NA---	No	No
	TRINITY_DN4044_c0_g1_i28	Highest	1.08	Upregulated	2.046412995	1.033097331	26.95054542	4.752242565	0.000887	cysteine dioxygenase type 1-like	No	No
	TRINITY_DN40481_c0_g1_i2	Highest	1.08	Upregulated	2.076713257	1.054302029	3.579338737	1.839693082	0.04790017	Ankyrin repeat-containing domain	No	No
	TRINITY_DN4099_c0_g1_i6	Highest	1.08	Upregulated	2.045940247	1.032764011	54.82342991	5.776720685	0.013774524	Glutathione peroxidase	No	No
	TRINITY_DN4152_c0_g1_i3	Highest	1.08	Upregulated	2.135048932	1.094269134	65.76312473	6.039206945	0.000551	vascular endothelial growth factor 2	No	No
	TRINITY_DN4191_c0_g1_i1	Highest	1.08	Upregulated	2.90012	1.536112597	89.92398181	6.490634014	4.90E-05	prophenoloxidase activating factor	No	No
	TRINITY_DN4191_c0_g1_i4	Highest	1.08	Upregulated	2.894250576	1.533189831	35.71922249	5.158628772	2.19E-05	prophenoloxidase activating factor	No	No
Un-weathered	TRINITY_DN4318_c5_g1_i2	Highest	1.08	Downregulated	-4.645716001	-2.215900963	11.82403605	3.563650668	0.00078	---NA---	No	No

TRINITY_DN4367_c0_g1_i2	Highest	1.08	Downregulated	-2.800315319	-1.485589286	17.05966659	4.092517546	0.013286851	---NA---	No	No
TRINITY_DN4548_c0_g1_i1	Highest	1.08	Upregulated	4.947484117	2.306695076	15.45061246	3.949592122	2.83E-07	Anti-lipopolysaccharide factor	No	No
TRINITY_DN500_c0_g1_i12	Highest	1.08	Upregulated	5.689189125	2.508223041	7.709729734	2.946680287	2.50E-06	---NA---	No	No
TRINITY_DN504_c0_g1_i10	Highest	1.08	Upregulated	3.341557923	1.740520882	24.3973904	4.608654937	0.000179	sarcosine dehydrogenase, mitochondrial-like	No	No
TRINITY_DN504_c0_g1_i33	Highest	1.08	Upregulated	2.542839259	1.346440267	72.13788973	6.172685315	0.000108	sarcosine dehydrogenase, mitochondrial-like	No	No
TRINITY_DN504_c0_g1_i5	Highest	1.08	Upregulated	2.944242171	1.557896342	61.86644679	5.951085272	7.81E-06	sarcosine dehydrogenase, mitochondrial-like	No	No
TRINITY_DN5071_c0_g1_i1	Highest	1.08	Upregulated	7.764513267	2.956895489	3.556835449	1.830594232	0.011477274	---NA---	Yes	No
TRINITY_DN5482_c0_g1_i13	Highest	1.08	Upregulated	2.685927822	1.425420536	5.534208449	2.468376985	0.000399	cytochrome P450 307a1-like	No	No
TRINITY_DN5567_c0_g1_i2	Highest	1.08	Upregulated	2.428311147	1.27995329	50.8263308	5.66750418	1.84E-05	adhesive plaque matrix protein-like	No	No
TRINITY_DN576_c0_g2_i4	Highest	1.08	Downregulated	-2.07720354	-1.054462589	5.992948042	2.583265866	0.030474457	deoxynucleoside triphosphate triphosphohydrolase SAMHD1-like	No	No
TRINITY_DN5791_c0_g1_i6	Highest	1.08	Upregulated	2.256497509	1.174085186	3.500655493	1.80762509	0.000137	---NA---	No	No
TRINITY_DN58469_c0_g1_i3	Highest	1.08	Upregulated	2.19928259	1.137032991	50.571353	5.660248472	1.77E-09	Gamma-interferon-inducible lysosomal thiol reductase	No	No
TRINITY_DN5963_c0_g1_i3	Highest	1.08	Upregulated	4.854945889	2.279455216	50.58487847	5.660634274	0.000858	CUB domain	No	No
TRINITY_DN6098_c0_g1_i1	Highest	1.08	Upregulated	5.143567718	2.362769399	26.63128505	4.73505014	2.08E-05	hypothetical protein Anas_12496	Yes	No
TRINITY_DN6257_c0_g1_i7	Highest	1.08	Upregulated	2.470983627	1.305085451	88.4959835	6.467540073	1.97E-06	chymotrypsin BII-like	No	No
TRINITY_DN6433_c0_g1_i5	Highest	1.08	Upregulated	2.350105692	1.232725641	3.074626221	1.620411034	0.035698465	---NA---	No	No
TRINITY_DN6589_c0_g1_i1	Highest	1.08	Upregulated	2.989552708	1.579929647	7.135511667	2.835016885	1.36E-12	molt-inhibiting hormone	No	No
TRINITY_DN6598_c0_g2_i1	Highest	1.08	Downregulated	-2.293853733	-1.197773401	21.13884478	4.401824632	0.003581301	gamma-butyrobetaine dioxygenase-like isoform X1	No	No
TRINITY_DN6695_c0_g2_i4	Highest	1.08	Upregulated	2.465001296	1.301588405	309.9650782	8.275961875	0.001751478	uncharacterized protein LOC119573322	No	Yes
TRINITY_DN6695_c0_g2_i5	Highest	1.08	Upregulated	3.834834405	1.939164281	79.41365914	6.311315267	0.000258	uncharacterized protein LOC119573322	No	Yes
TRINITY_DN6710_c3_g1_i5	Highest	1.08	Upregulated	2.008093	1.005826086	196.1798363	7.616032956	0.042256819	uncharacterized protein LOC113806809	No	Yes
TRINITY_DN672_c0_g1_i20	Highest	1.08	Upregulated	5.214598853	2.382556274	27.07247447	4.758754853	2.18E-08	papilin isoform X4	Yes	No
TRINITY_DN672_c0_g1_i8	Highest	1.08	Upregulated	4.384019891	2.132254344	20.0928035	4.328606969	1.46E-06	---NA---	No	No
TRINITY_DN7166_c1_g1_i9	Highest	1.08	Upregulated	2.079105376	1.055962881	93.48304705	6.546632854	1.84E-05	i-type lysozyme 3 precursor	No	No
TRINITY_DN7237_c0_g1_i3	Highest	1.08	Upregulated	5.445188671	2.444982038	3.785802627	1.920599198	0.013774524	Apolipoprotein D	Yes	No
TRINITY_DN7294_c0_g1_i1	Highest	1.08	Upregulated	2.195994152	1.134874212	9.704001672	3.278579799	0.001312724	PREDICTED: uncharacterized protein LOC108673431	No	No
TRINITY_DN7353_c0_g1_i1	Highest	1.08	Upregulated	2.234185539	1.159749	16.86918185	4.07631881	1.46E-06	heat shock protein 21	No	No
TRINITY_DN7549_c0_g1_i9	Highest	1.08	Upregulated	2.260724904	1.176785449	134.3548113	7.069904176	0.001352029	---NA---	No	No
TRINITY_DN7665_c0_g1_i1	Highest	1.08	Upregulated	4.885035976	2.288369187	9.101726966	3.186140309	0.028636681	Fatty acid amide hydrolase 1	No	No
TRINITY_DN789_c1_g1_i4	Highest	1.08	Upregulated	2.040956086	1.029245141	6.115937214	2.612573596	0.000816	F-box/LRR-repeat protein 20	No	No
TRINITY_DN8241_c0_g1_i2	Highest	1.08	Upregulated	7.993197717	2.998772776	21.76563694	4.443980334	2.23E-06	hypothetical protein Anas_12496	Yes	No
TRINITY_DN8838_c2_g1_i19	Highest	1.08	Downregulated	-2.622072067	-1.390707338	71.8265148	6.166444609	0.000401	phosphoethanolamine N-methyltransferase-like	No	No
TRINITY_DN8563_c0_g1_i9	Highest	1.08	Upregulated	2.547955038	1.34933982	12.39437237	3.631613312	0.000742	PREDICTED: uncharacterized protein LOC108678532	No	No
TRINITY_DN8807_c0_g1_i13	Highest	1.08	Upregulated	2.026182747	1.018764301	14.50944721	3.858920651	0.011428967	kynureninase-like	No	No
TRINITY_DN8938_c0_g1_i1	Highest	1.08	Upregulated	2.22639049	1.154706651	10.55730847	3.400170169	1.37E-05	---NA---	No	No
TRINITY_DN9010_c0_g1_i12	Highest	1.08	Upregulated	2.531643989	1.340074541	14.85828506	3.893195705	0.000179	cytochrome b5	No	No
TRINITY_DN9172_c3_g1_i7	Highest	1.08	Upregulated	3.118378106	1.640795867	76.15864666	6.250935937	0.042833059	apolipoprotein D-like	No	No
TRINITY_DN9177_c0_g1_i1	Highest	1.08	Upregulated	4.125624633	2.044612565	31.62409044	4.982952081	1.53E-07	MAP kinase-interacting serine/threonine-protein kinase 1	No	No
TRINITY_DN921_c0_g1_i4	Highest	1.08	Downregulated	-2.188763687	-1.1301162	24.12792955	4.592632216	0.000749	probable phosphoserine aminotransferase	No	No
TRINITY_DN9238_c0_g1_i6	Highest	1.08	Upregulated	2.757642211	1.463435287	190.7166384	7.575286902	2.15E-08	low-density lipoprotein receptor-like	No	Yes
TRINITY_DN929_c0_g1_i6	Highest	1.08	Upregulated	2.995947438	1.583012313	8.701507032	3.121265286	0.033919134	putative phospholipase A2	No	No
TRINITY_DN9401_c0_g1_i1	Highest	1.08	Upregulated	2.063707782	1.045238701	6.035284858	2.593421866	0.011078738	Reverse transcriptase domain	No	No
TRINITY_DN9743_c0_g2_i2	Highest	1.08	Upregulated	2.005072805	1.003654622	39.52077875	5.30453947	0.000282	protein suppressor of forked	No	No
TRINITY_DN993_c1_g1_i2	Highest	1.08	Downregulated	-2.193019025	-1.132918328	63.61538029	5.991303703	1.84E-05	---NA---	No	No
TRINITY_DN4509_c11_g1_i1	Middle	0.54	Downregulated	-2.484265743	-1.312819507	4.999443718	2.321767577	0.023648375	---NA---	No	No
TRINITY_DN804_c0_g1_i2	Middle	0.54	Upregulated	2.138253859	1.096433144	5.959433498	2.575175195	0.023648375	serine/threonine-protein kinase MAK-like isoform X2	No	No
TRINITY_DN81243_c0_g1_i1	Middle	0.54	Upregulated	3.010685975	1.590092238	4.902994686	2.293663198	0.027666109	---NA---	No	No
TRINITY_DN9642_c0_g1_i1	Middle	0.54	Upregulated	2.129010549	1.090183098	15.35373445	3.940517696	0.009854605	EF-hand calcium-binding domain-containing protein 4B	No	No
TRINITY_DN11720_c0_g1_i12	Lowest	0.27	Downregulated	-12.55878927	-3.650625483	6.847256034	2.775525959	0.046816102	glycine-rich cell wall structural protein 1-like	Yes	No
TRINITY_DN29156_c0_g1_i2	Lowest	0.27	Upregulated	2.042533763	1.030359926	6.078375542	2.603685812	0.006341129	---NA---	No	No
TRINITY_DN13160_c0_g1_i5	Highest, Middle	1.08	Downregulated	-6.899624444	-2.786517836	83.10495887	6.37686266	5.87E-09	chitinase-3-like protein 1	Yes	No
		0.54	Downregulated	-5.146994781	-2.36373032	83.10495887	6.37686266	1.06E-05		Yes	No
TRINITY_DN24816_c0_g2_i5	Highest, Middle	1.08	Upregulated	14.90957628	3.898167353	6.127385448	2.615271608	0.001566804	---NA---	Yes	No
		0.54	Upregulated	14.5155819	3.859530503	6.127385448	2.615271608	0.014777486		Yes	No
TRINITY_DN2594_c0_g1_i5	Highest, Middle	1.08	Upregulated	4.313414108	2.108830228	10.65061695	3.412865097	4.97E-05	pentraxin-related protein PTX3-like	No	No
		0.54	Upregulated	2.954808685	1.563064723	10.65061695	3.412865097	0.033346443		No	No
TRINITY_DN2935_c0_g1_i11	Highest, Middle	1.08	Upregulated	58.76203044	5.876812342	32.06365237	5.002866867	1.68E-07	putative ankyrin repeat protein RF_0381 isoform X4	Yes	No
		0.54	Upregulated	11.86975825	3.569218646	32.06365237	5.002866867	0.014777486		Yes	No
TRINITY_DN5090_c4_g2_i3	Highest, Middle	1.08	Upregulated	3.626464374	1.858563676	435.550561	8.766696394	1.77E-09	PREDICTED: uncharacterized protein LOC108673189	No	Yes
		0.54	Upregulated	2.318884251	1.213430808	435.550561	8.766696394	0.00406362		No	Yes
TRINITY_DN672_c0_g1_i29	Highest, Middle	1.08	Upregulated	5.824950224	2.542245722	8.907240901	3.154978613	2.84E-06	---NA---	Yes	No
		0.54	Upregulated	3.22224487	1.688066134	8.907240901	3.154978613	0.031095115		No	No
TRINITY_DN6949_c6_g1_i5	Highest, Middle	1.08	Upregulated	4.492913508	2.167651289	47.15184095	5.559242194	6.26E-06	proton-coupled folate transporter-like	No	No
		0.54	Upregulated	3.013225734	1.591308756	47.15184095	5.559242194	0.016257498		No	No
TRINITY_DN734_c0_g1_i13	Highest, Middle	1.08	Upregulated	5.252006745	2.392868769	4.901837498	2.293322658	1.84E-05	uncharacterized protein LOC119576313	Yes	No
		0.54	Upregulated	3.957915695	1.984740883	4.901837498	2.293322658	0.007040766		No	No
TRINITY_DN734_c0_g1_i20	Highest, Middle	1.08	Upregulated	76.12880247	6.250370479	38.7308291	5.27541048	1.77E-09	uncharacterized protein LOC119576313	Yes	No
		0.54	Upregulated	29.89980079	4.902063967	38.7308291	5.27541048	1.12E-05		Yes	No
TRINITY_DN9575_c0_g2_i1	Highest, Middle	1.08	Downregulated	-4.685377489	-2.228165287	1401.926424	10.45319492	3.78E-12	protein obstructor-E-like isoform X1	No	Yes
		0.54	Downregulated	-2.329283224	-1.219886071	1401.926424	10.45319492	0.007040766		No	Yes
TRINITY_DN736_c0_g1_i15	Highest, Lowest	1.08	Upregulated	2.095506284	1.067298848	4.176009654	2.062125047	0.033919134	Glycine N-methyltransferase	No	No
		0.27	Upregulated	2.616456874	1.38761448	4.176009654	2.062125047	0.043358719		No	No
TRINITY_DN6462_c0_g1_i1	Highest, Middle, Lowest	1.08	Upregulated	3.769403709	1.914336318	189.7761161	7.568154626	3.16E-17	Lysosomal protective protein	No	Yes
		0.54	Upregulated	2.833720803	1.502697622	189.7761161	7.568154626	6.59E-10		No	Yes
		0.27	Upregulated	2.141526443	1.098639491	189.7761161	7.568154626	0.00037		No	Yes

Appendix E

The contig IDs, type of dysregulation (up- or down-regulation), and orthologous gene descriptions for the 57 shared contigs between weathering treatment groups, the 23 unique contigs in the weathered leachate group, and the 82 unique contigs in the un-weathered leachate group, as displayed in Figure 7.

Treatment	Dysregulation	Contig ID found in *A. bahia* (from *de novo* assembly)	Gene description - orthologous genes in arthropods (from annotation file)
Both	Upregulated	TRINITY_DN22848_c0_g1_i1	Hemocyanin A chain
Both	Upregulated	TRINITY_DN11842_c0_g1_i11	---NA---
Both	Upregulated	TRINITY_DN19142_c0_g1_i5	acetylcholinesterase-like precursor
Both	Upregulated	TRINITY_DN15803_c0_g1_i3	oplophorus-luciferin 2-monooxygenase non-catalytic subunit-like
Both	Upregulated	TRINITY_DN4191_c0_g1_i4	prophenoloxidase activating factor
Both	Upregulated	TRINITY_DN7665_c0_g1_i1	Fatty acid amide hydrolase 1
Both	Upregulated	TRINITY_DN500_c0_g1_i12	---NA---
Both	Upregulated	TRINITY_DN6098_c0_g1_i1	hypothetical protein Anas_12496
Both	Upregulated	TRINITY_DN58469_c0_g1_i3	Gamma-interferon-inducible lysosomal thiol reductase
Both	Upregulated	TRINITY_DN19891_c0_g1_i1	peritrophin-44-like protein
Both	Upregulated	TRINITY_DN504_c0_g1_i5	sarcosine dehydrogenase, mitochondrial-like
Both	Upregulated	TRINITY_DN5090_c4_g2_i3	PREDICTED: uncharacterized protein LOC108673189
Both	Upregulated	TRINITY_DN672_c0_g1_i8	---NA---
Both	Upregulated	TRINITY_DN672_c0_g1_i20	papilin isoform X4
Both	Upregulated	TRINITY_DN672_c0_g1_i29	---NA---
Both	Upregulated	TRINITY_DN22896_c0_g1_i3	C-type lectin 3
Both	Upregulated	TRINITY_DN9177_c0_g1_i1	MAP kinase-interacting serine/threonine-protein kinase 1
Both	Upregulated	TRINITY_DN8241_c0_g1_i2	hypothetical protein Anas_12496
Both	Upregulated	TRINITY_DN16678_c0_g1_i2	sequestosome-1 isoform X1
Both	Upregulated	TRINITY_DN2003_c0_g2_i1	juvenile hormone binding protein 7
Both	Upregulated	TRINITY_DN12572_c0_g1_i10	Dual specificity protein phosphatase 14
Both	Upregulated	TRINITY_DN11355_c0_g1_i1	uncharacterized protein LOC113805697
Both	Upregulated	TRINITY_DN15559_c0_g1_i10	apolipoprotein D-like
Both	Upregulated	TRINITY_DN5071_c0_g1_i1	---NA---
Both	Upregulated	TRINITY_DN2376_c0_g1_i7	Acyl-coenzyme A thioesterase 1
Both	Upregulated	TRINITY_DN2594_c0_g1_i5	pentraxin-related protein PTX3-like
Both	Upregulated	TRINITY_DN736_c0_g1_i15	Glycine N-methyltransferase
Both	Upregulated	TRINITY_DN4099_c0_g1_i6	Glutathione peroxidase
Both	Upregulated	TRINITY_DN1475_c1_g1_i13	peritrophin-48-like isoform X1
Both	Upregulated	TRINITY_DN3295_c0_g1_i10	C-type lectin
Both	Upregulated	TRINITY_DN3295_c12_g1_i5	serine protease 1
Both	Upregulated	TRINITY_DN4548_c0_g1_i1	Anti-lipopolysaccharide factor
Both	Upregulated	TRINITY_DN6695_c0_g2_i5	uncharacterized protein LOC119573322
Both	Upregulated	TRINITY_DN6695_c0_g2_i4	uncharacterized protein LOC119573322
Both	Upregulated	TRINITY_DN2935_c0_g1_i11	putative ankyrin repeat protein RF_0381 isoform X4
Both	Upregulated	TRINITY_DN2935_c0_g1_i12	putative ankyrin repeat protein RF_0381 isoform X4
Both	Upregulated	TRINITY_DN5963_c0_g1_i3	CUB domain
Both	Upregulated	TRINITY_DN6589_c0_g1_i1	molt-inhibiting hormone
Both	Upregulated	TRINITY_DN3120_c0_g1_i35	carboxypeptidase B
Both	Upregulated	TRINITY_DN2668_c0_g1_i5	prophenoloxidase 2
Both	Upregulated	TRINITY_DN3592_c3_g1_i1	putative zinc metalloproteinase
Both	Upregulated	TRINITY_DN734_c0_g1_i13	uncharacterized protein LOC119576313
Both	Downregulated	TRINITY_DN6598_c0_g2_i1	gamma-butyrobetaine dioxygenase-like isoform X1
Both	Downregulated	TRINITY_DN993_c1_g1_i2	---NA---
Both	Downregulated	TRINITY_DN22786_c0_g1_i1	delta(24)-sterol reductase-like
Both	Downregulated	TRINITY_DN11316_c0_g1_i17	probable deoxycytidylate deaminase
Both	Downregulated	TRINITY_DN4367_c0_g1_i2	---NA---
Both	Downregulated	TRINITY_DN4318_c5_g1_i2	---NA---
Both	Downregulated	TRINITY_DN13160_c0_g1_i5	chitinase-3-like protein 1
Both	Downregulated	TRINITY_DN9575_c0_g2_i1	protein obstructor-E-like isoform X1
Both	Downregulated	TRINITY_DN4509_c11_g1_i1	---NA---
Both	Upregulated	TRINITY_DN29156_c0_g1_i2	---NA---
Both	Upregulated	TRINITY_DN6949_c6_g1_i5	proton-coupled folate transporter-like
Both	Upregulated	TRINITY_DN6462_c0_g1_i1	Lysosomal protective protein
Both	Upregulated	TRINITY_DN734_c0_g1_i20	uncharacterized protein LOC119576313
Both	Upregulated	TRINITY_DN11122_c0_g1_i13	---NA---
Both	Upregulated	TRINITY_DN24816_c0_g2_i5	---NA---
Un-weathered	Upregulated	TRINITY_DN9743_c0_g2_i2	protein suppressor of forked
Un-weathered	Upregulated	TRINITY_DN20635_c0_g1_i1	Anti-lipopolysaccharide factor
Un-weathered	Upregulated	TRINITY_DN4152_c0_g1_i3	vascular endothelial growth factor 2
Un-weathered	Upregulated	TRINITY_DN8938_c0_g1_i1	---NA---

Un-weathered	Upregulated	TRINITY_DN7353_c0_g1_i1	heat shock protein 21
Un-weathered	Upregulated	TRINITY_DN25454_c0_g1_i7	uncharacterized protein LOC113804027
Un-weathered	Upregulated	TRINITY_DN9010_c0_g1_i12	cytochrome b5
Un-weathered	Upregulated	TRINITY_DN2382_c0_g1_i16	rhythmically expressed gene 5 protein-like
Un-weathered	Upregulated	TRINITY_DN6710_c3_g1_i5	uncharacterized protein LOC113806809
Un-weathered	Upregulated	TRINITY_DN504_c0_g1_i10	sarcosine dehydrogenase, mitochondrial-like
Un-weathered	Upregulated	TRINITY_DN4191_c0_g1_i1	prophenoloxidase activating factor
Un-weathered	Upregulated	TRINITY_DN504_c0_g1_i33	sarcosine dehydrogenase, mitochondrial-like
Un-weathered	Upregulated	TRINITY_DN2138_c0_g1_i17	---NA---
Un-weathered	Upregulated	TRINITY_DN3747_c1_g1_i3	DNA topoisomerase 2-alpha
Un-weathered	Upregulated	TRINITY_DN27_c0_g1_i2	putative inorganic phosphate cotransporter
Un-weathered	Upregulated	TRINITY_DN7549_c0_g1_i9	---NA---
Un-weathered	Upregulated	TRINITY_DN929_c0_g1_i6	putative phospholipase A2
Un-weathered	Upregulated	TRINITY_DN789_c1_g1_i4	F-box/LRR-repeat protein 20
Un-weathered	Upregulated	TRINITY_DN2496_c0_g1_i2	---NA---
Un-weathered	Upregulated	TRINITY_DN15085_c0_g1_i1	Ankyrin repeat, SAM and basic leucine zipper domain-containing protein 1
Un-weathered	Upregulated	TRINITY_DN16120_c0_g1_i5	venom protease-like
Un-weathered	Upregulated	TRINITY_DN17832_c0_g1_i4	uncharacterized protein LOC113799941 isoform X1
Un-weathered	Upregulated	TRINITY_DN2620_c0_g1_i13	---NA---
Un-weathered	Upregulated	TRINITY_DN5567_c0_g1_i2	adhesive plaque matrix protein-like
Un-weathered	Upregulated	TRINITY_DN22402_c0_g1_i11	cuticle protein 8-like
Un-weathered	Upregulated	TRINITY_DN7294_c0_g1_i1	PREDICTED: uncharacterized protein LOC108673431
Un-weathered	Upregulated	TRINITY_DN12772_c0_g1_i7	pancreatic lipase-related protein 2-like
Un-weathered	Upregulated	TRINITY_DN7237_c0_g1_i3	Apolipoprotein D
Un-weathered	Upregulated	TRINITY_DN25116_c0_g1_i2	uncharacterized protein LOC113805499
Un-weathered	Upregulated	TRINITY_DN8807_c0_g1_i13	kynureninase-like
Un-weathered	Upregulated	TRINITY_DN40481_c0_g1_i2	Ankyrin repeat-containing domain
Un-weathered	Upregulated	TRINITY_DN1328_c2_g1_i3	Serine proteases trypsin domain
Un-weathered	Upregulated	TRINITY_DN4044_c0_g1_i28	cysteine dioxygenase type 1-like
Un-weathered	Upregulated	TRINITY_DN1452_c1_g1_i19	---NA---
Un-weathered	Upregulated	TRINITY_DN12171_c0_g3_i1	serine protease 1
Un-weathered	Upregulated	TRINITY_DN6257_c0_g1_i7	chymotrypsin BII-like
Un-weathered	Upregulated	TRINITY_DN9401_c0_g1_i1	Reverse transcriptase domain
Un-weathered	Upregulated	TRINITY_DN1879_c2_g1_i6	serine protease-like protein 3
Un-weathered	Upregulated	TRINITY_DN2934_c0_g1_i15	phenoloxidase-activating factor 2-like
Un-weathered	Upregulated	TRINITY_DN5791_c0_g1_i6	---NA---
Un-weathered	Upregulated	TRINITY_DN13160_c3_g1_i1	---NA---
Un-weathered	Upregulated	TRINITY_DN6433_c0_g1_i5	---NA---
Un-weathered	Upregulated	TRINITY_DN10614_c0_g1_i10	PREDICTED: elastin-like
Un-weathered	Upregulated	TRINITY_DN9238_c0_g1_i6	low-density lipoprotein receptor-like
Un-weathered	Upregulated	TRINITY_DN3431_c0_g1_i11	---NA---
Un-weathered	Upregulated	TRINITY_DN5482_c0_g1_i13	cytochrome P450 307a1-like
Un-weathered	Upregulated	TRINITY_DN21273_c0_g1_i5	SCYLLA-like protein
Un-weathered	Upregulated	TRINITY_DN20289_c0_g1_i15	Cystathionine beta-synthase
Un-weathered	Upregulated	TRINITY_DN20289_c0_g1_i12	Cystathionine beta-synthase
Un-weathered	Upregulated	TRINITY_DN12717_c0_g1_i6	---NA---
Un-weathered	Upregulated	TRINITY_DN2077_c3_g2_i3	---NA---
Un-weathered	Upregulated	TRINITY_DN12572_c0_g1_i8	Dual specificity protein phosphatase 14
Un-weathered	Upregulated	TRINITY_DN1955_c0_g1_i3	serine protease 2
Un-weathered	Upregulated	TRINITY_DN8563_c0_g1_i9	PREDICTED: uncharacterized protein LOC108678532
Un-weathered	Upregulated	TRINITY_DN30383_c0_g1_i13	ERAD-associated E3 ubiquitin-protein ligase HRD1B-like
Un-weathered	Upregulated	TRINITY_DN3318_c0_g1_i15	tolloid-like protein 2
Un-weathered	Upregulated	TRINITY_DN9172_c3_g1_i7	apolipoprotein D-like
Un-weathered	Upregulated	TRINITY_DN3753_c5_g1_i2	---NA---
Un-weathered	Upregulated	TRINITY_DN7166_c1_g1_i9	i-type lysozyme 3 precursor
Un-weathered	Upregulated	TRINITY_DN14779_c0_g1_i17	serine-rich adhesin for platelets-like isoform X15
Un-weathered	Downregulated	TRINITY_DN13699_c0_g1_i8	Hemocyanin A chain
Un-weathered	Downregulated	TRINITY_DN1660_c3_g1_i1	protein croquemort-like
Un-weathered	Downregulated	TRINITY_DN1264_c0_g1_i4	transient-receptor-potential-like protein
Un-weathered	Downregulated	TRINITY_DN3666_c0_g1_i12	D-3-phosphoglycerate dehydrogenase
Un-weathered	Downregulated	TRINITY_DN1409_c1_g1_i7	carotenoid isomerooxygenase
Un-weathered	Downregulated	TRINITY_DN2261_c4_g1_i1	zinc proteinase Mpc1
Un-weathered	Downregulated	TRINITY_DN838_c2_g1_i19	phosphoethanolamine N-methyltransferase-like

Un-weathered	Downregulated	TRINITY_DN11316_c0_g1_i10	probable deoxycytidylate deaminase
Un-weathered	Downregulated	TRINITY_DN11999_c0_g1_i10	Xylulose kinase
Un-weathered	Downregulated	TRINITY_DN3720_c0_g1_i4	---NA---
Un-weathered	Downregulated	TRINITY_DN2821_c0_g1_i4	7,8-dihydro-8-oxoguanine triphosphatase-like
Un-weathered	Downregulated	TRINITY_DN576_c0_g2_i4	deoxynucleoside triphosphate triphosphohydrolase SAMHD1-like
Un-weathered	Downregulated	TRINITY_DN12999_c0_g1_i11	betaine--homocysteine S-methyltransferase 1-like
Un-weathered	Downregulated	TRINITY_DN11316_c0_g1_i7	deoxycytidylate deaminase
Un-weathered	Downregulated	TRINITY_DN309913_c0_g1_i2	phosphatidylserine decarboxylase proenzyme, mitochondrial-like isoform X1
Un-weathered	Downregulated	TRINITY_DN3387_c0_g1_i1	Laminin subunit alpha
Un-weathered	Downregulated	TRINITY_DN921_c0_g1_i4	probable phosphoserine aminotransferase
Un-weathered	Downregulated	TRINITY_DN2231_c1_g3_i1	oplophorus-luciferin 2-monooxygenase non-catalytic subunit-like
Un-weathered	Upregulated	TRINITY_DN9642_c0_g1_i1	EF-hand calcium-binding domain-containing protein 4B
Un-weathered	Upregulated	TRINITY_DN81243_c0_g1_i1	---NA---
Un-weathered	Upregulated	TRINITY_DN804_c0_g1_i2	serine/threonine-protein kinase MAK-like isoform X2
Un-weathered	Downregulated	TRINITY_DN11720_c0_g1_i12	glycine-rich cell wall structural protein 1-like
Weathered	Upregulated	TRINITY_DN27246_c0_g1_i19	microsomal glutathione S-transferase 1-like
Weathered	Upregulated	TRINITY_DN7493_c0_g1_i1	trypsin 3A1-like
Weathered	Upregulated	TRINITY_DN1475_c1_g1_i1	peritrophin-48-like isoform X1
Weathered	Upregulated	TRINITY_DN4854_c0_g1_i1	uncharacterized protein LOC119573628
Weathered	Upregulated	TRINITY_DN1613_c0_g1_i15	obstructor F2
Weathered	Upregulated	TRINITY_DN8283_c0_g1_i8	---NA---
Weathered	Upregulated	TRINITY_DN11617_c0_g1_i3	rhomboid-related protein 2-like isoform X1
Weathered	Upregulated	TRINITY_DN5399_c0_g1_i1	fibrocystin-L-like
Weathered	Upregulated	TRINITY_DN6257_c0_g1_i10	chymotrypsin-like proteinase
Weathered	Downregulated	TRINITY_DN6849_c3_g1_i4	oplophorus-luciferin 2-monooxygenase non-catalytic subunit-like
Weathered	Downregulated	TRINITY_DN28702_c0_g1_i8	---NA---
Weathered	Downregulated	TRINITY_DN19212_c0_g1_i2	---NA---
Weathered	Upregulated	TRINITY_DN9383_c0_g1_i1	calcium homeostasis endoplasmic reticulum protein-like isoform X2
Weathered	Downregulated	TRINITY_DN4654_c0_g1_i11	pre-mRNA-processing factor 40 homolog B-like isoform X3
Weathered	Downregulated	TRINITY_DN1676_c0_g2_i2	Protein wos2
Weathered	Downregulated	TRINITY_DN8131_c0_g1_i18	---NA---
Weathered	Downregulated	TRINITY_DN16133_c0_g1_i9	Glycogen-binding subunit 76A
Weathered	Downregulated	TRINITY_DN1069_c0_g1_i5	proteoglycan 4-like
Weathered	Downregulated	TRINITY_DN11818_c0_g1_i5	uncharacterized protein LOC119575634
Weathered	Downregulated	TRINITY_DN18080_c0_g2_i1	protein broad-minded-like
Weathered	Downregulated	TRINITY_DN16423_c0_g1_i1	nucleoprotein TPR-like
Weathered	Downregulated	TRINITY_DN1952_c0_g1_i5	nucleolar protein 9
Weathered	Downregulated	TRINITY_DN37484_c0_g1_i1	Molybdenum cofactor sulfurase